July 2018

Intersection Signal Control and Design for Improved Person Mobility and Air Quality in Urban Multimodal Transportation Systems

Farnoush Khalighi

INTERSECTION SIGNAL CONTROL AND DESIGN FOR IMPROVED PERSON MOBILITY AND AIR QUALITY IN URBAN MULTIMODAL TRANSPORTATION SYSTEMS

A Dissertation Presented

by

FARNOUSH KHALIGHI

Submitted to the Graduate School of the
University of Massachusetts Amherst in partial fulfillment
of the requirements for the degree of

DOCTOR OF PHILOSOPHY

May 2018

Civil and Environmental Engineering

INTERSECTION SIGNAL CONTROL AND DESIGN FOR IMPROVED PERSON MOBILITY AND AIR QUALITY IN URBAN MULTIMODAL TRANSPORTATION SYSTEMS

A Dissertation Presented

by

FARNOUSH KHALIGHI

Approved as to style and content by:

Eleni Christofa, Chair

Song Gao, Member

Ahmed Ghoniem, Member

Eric Gonzales, Member

Michael Knodler, Member

Richard Palmer, Department Chair
Civil and Environmental Engineering

ABSTRACT

INTERSECTION SIGNAL CONTROL AND DESIGN FOR IMPROVED PERSON MOBILITY AND AIR QUALITY IN URBAN MULTIMODAL TRANSPORTATION SYSTEMS

MAY 2018

FARNOUSH KHALIGHI

B.Sc., SHARIF UNIVERSITY OF TECHNOLOGY, IRAN

Ph.D., UNIVERSITY OF MASSACHUSETTS AMHERST

Directed by: Professor Eleni Christofa

Alternative geometric designs (e.g. roundabouts) and multi-objective signal control strategies are promising measures to improve sustainability of traffic networks. However, roundabouts are mostly used because of their safety and operational advantages. There has been less attention to the environmental performance of roundabouts. Also, the existing studies have been mostly used through field measurements and current simulation models, which need high calibration efforts and they are not inclusive in terms of considering all influencing factors on vehicular emissions at roundabouts. Furthermore, the existing real-time signal control strategies do not account for the emission rates of different vehicle types (e.g. cars and buses). In addition, the real-time multi-objective signal control systems does not consider environmental objectives. This dissertation develops a real-time bi-objective signal control system for isolated intersections, which operate at undersaturated traffic conditions that mini-

mizes a weighted combination of vehicle delay (or person delay) and emissions of auto and transit vehicles. Pareto Frontiers of the optimal solutions are presented to help decision makers select the most appropriate combinations of objectives to achieve desirable levels of delay and emissions. Additionally, a simple simulation tool based on Cellular Automata (CA) model of traffic simulation is developed to estimate delay and reproduce vehicle trajectories for emission estimation. The models are used to compare the operational and environmental performance of roundabouts and signalized intersections and perform sensitivity analysis with respect to total traffic demand, left turn ratio, and pedestrian volume. Evaluation tests show that replacing a signalized intersection with a roundabout results in improved delay and emissions at undersaturated traffic conditions and any pedestrian volume. It also shows that roundabouts' performance is less affected by high left turning demand compared to signalized intersections. On the contrary, roundabouts' performance is sensitive to frequent pedestrian crossings while the performance of signalized intersections is not affected by pedestrian crossings.

TABLE OF CONTENTS

LIST OF TABLES

Table **Page**

LIST OF FIGURES

Figure **Page**

LIST OF SYMBOLS

λ_d	weight of the delay term in the objective function
λ_e	weight of the emission term in the objective function
$g_{i,T}$	green time of phase i in cycle T $[sec]$
y_i	yellow time of phase i $[sec]$
k_j	the first phase that serves lane group j
l_j	the last phase that serves lane group j
I	the number of phases in a cycle
J	the number of lane groups
C	cycle length $[sec]$
$R_j^{(1)}(g_{i,T})$	the first red duration of lane group j in cycle T, shown in figure 2.1 $[sec]$
$R_j^{(2)}(g_{i,T})$	the second red duration of lane group j in cycle T, shown in figure 2.1 [sec]
$G_j^e(g_{i,T})$	effective green time of lane group j in cycle T $[sec]$
τ_j^T	end of the green phases in cycle T that serves lane group j $[sec]$
$D_{j,T}$	total auto delay in cycle T $[veh - sec]$
$\hat{D}_{j,T+1}$	total auto delay in cycle $T+1$ $[veh - sec]$
$E_{j,T}$	total auto emission in cycle T $[gr]$
$\hat{E}_{j,T+1}$	total auto emission in cycle $T+1$ $[gr]$
$d_{b,T}$	delay of bus b $[sec]$
$e_{b,T}$	emission of bus b $[gr]$
b_{max}	the number of buses considered in an optimization cycle
$g_{i,min}$	minimum green time of phase i $[sec]$
$g_{i,max}$	maximum green time of phase i $[sec]$
$g_{i,next}$	assumed fixed duration of phase i in cycle $T+1$ when cycle T is being optimized $[sec]$
q_j	arrival flow rate of auto vehicles in lane group j $[\frac{veh}{hr}]$
s_j	saturation flow rate of auto vehicles in lane group j $[\frac{veh}{hr}]$
o_a	average passenger occupancy of auto vehicles $[\frac{pax}{veh}]$
o_b	passenger occupancy of transit vehicle b $[\frac{pax}{veh}]$
$N_{j,T}^q$	the length of queue of lane group j in cycle T veh
$N_{j,T}^{\star,a}$	the number of vehicles in lane group j and cycle T that experience a complete stop
$\bar{N}_{j,T}^a$	the number of auto vehicles in lane group j and cycle T that experience a partial stop
L_1	traveling distance upstream the intersection m
L_2	traveling distance downstream the intersection m

t_a	arrival time of auto vehicle a sec
t_b	arrival time of transit vehicle b sec
$t_{j,T}^{\star,a}$	the arrival time of the last auto vehicle in lane group j and cycle T that experiences a complete stop sec
$t_{j,T}^{\star,b}$	the arrival time of the last transit vehicle in lane group j and cycle T that experiences a complete stop sec
$t_{j,T}^{q}$	the arrival time of the last vehicle that arrives at the back of the queue in lane group j and cycle T sec
$\alpha_a, \beta_a, \gamma_a$	symbols for the time interval an auto vehicle could possibly arrive
$\alpha_b, \beta_b, \gamma_b, \delta_b$	symbols for the time interval a transit vehicle could possibly arrive
v_f^a	cruising speed of auto vehicles $[\frac{m}{s}]$
v_f^b	cruising speed of transit vehicles $[\frac{m}{s}]$
α_{acc}^a	constant acceleration rate of auto vehicles $[\frac{m}{s^2}]$
α_{dec}^a	constant deceleration rate of auto vehicles $[\frac{m}{s^2}]$
α_{acc}^b	constant acceleration rate of transit vehicles $[\frac{m}{s^2}]$
α_{dec}^b	constant deceleration rate of transit vehicles $[\frac{m}{s^2}]$
$T_{m,j,T}^a$	total time spent in operation mode m by all auto vehicles that arrive in lane group j and cycle T, where $m \in \{acc, dec, id, cr\}$ $[veh - sec]$
$t_{m,j,T}^k$	total time spent in operation mode m by all auto vehicles that arrive in time interval k in lane group j and cycle T, where $m \in \{acc, dec, id, cr\}$ and $k \in \{\alpha_a, \beta_a, \gamma_a\}$ $[veh - sec]$
e_m^a	emission rate of auto vehicles in operation mode m, where $m \in \{acc, dec, id, cr\}$ $[\frac{gr}{sec}]$
e_m^b	emission rate of transit vehicles in operation mode m, where $m \in \{acc, dec, id, cr\}$ $[\frac{gr}{sec}]$
$d_{b,T}^k$	delay of transit vehicle b that arrives in time interval k of cycle T, where $k \in \{\alpha_b, \beta_b, \gamma_b, \delta_b\}$ sec
$t_{b,m}^k$	the time that a transit vehicle b that arrives in interval k spends in operation mode m where $m \in \{acc, dec, id, cr\}$ and $k \in \{\alpha_b, \beta_b, \gamma_b, \delta_b\}$ sec
ω_b^k	binary variable that determines the time interval in which transit vehicle b could possibly arrive where $k \in \{\alpha_b, \beta_b, \gamma_b, \delta_b\}$
M_1/M_2	big numbers
$g_{i,b}^k$	continuous variable of green times for a time interval that transit vehicle b could possibly arrive where $k \in \{\alpha_b, \beta_b, \gamma_b, \delta_b\}$ sec
Y	intersection flow ratio

INTRODUCTION

Motivation

Severe traffic congestion and high levels of air pollutants produced by vehicles have threaten people's quality of life in urban areas. Traffic intersections are responsible for a significant portion of delay that users experience during their travel in a traffic network. They also have major contributions to air quality and consequently public health. Furthermore, serving multiple modes at signalized intersections has been a challenge for transportation authorities. Traffic intersections can adversely affect transit operations and ridership by holding transit vehicles back from their schedule and imposing excessive delays to transit users. However, minimizing all negative impacts of traffic intersections cannot be achieved at the same time and there is a need for a solution that balances all these impacts.

The improvement of traffic externalities at intersections can be achieved through optimized signal control strategies. These strategies are cost-effective tools to mitigate traffic congestion and air pollution in traffic networks because they can be implemented within existing infrastructure. Signal control systems are traditionally designed to improve traffic operations by minimizing vehicle delay or maximizing intersection capacity. However, minimized delay or maximized capacity does not guarantee decreases vehicular emissions at intersections. With increased concerns about levels of transportation-related air pollutants in urban areas and the major role of intersections in exacerbating air quality, attention has shifted towards environmental-friendly signal control strategies. In recent years, a few signal control systems to minimize emission or energy consumption have been developed.

The development of signal control systems with environmental objectives has been a major step towards sustainability. However, improving emissions or energy consumption can be conflicting with operational objectives such as minimizing delay. As studies have shown, emission rates of vehicles are significantly higher during the acceleration mode. Therefore, operational and environmental objectives should be directly considered in signal control strategies at the same time. To meet certain thresholds for operational and environmental performance measures, the objectives should be combined with appropriate weights. Furthermore, depending on the vehicle types in a fleet and the air pollutants of concern, transportation modes can have different impacts on emissions. Therefore, there is an imperative need for multi-objective signal control systems that account for the needs and impacts of different modes present at an intersection.

In additions to signal control strategies, alternative intersection designs (e.g. roundabouts) can help to improve sustainability of traffic networks. Roundabouts are another important element traffic networks, which are mostly used because of their safety and operational advantages over signalized intersections. However, roundabouts and signalized intersections lead to different vehicle speed profiles, which are directly associated with vehicular emission levels. Thus, the impact of roundabouts on vehicular emission should be considered as well as their operational impacts.

Research Question

Specifically, the questions that motivate this research are:

- How should a signal control system be designed to keep a balance between operational and environmental performance of signalized intersections?
- Under what conditions roundabouts lead to better operational and environmental performance compared to signalized intersections?

Research Contribution

In this dissertation a real-time bi-objective signal control system is developed to minimize delay (or person delay) and emissions. The delay and emission estimations within the signal control system are based on analytical models, which result in low computation times and make the use of the system for real-time signal timings possible. Additionally, different emission rates across vehicle operation modes and for two vehicle types (i.e. auto and transit vehicles) have been taken into account. Trade-offs between delay (or person delay) and emissions for two important air pollutants, CO and NO_x, are presented by Pareto Frontiers of optimal solutions. The Pareto curves and provided insights into them help decision makers select appropriate combination of objectives to achieve desirable improvements in traffic operation and air quality.

In addition, this study provides a simple simulation tool based on Cellular Automata model of traffic simulation to estimate delay and emission at roundabouts and signalized intersections with single-lane approaches. The CA-based model is advantageous in that it needs less calibration efforts than the existing microsimulation models. This model is validated for undersaturated conditions. The CA-based models are used to study the effects of total traffic demand, left turn ratios, and pedestrian demand on the performance of the two type of intersections.

Dissertation Organization

This dissertation is organized as follows. Chapter 1 presents a review of the literature on existing emission models, signal control strategies with environmental objectives, multi-objective signal control systems, studies on the environmental and operational performance of roundabouts, and the applications of cellular automata model in traffic simulation and emission estimation. Chapter 2 describes the proposed bi-objective signal control strategy to minimize delay and emissions. It first presents the general mathematical optimization model to minimize a weighted combination of delay (or person delay) and emissions. Then, the methodology to estimate delay and emis-

sions and the reformulated mathematical model are presented. The rest of Chapter 2 presents the evaluation tests and discusses the results and conclusions. Chapter 3 evaluates the operational and environmental performance of roundabouts and signalized intersections with single-lane approaches. First, the cellular automata model of traffic simulation is described. Then, CA-based models to simulate traffic at roundabouts and signalized intersections are calibrated and validated against a microsimulation model in Aimsun. Then the method to estimate emissions is presented. Next, the performance of roundabouts and signalized intersections under different demand conditions and pedestrian volumes is evaluated and compared against each other and conclusions are presented. The final chapter summarizes this dissertation's key findings, contributions, and future work.

CHAPTER 1

LITERATURE REVIEW

This chapter first presents a brief description of the emission models in two categories; macroscopic and microscopic models. Then, a review of existing research on vehicular emissions at signalized intersections and signal control strategies to minimize emissions is presented. This is organized by type of study: field measurements, simulation studies, and analytical models. Existing multi-objective signal timing plans are presented next and are organized into two groups of strategies that consider environmental objectives (e.g. emission and fuel consumption) and strategies that do not include environmental objectives. The next section reviews existing literature on the environmental performance of roundabouts through field measurements and simulation studies. Then, a description of Cellular Automata (CA) traffic model in reproducing traffic conditions, and its applications in studying traffic operations, safety, and environmental performance of roundabouts is presented. The last section, provides a summary of the literature and identifies the gaps in the literature that this dissertation aims to address.

1.1 Vehicle Emission Models

The need for estimating vehicular emission inventories at different levels (i.e. from local to national scales) and the impact of transportation projects on air pollution as well as emission requirements developed by the Environmental Protection Agency (EPA) has led to the development of several macroscopic and microscopic emission models.

Earlier models estimate aggregate emission levels based on average speed and traveled distance (i.e. macroscopic models). However, several field measurements have shown that emission rates during acceleration and cruising modes are usually higher than other operation modes (i.e. idling and deceleration) because of the higher level of the vehicle's engine power at these modes [30]. Generally, a vehicle's emission rates depend on its speed and acceleration rates [15]. Therefore, more recent emission models account for sensitivity of emission to speed changes (i.e. microscopic models). The next subsection presents a review of commonly-used emission models.

1.1.1 Macroscopic Emission Models

Macroscopic emission models estimate aggregate emissions based on average speed of a road section and total vehicle miles traveled and do not account for speed changes in vehicles' trips. Their application is mostly for large-scale projects and they are not appropriate for project-level emission analyses. Two macroscopic emission models used by agencies at national, state, or local [1] levels are Mobile source Emission Factor Model (MOBILE) and EMission FACtors (EMFAC), which are reviewed in this section.

1.1.1.1 Mobile source Emission Factor Model (MOBILE)

MOBILE is one of the earliest emission models, which was initially developed in the late 1970s as MOBILE1, and has been updated a few times to incorporate improved data, and changes in vehicle, engine, and emission control system technologies as well, changes in applicable regulations, emission standards, and test procedures. The last version of MOBILE, which incorporates all aforementioned updates was developed in 2004 as MOBILE6.2. It is worth noting that MOBILE models are not in use

[1] It should be noted that terms "local-level" and "project-level" have different meanings. Local-level emission refers to the total emission inventories in a specific geographical area while project-level emission refers to the emissions produced as a result of implementing a transportation project such as traffic signal coordination

for regulatory analysis anymore because they account for neither emission requirements established after 2004 nor improved data. MOBILE has now been replaced by MOVES, which is developed to address new requirements by the government [4].

MOBILE is an EPA's approved model and was used by the U.S. government for local, state, and national emission estimation purposes. The model specifies emission rates for different vehicle classes for predefined driving cycles. Then, it adjusts the default emission rates using some correction factors to account for vehicle population, fuel quality, temperature, and humidity. The adjusted emission rates are then paired with vehicle activity data to estimate emission inventories in tons of pollutants per hour, day, month, or year [8]. MOBILE6.2 calculates emissions of hydrocarbons (HC), oxides of nitrogen (NOx) and carbon monoxide (CO), particulate matters (PM), and some air toxics such as Benzene from passenger cars, motorcycles, light and heavy-duty trucks.

MOBILE integrates emission factors (for highway vehicle emissions) in the unit of grams per hour or grams per mile with total vehicle miles traveled (VMT) to estimate total emission (i.e. it does not account for variations in vehicles' speed profiles). It also presents aggregate emission outputs and not emissions produced by individual vehicles [4]. As a result, it is considered a macroscopic model, which is able to estimate large-scale inventories and is not appropriate for operational-level projects [59].

1.1.1.2 EMission FACtors (EMFAC)

The EMFAC emission model was developed in 1990 by the California Air Resources Board (CARB) and approved by the EPA to assess emissions from on-road vehicles including passenger cars, trucks, motor cycles, motor homes, and buses in California. Different versions of EMFAC have been released to date to incorporate improved data as well as updates in emission standards and requirements. Like MOBILE, EMFAC uses default emission rates, correction factors (to account for temperature, humidity,

etc), and vehicle activity data (i.e. VMT) to estimate emissions in tons/day for a specific month, year, or season [8].

EMFAC is used to estimate emissions of PM, CO, HC, NO_x, CO_2, Lead, and sulfur oxides at local (i.e. air district[2], air basin[3], or county) and state (California) levels. Pollutants considered in EMFAC include the exhaust, evaporative, and tire/brake emissions [8].

1.1.2 Microscopic Emission Models

The aggregate nature of MOBILE and EMFAC makes them inadequate for project-level emission analyses such as signal control strategies and many Intelligent Transportation System (ITS) strategies. The need for models that are capable of estimating emissions at finer scales as well as considering the modal operation of vehicles (i.e., idle, cruise, and various levels of acceleration/deceleration) for estimating emissions has led to the development of microscopic emission models. These models estimate emission based on either speed/acceleration levels or power demand modes of vehicle's operation (i.e. modal emission models). An example of the former is the VT-Micro emission model and two examples of the latter are the Comprehensive Modal Emission Model (CMEM) and the Motor Vehicle Emission Simulator (MOVES). This section presents these three emission models.

1.1.2.1 Virginia Tech Microscopic (VT-Micro)

Virginia Tech Microscopic model (VT-Micro) is a vehicle emission model developed by researchers at the Virginia Tech University. It has been developed using chasis dynamometer data of 60 light-duty vehicles and trucks (the first version of the model

---

[2] "The state of California is divided into Air Pollution Control Districts (APCD) and Air Quality Management Districts (AQMD), which are also called air districts [6]."

[3] "An air basin is an area within a ring or partial ring of mountains that in the absence of winds holds air and smog within the area [2]."

was developed based on data of 9 light-duty vehicles, but in the last version data of 60 light-duty vehicles and trucks is incorporated.). VT-Micro can be used to estimate emissions of HC, CO, CO_2, and NO_x at the project-level [59].

VT-Micro emission models (i.e. models for different vehicle classes) are developed by aggregating data based on vehicle and operational variables. The instantaneous speed and acceleration levels are used as operational variables. Also, vehicles are categorized into homogeneous categories in terms of emission rates. Three steps of vehicle categorization are: 1) categorizing vehicles into Light Duty Vehicles (LDV), Light Duty Trucks (LDT), and Heavy Duty Trucks (HDT); 2) grouping based on fuel type (i.e. diesel or gasoline); and 3) using statistical algorithms to further group vehicles into categories with the same emission characteristics (parameters used in this step are vehicle model year, engine technology, engine size, and vehicle mileage). VT-Micro presents emission models for 5 different LDV classes and 2 LDT classes [59].

1.1.2.2 Comprehensive Modal Emission Model (CMEM)

CMEM is a modal-based emission model initially developed in the late 1990's by research groups at the University of California, Riverside, the University of Michigan, and the Lawrence Berkeley National laboratory to fulfill the need for microscopic emission modeling. CMEM is comprehensive in a sense that it includes a variety of vehicle types and technologies in various states of conditions (e.g. properly functioning, deteriorated, and malfunctioning) [3]. The last version of the model estimates emissions of 28 light-duty vehicle categories and 3 heavy-duty vehicle/technology categories [15].

An important difference of CMEM with past models is its approach in estimating emissions. The modal emission models developed before CMEM used speed/acceleration profiles of vehicles, but CMEM is developed using a power-demand approach. In

speed/acceleration approach many parameters that affect emissions such as road grade and use of accessories have not been accounted for [60]. However, in the approach used by CMEM, the entire emission production process is broken down into smaller components that correspond to physical phenomena, which are associated with vehicle operation and emission production. Each component is represented by an analytical model based on various parameters such as vehicle mass, engine size, aerodynamic drag coefficient, etc. This way of estimating emissions not only accounts for a more complete set of parameters, but also allows considering new parameters by easily adding them to the analytical representation of each component [15].

The power demand-based approach of emission estimation is centered around the concept of Vehicle Specific Power (VSP). VSP is an indicator of a vehicle's engine power, which is impacted by the aerodynamic drag force, acceleration, rolling resistance, and hill climbing. VSP is reported in kilowatts per tonne, the instantaneous power demand of the vehicle divided by its mass. VSP is presented with an equation that has the following general form.

$$VSP = v * (a + g * \sin\phi + \psi) + \zeta * v^3 \tag{1.1}$$

where:

v: vehicle speed $[\frac{m}{s}]$

a: vehicle acceleration $[\frac{m}{s^2}]$

g: acceleration due to gravity $[\frac{m}{s^2}]$

ϕ: road grade %

ψ: rolling resistance coefficient $[\frac{m}{s^2}]$

ζ: drag coefficient $[\frac{1}{m}]$)

The coefficients of the equation are determined for specific vehicle type [86]. The calculation of VSP on a second-by-second basis facilitates obtaining a vehicle's power

distribution throughout a trip. The calculated VSP values are then used to determine the instantaneous VSP bins and associated emission rates (presented in grams per second). VSP bins represent different ranges of VSP values such that emission rates associated with each bin are significantly different than those of other bins. Total emissions for a trip can be then estimated by adding the emissions produced in each VSP mode.

The inputs to the CMEM are vehicle activity data (at least, second-by-second speed) and fleet composition. The model estimates tailpipe emissions of CO, HC, CO_2, NO_x, and PM, and fuel consumption [15].

1.1.2.3 Motor Vehicle Emission Simulator (MOVES)

MOVES is a comprehensive emission estimation package developed by the EPA to estimate emissions of on-road and off-road (such as cranes and bulldozers) mobile sources. The need for emission assessment of finer-scale projects such as installing traffic signals or adding lanes led to the development of this model. MOVES is able to estimate emission inventories at very fine-scales to national-scales. Diverse uses of MOVES include national-scale uses (e.g. inventory of the U.S. Greenhouse Gas emission), local inventory (e.g. State Implementation Plans), hot-spot and project-level analysis (e.g. PM and CO conformity, and toxic exposures), model interaction (e.g. microscopic models and dispersion models), and policy evaluation (e.g. cleaner vehicles and fuel types) [42].

MOVES applies a four-step approach to estimate emissions: 1) calculating total activity, which is the product of population and per-source activity; 2) distributing total activity into source and mode bins (Source bin is determined based on several parameters such as fuel type, mileage, technology, standard, and emitter category, and operating mode is determined based on the power bin (VSP bin)); 3) calculating emission rates based on source and operation mode bins; and 4) aggregating emission

rates across these modes. It should be noted that unlike MOBILE and EMFAC, MOVES represents activity data by source-time and number and not VMT. This is due to the fact that both on-road idling vehicles and off-road equipment produce emissions without traveling any distance. Also, some activities that produce emissions (such as start exhaust emissions) are non-time and should be presented in number[42].

1.2 Emission Estimation at Signalized Intersections

The effect of traffic intersections on vehicular emissions has been studied through field measurements, simulation studies, and analytical models, all of which present some advantages and disadvantages. Cost-effectiveness, accuracy, calibration effort, and simplicity are the key elements that should be considered in selecting a method to conduct a study.

This section reviews existing literature on emission estimation at signalized intersections as well as existing signal control strategies aimed at improving air quality.

1.2.1 Field Studies

Field experiments to study vehicular emissions have been performed in two ways. One approach is to use a Portable Emission Measurement System (PEMS) that can be installed in the vehicle to measure tailpipe emissions. The second approach is to only record the real-world operation of vehicles and use the vehicle operation data (e.g. vehicles' trajectory) along with an available emission model or emission database to estimate emissions associated with a certain speed profile. Although both methods usually provide acceptable estimates, the first method that directly measures tailpipe emissions is more reliable because it measures emissions under real-world conditions. However, it is not always feasible due to the high cost of the required devices.

In recent years, with the development of affordable mobile emission measurement devices, field measurements have become more popular. An on-board emission de-

vice was used by Zhang et al. [88] to measure and compare real-world emissions produced under signal coordination and non-coordination. Several researchers have used On-board Emission Measurement (OEM 2100^{TM}) units developed by the Clean Air Technologies International, Inc [30, 63, 76, 23]. OEM 2100 is a portable instrument and has three connections with the vehicle: a power cable that connects to the power port, a link that connects On-Board Diagnostic (OBD) link to the engine to get engine's activity data, and an emission sampling probe, which should be inserted to the tailpipe. These connections make it possible to establish the relationship between a vehicle's operation (i.e., speed and acceleration rates) and tailpipe emissions [23].

The OEM 2100 was first used to study the effect of traffic flow on a signalized arterial on real-world vehicle emissions and investigate the relationship between vehicle emission and a commonly used traffic performance measure, control delay [63]. After that, field studies were conducted using OEM device to estimate emission rates [30]. Also, OEM units have been used in some studies to evaluate the environmental effects of signal control strategies such as signal coordination [76, 74].

The second type of field studies has been utilized to show improvements obtained by an adaptive signal control strategy on produced emissions of CO, HC, CO_2, NO_x, and fuel consumption. This study utilizes traffic data including idle time and stop rate monitored by camera sensors along with available speed profile databases and their corresponding emission records [54].

1.2.2 Simulation Studies

Most of the studies to estimate the impact of signal control strategies on emissions have been performed using simulation tools. Usually, an integration of a traffic simulation tool with an emission model is used to estimate emissions, which is commonly used in a variety of ITS and transportation control measure evaluations. Some researchers have used macroscopic traffic simulation tools such as AVENUE along with

emission models to evaluate emission impacts of signal timings [56]. However, the majority of research has been performed using microscopic traffic and emission models.

There are microsimulation studies using an integration of CMEM and Paramics traffic simulation package to assess the effect of advisory speed limits on produced emissions at a single signalized intersection or on an signalized arterial. The proposed system by Li et al. [47] informs connected vehicles' drivers if they are not able to pass the intersection based on their estimated travel time to the intersection and the remained time of the signal's green phase. This information helped drivers to avoid harsh braking and consequent additional CO_2 emission (improvement of around 7%) and fuel consumption (improvement of around 8%) in medium traffic conditions (v/c ratio of 0.7).

Another eco-approach technology developed by Xia et al. [81] provides drivers with more detailed information than the system presented in the last study. The system uses the intersection map and signal timings to estimate the speed at which a vehicle can pass the intersection (if possible) or gently decelerate to a stop. This system has been evaluated through field measurement and simulation (using CMEM and Paramics) on a single intersection and showed on average of 14% reduction in fuel consumption and CO_2 emissions. The authors also evaluated the performance of the proposed eco-friendly system on a signalized arterial through simulation [80]. The application of the system on vehicles traveling on a signalized arterial resulted in 10-15% reduction (depending on the corridor's traffic condition) in fuel consumption and CO_2 emission of an equipped vehicle, as well as a network-wide reduction of 3.39% at penetration rate of 20%.

The VISSIM traffic simulation tool has been used along with MOVES [32], CMEM [69, 43, 72], or MOVElite [48] to assess emissions. Guo and Zhang [32] evaluated the relationship between mobility and environmental externalities at two signalized inter-

sections. They used SYNCHRO (to obtain mobility-based optimal signal timings), VISSIM (to simulate traffic conditions and obtain vehicle trajectories resulted from SYNCHRO signal plans), and MOVES (to estimate emissions and fuel consumption resulted from output trajectories from VISSIM). Then, they applied statistical analysis to explore the relationship between mobility measurements and environmental externalities. The analysis showed that among mobility measurements, total delay and total number of stops are more correlated with emissions and fuel consumption.

An integration of VISSIM and CMEM was used by Stathopoulos and Noland [69] to examine long-term impacts of signal coordination (coordination plan developed by TRANSYT) on emissions. They showed that although in the short-run emissions of different pollutants (i.e. CO, HC, NO_x, and CO_2) are improved, in the long-run the potential induced trips cancels off the effects of signal coordination. Kun and Lei [43] also used a traffic-emission platform of VISSIM and CMEM to model a traffic network to 1) analyze the relationship between emission/fuel consumption and vehicle's speed/acceleration profile; 2) estimate emissions for a variety of vehicle types (including cars, buses, and Light Goods Vehicles (LPG)); and 3) investigate the emission impacts of an alternative signal timing plan (i.e. extending green phase of the major street by 5% while keeping cycle length constant). This study showed significant impacts of acceleration rate on emissions as well as improvements in emissions through the alternative signal timing plan.

Stevanovic et al. [72] used an integration of VISSIM, CMEM, and VISSIM-based Genetic Algorithm for Optimization of Signal Timings (VISGAOST) [4] to optimize signal timings and the effects on fuel consumption and CO_2 emission. They evaluated seven different objectives including operational and environmental objectives and

[4]VISGAOST is a signal timing optimization tool, which develops optimized signal plans based on their performance in VISSIM.

showed that minimizing CMEM-estimated fuel consumption results in the minimum level of fuel consumption and CO_2 emissions.

Furthermore, Zhang et al. [88] used the integration of VISSIM and the VSP approach in addition to field measurements to investigate the environmental performance of different signal control strategies. The integration of the CORSIM traffic microsimulation model with VT-micro to estimate emissions and fuel consumption was used in the development of a sustainable signal control system that minimized emissions by introducing a speed management strategy [18]. A study to evaluate the impact of different levels of signal coordination (poor, real-time, and good coordination) on emissions was conducted with the use of the INTEGRATION traffic microsimulation tool along with microscopic emission regression models [61].

1.2.3 Analytical Models

The first analytical emission models estimated emissions based on average travel characteristics such as average speed or number of stops. The 2nd edition of the Canadian Capacity Guide (CCG) presents a model for estimating emissions as a function of the number of stops and average stopped delay, average cruising speed, and distance [75]. Another analytical emission model based on traffic demand, roadway characteristics, and traffic signal timing parameters such as cycle length or green splits was developed by Hellinga et al. [34].

Studies have shown that average travel characteristics like average speed are not reliable parameters to estimate emissions since emission levels are significantly affected by speed changes and the acceleration levels of vehicles. Therefore, a number of researchers accounted for different vehicle operation modes (i.e. acceleration, deceleration, cruising, and idling) and used corresponding emission rates for each mode to estimate emissions [68, 66]. However, these models have focused on only autos. None of the above studies have modeled other modes' emissions such as buses at

signalized intersections. Khalighi and Christofa [39] developed an analytical model based on modal vehicle operation times and VSP approach to estimate emissions of autos and buses at a traffic signal. This model has then been used within a real-time signal control system to minimize emissions.

1.2.4 Summary of Emission Studies at Signalized Intersections

A review of the literature shows that emission impacts of traffic signals have been evaluated through three types of studies; field measurements, simulation studies, and analytical models, each of which has some advantages and disadvantages.

Field studies provide more accurate emission measurements because they measure emissions under real-world conditions. Also, they can be utilized to establish the relationship between a vehicle's operation and its emissions and develop emission rates based on speed/acceleration levels. However, field studies are time-consuming, sometimes costly (depending on the cost of emission measurement device), and cannot be used to evaluate the environmental impacts of a project before implementing it.

Most of the existing emission studies have been performed through simulation models. Integration of traffic simulation tools with emission models has been used in several studies to evaluate the emission impact of a wide variety of signal control strategies. A key advantage of simulation models (only microscopic models) is that they can estimate emissions based on second-by-second trajectories. In addition, simulation packages can be used in before/after studies for transportation projects. However, they often require intensive data collection and calibration efforts to accurately reproduce real-world conditions.

Analytical models are the simplest forms of emission models either using modal emission rates or average speed to estimate emissions. These models can be implemented within real-world signal control strategies due to their relatively low compu-

tation times and simplicity. However, the majority of these anlytical models are for autos and there is only one study that estimates bus emissions at traffic signals.

1.3 Multi-Objective Signal Timing Optimization

Traditionally, signal timing optimization has focused on minimizing vehicle delay or maximizing intersection throughput. However, sustainability goals have shifted the objectives towards improving person mobility, air quality, fuel consumption, safety, and providing conditions for smoother traffic operations, which can be achieved by considering various objectives such as minimizing delay and stops, queue length, and so forth.

Several studies have shown that single-objective signal control systems are inadequate for improving the performance of the system in different aspects at the same time. Leonard and Rodegerdts [46] developed different single-objective signal timing plans to separately minimize delay, stops, fuel consumption, and maximize progression. They demonstrated that signal settings obtained by each of these objectives may have significantly different impacts on the performance of the system and one objective could be even conflicting with others (i.e. improving one objective may worsen another one). Zeng et al. [85] validates the claim that some signal timing objectives could be conflicting by evaluating the impact of signal timing on vehicle delay, stop rate, capacity, queue length, and pedestrian delay. This study showed that vehicle delay, pedestrian delay, and queue length are consistent (i.e. improving vehicle delay results in improved pedestrian delay and queue length) while vehicle delay is not consistent with stopping rate and intersection capacity. This is due to the fact that minimizing delay can be usually achieved by decreasing the cycle length, while minimizing number of stops is obtained by increasing the cycle length. Therefore, in an effort to balance objectives, recent studies have developed multi-objective signal timing plans.

A survey was carried out by the Transport Operation Research group at the University of Newcastle, UK amongst the UK transport community about the best objective function that can be used for a signal timing plan [13]. Based on this survey, it is not recommended to develop a single solution for all situations even if this solution accounts for multiple measures such as operational and environmental measures. This is due to the fact that each site has different constraints and requirements, which may vary over time. For example, for an intersection that serves buses, improving the operation of buses may be prioritized over the operation of general traffic. In addition, studies show that vehicular emissions are higher at low temperatures [21]. Therefore, increasing the weight of emission in the objective function of a signal timing plan during winter might be an appropriate strategy. A proper technique is to present a set of optimal solutions, which reflect the trade-off between desired objectives. Therefore, all of these solutions are optimal, but with respect to different objective criteria and priorities. When implementing the signal control system, the solution that matches the desired objective criteria the most should be chosen.

The optimal solution set can be presented as a Pareto Frontier. The concept of Pareto Frontier was initially introduced and formulated by Vilfredo Pareto [58], an Italian economist in the nineteenth century. Pareto frontier was first used in studies of economic efficiency and income distribution, but it currently has a lot of applications in engineering and science. Given an initial allocation of resources amongst a set of users, a change to a different allocation that makes at least one user better off without making any other user worse off is called a Pareto improvement. An allocation is defined as "Pareto efficient" when no further Pareto improvements can be made. In a nutshell, a Pareto frontier is the set of Pareto efficient solutions for a certain set of objective criteria [9]. In some studies that have developed multi-objective signal timing plans, the Pareto Frontier is presented to help decision makers select the most suitable solutions given their objective criteria.

The two following subsections present a review of the existing multi-objective signal control strategies. The first subsection present studies that have considered environmental objectives (in addition to other objectives) and the second subsection presents studies that have not included environmental objectives. The final subsection provides a summary of these studies and identifies the gaps that should be addressed.

1.3.1 Signal Control Strategies with Environmental Objectives

Li et al. [49] optimized signal cycle length of a single intersection through minimizing a performance index defined as a combination of delay, fuel consumption, and emissions. The optimization problem was constrained by minimum green times to allow pedestrian crossings. They showed that the optimal cycle length increases as traffic flow increases. Zhou and Cai [90] also developed a multi-objective signal control strategy with the same objectives (i.e. minimizing vehicle delay, fuel consumption, and emissions). The signal control system was developed in a simulation framework combining Paramics, CMEM, and a genetic algorithm to find the optimal solutions and it was evaluated on a single intersection. They used the concept of comprehensive economic cost, which was defined as the summation of emission, fuel, and delay cost to evaluate their proposed signal timing strategy. They showed that the developed system has a better performance than Webster signal timings (which minimizes vehicle delay) in terms of comprehensive cost.

Some studies have evaluated the relationship between optimized signal timing and users' behavior of route choice. Zhou et al. [89] examined the effect of users' route choice on the performance of a signal timing strategy. They developed a bi-objective signal timing optimization problem with emission minimization as the upper-level objective, a user equilibrium model as the lower-level objective, and signal cycle length and green times as the variables. Emissions were estimated as the summation of running and idling emissions. The evaluation of their model was performed on a

small network with a signalized intersection and 6 links between the origin and destination nodes and showed improvements in traffic quality and emissions. Li and Ge [50] developed a bi-level programming model, which maximizes reserve capacity and minimizes emissions (estimated as the summation of running and idling emissions) in the upper-level and the lower-level accounting for network equity (i.e. difference between users' travel cost across the network, which considers flow-dependent travel time and stop delay at traffic signals). The model presents optimal green ratios for fixed-time signal control systems in a network, which operates under congested traffic conditions. This study only considers auto vehicles and does not account for the effect of other modes such as buses. They evaluated the model for two networks of different sizes (one of them has only one signalized intersection and the other has multiple signalized intersections) and presented the Pareto Frontier of the optimal solutions.

Zhang et al. [87] developed a fixed-time bi-objective signal timing plan to minimize total traffic delay and the risk of human exposure to emissions on a coordinated signalized arterial. They used the Cell Transmission Model (CTM) to capture dynamics in traffic conditions (only considering passenger cars), modal emission rates (i.e. idling, cruising, acceleration, and deceleration), Gaussian plume air dispersion model along with population densities to estimate delay and the risk of human exposure to emissions. A genetic algorithm was used to optimize the signal's cycle length, offsets, green splits, and phase sequence and the Pareto Front of optimal solutions was presented. Stevanovic et al. [71] developed a simulation-based multi-objective optimization by integrating VISSIM, CMEM, Surrogate Safety Assessment Model (SSAM), and VISGAOST. Three objectives including throughput, fuel consumption, and number of vehicular conflicts were considered. Signal cycle length, offsets, green splits, and phase sequence were optimized and Pareto optimal solutions were presented. Evaluating the model on a road link with 5 signalized intersections showed that safety and environmental measures coincide, but they contradict throughput.

1.3.2 Signal Control Strategies without Environmental Objectives

Signal control strategies presented in this section are optimized for two or more operational or safety objectives such as the combination of travel delay, number of stops, and capacity [82], delay and number of stops [85], vehicle delay, stop rate, capacity, queue length, and pedestrian delay [85], or safety measures (such as probability of crash occurrence) and traffic efficiency [70].

Stevanovic et al. [70] analyzed the trade-off between safety (i.e. number of vehicular conflicts) and traffic efficiency (i.e. throughput) using a simulation framework of VISSIM, SSAM, and VISGAOST. They showed that an optimal balance between safety and efficiency can be reached by a single-objective signal timing plan, which minimizes the ratio of number of conflicts to throughput while penalizing inefficient timing plans during optimization. This signal control strategy reduces vehicle conflicts by 7% with only 1% decrease in efficiency on a 12-intersection corridor compared to the initial signal timing plan. They also developed Pareto Frontier a of bi-objective signal timing optimization problem considering the two aforementioned objectives.

Head et al. [84] presented the Pareto Frontier of optimal solutions to a signal timing optimization problem when there are multiple priority requests from different transportation modes present at the intersections. The objective function they optimized was the weighted total delay of different modes constrained to certain requirements for signal timing principles such as coordination. The selection of weights in the objective function reflects the decision makers' priorities such as favoring transit vehicles, general traffic, or pedestrians.

Searching for several non-dominated solutions could be computationally intensive and requires efficient methods and powerful computers. Sun et al. [73] focused on improving the efficiency of optimization method by using a non-dominated sorting genetic algorithm to estimate the Pareto solutions of a bi-objective signal timing optimization for a two-phase isolated traffic signal. The conflicting objectives they

considered were the Webster-based delay and the stop rate of cars, and the design variable was effective green time. Hitchcock and Gayah [35] developed a method to reduce the number of metrics in the objective function by removing noncompeting objectives and further reducing the number of Pareto optimal solutions utilizing a ranking method. They assessed the model on a set of objectives initially including vehicle delay, vehicle delay inequity (i.e. the difference between delay of the lane group with maximum delay and the average of all lane groups' delay), total passenger delay, passenger delay inequity (i.e. similar to vehicle delay inequity, but for passenger delay of each lane group), total number of stops, and total pedestrian delay. Using their proposed method, they could recognize and remove redundant objectives (i.e. total passenger delay and passenger delay inequity). They also achieved a large decrease in the number of solutions (from 1600 to 3 solutions) after applying the ranking method.

There are some multi-objective signal control systems that have applied a fuzzy rule-based method. In fuzzy logic method, metrics' values are represented by qualitative terms (e.g. a queue of 1 to 5 vehicles can be represented by the term "short queue"). The main element of a fuzzy logic control system is a set of rules (e.g. if the queue is long, then extend green). Pappis and Mamdani [57] were the first to implement the fuzzy logic concept in a signal control system with a single objective to minimize average vehicle delay. They showed the fuzzy-based signal control strategy outperforms conventional actuated controllers.

Fuzzy logic has been also used in the development of multi-objective signal control strategies. Lee et al. [45] developed a bi-objective signal control system to reduce total delay of waiting cars, control spill-back, and improve load balancing by controlling out-going cars of an intersection when it has too many waiting cars in its vicinity. Kosonen [41] utilized an on-line (real-time) simulation system along with detector data to reproduce real-time traffic conditions and used that information to optimize a multi-agent fuzzy signal control system. In this signal control system each signal in-

teracts with its neighboring signals, but operates individually and locally. The whole system has multiple objectives including safety, equality (assuring each direction has a possibility of getting green), timing objectives (contains several contradictory objectives such as efficiency and safety), and minimizing transition (optimal rest state when there is no traffic). Schmöcker [65] used fuzzy logic and set acceptability thresholds for each objective and optimized signal green times based on Bellman-Zadeh principal that suggests maximizing the minimum degree of acceptability for all objectives [16].

1.3.3 Summary of Multi-Objective Signal Control Strategies

A review of the literature shows that there are several multi-objective signal control strategies to improve the operational, safety, and environmental performance of signalized intersections. Some studies present trade-offs between desired objectives by demonstrating the Pareto Front of optimal signal timing solutions to help decision makers select the most appropriate solution based on their priorities.

Although some studies have considered the combination of operational and environmental (i.e. fuel consumption or emission) objectives, most of them have used rough estimations for emissions (only from passenger cars) by using average trip speed or the sum of running and idling emissions. There is only one study that optimizes signal timings based on modal-based emissions, but it does not account for bus emissions. In addition, traffic performance is mainly represented by capacity or vehicle delay and not passenger delay, which is a better representative of delay imposed to all users. Therefore, accounting for buses is particularly important due to their higher emission rates and passenger occupancy. Furthermore, all of the existing multi-objective signal control strategies with environmental concerns are fixed time and cannot be implemented within real-time control systems.

1.4 Environmental Performance of Roundabouts

Although roundabouts are considered as promising alternatives for signalized intersections due to their improved safety aspects and operational performance, their environmental performance has not been investigated comprehensively. Additionally, the limited resources on the emission impacts of roundabouts do not suggest consistent results. As roundabouts perform differently compared to signalized intersections in terms of safety and operation, their environmental performance is also different under various traffic conditions. Most of the studies on vehicular emissions at roundabouts are performed through field measurements and simulation tools.

This section reviews the existing literature on the environmental performance of roundabouts in two groups of field measurements and simulation studies. Then, a description of Cellular Automata (CA) model and its application in roundabout studies is provided. Finally, a summary of these studies as well as their shortcomings are presented.

1.4.1 Field Studies

OEM units have been used in many studies to measure a vehicle's tailpipe emissions at roundabouts under real-world operations [44, 91, 77, 33]. Züger et al. [91] utilized an OEM unit to measure vehicle emissions under various traffic and pedestrian volumes and turning ratios. They showed that roundabouts improve emissions compared to signalized intersections for most traffic conditions, but they are outperformed by stop-controlled intersections. Várhelyi [77] showed decreases in emissions and fuel consumption at small roundabouts by conducting a different type of field test. They randomly selected traveling cars at the test site and followed them with an instrumented car, the driver of which tried to imitate the followed car's driving pattern as closely as possible. They used instantaneous speed profiles obtained from the field test along with existing emission rates. Their experiments showed a decrease of up

to 29% and an increase of 6% in emissions when a roundabout replaced a signalized intersection and a yield-control junction, respectively.

Unlike the previous studies, some field measurements show emission increases at roundabouts compared to signalized intersections. Hallmark et al. [33] investigated vehicular emissions at roundabouts and signalized intersections under uncongested traffic conditions and observed increased emissions at roundabouts. They suggested that the emission increase is due to the geometric design of roundabouts that makes drivers slow down when approaching a roundabout and accelerate while exiting a roundabout. Salamati et al. [64] presented an empirical-based macroscopic methodology built on a large sample size of second-by-second real world trajectories. They grouped trajectories into three categories of vehicles with no stop, one stop, or multiple stops. They used the VSP model to estimate and compare the pollutant emissions at roundabouts and signalized intersections. They evaluated the impact of intersection capacity, demand-to-capacity ratio, cycle length, green ratio, signal progression (HCM arrival type), and number of lanes in their study. They showed that at low traffic conditions, roundabouts have lower emissions than signalized intersections while at high traffic volumes, signalized intersections with favorable progression (i.e. main portion of traffic arrives during green time) outperforms roundabouts. They also illustrated that at oversaturated conditions, roundabouts have a steady increase in emissions but signalized intersections lead to a sharp increase in the amount of emissions produced.

1.4.2 Microsimulation Studies

There are several studies that have integrated an emission estimation package and a traffic simulation tool to investigate vehicular emissions at roundabouts. An integration of the Paramics traffic simulation tool with two emission models, CMEM and MOVES, has been used to compare emissions produced at roundabouts and signal-

ized intersections [19]. The study shows higher emission rates for roundabouts under all traffic conditions. In contrary, Jackson and Rakha [37] showed that roundabouts outperform other types of intersections (i.e. stop-controlled and signalized intersections) in terms of produced emissions and fuel consumption. In this study, they used the VT-micro emission model along with INTEGRATION traffic simulation tool and developed multiple scenarios that varied in total demand and left turning ratios.

Coelho et al. [24] used a roundabout traffic simulation tool, aaSIDRA, and VSP-based emission rates to investigate emissions at roundabouts based on reproduced speed profiles by aaSIDRA. They showed that the difference between circulating speed and cruising speed is a key factor affecting emissions because a higher speed difference results in higher acceleration rates and consequently emission rates.

Most of the existing simulation models use continuous car following traffic models as the underlying model to predict traffic state and vehicles' operations. These models are defined by ordinary differential equations describing the complete dynamics of a vehicle's position and velocity. Although the high resolution of continuous CF models results in good representation of traffic operations, the existing CF-based models need high calibration efforts.

1.4.3 Cellular Automata Simulation Models

In 1992 a discrete traffic model, Cellular Automata (CA), was introduced by Nagel and Schreckenberg [55] for the simulation of freeway traffic. Like the continuous CF model, CA can reproduce traffic properties for the entire range of conditions (free flow to congested condition) with acceptable accuracy, but at a lower resolution, which can potentially save a significant amount of simulation time. The next sections present CA-based traffic simulation models and their applications in roundabout studies.

A cellular automaton consists of a grid of cells, each being in a state of a finite number of states. In traffic simulation, the road sections are divided into short cells with

a length that can hold one car (or the shortest particle considered in the simulation). Longer vehicles can fit into more than one cells depending on their length. Vehicles move in these cells based on certain rules, which are explained in more detailed in Section 3.1.

There are some packages that use cellular automata as their underlying traffic model. The Transportation Analysis and SIMulation System (TRANSIMS) is the most comprehensive package using CA. TRANSIMS was initially introduced at the Los Alamos National Laboratory, but is now available and further-developed as an open source project. TRANSIMS is an integrated set of tools mainly used to forecast travel demand at the individual user level. It also has a traffic microsimulator and an emission module, which estimates emissions based on the output from the microsimulator. The emission module was built to address the most common issues in the other emission models that used average speed and vehicle miles traveled to estimate emissions (before TRANSIMS the emission model used by the U.S. government was MOBILE6, which was a macroscopic model). The time step and cell length used in TRANSIMS are 1 sec and 7.5 m, respectively, which result in speed bins of 7.5 m/s. Since this is a rough representation of speed for emission estimation, the model generates smooth vehicle trajectories before estimating emissions. The TRANSIMS emission module is based on three sets of data: 1) CMEM data; 2) EPA three-cities data; and 3) California Air Resource Board (CARB) data. It is able to estimate tailpipe emissions for LDVs, HDVs, and evaporative emissions as a function of fleet composition, fleet status, and fleet dynamics.

A study was conducted by Jeihani et al. [38] aiming at comparing TRANSIMS with emission field measurements and emission estimations of CMEM, VT-Micro, and MOBILE6. They showed that the magnitude of TRANSIMS emission estimates is more consistent with the field measurements while VT-Micro emission trends fit better to the field data. They also showed that the magnitude and trend of TRANSIMS

fuel consumption estimates is not consistent with the real-world consumption [11]. TRANSIMS can be used for transportation planning on a regional-scale and not for a single intersection study outside of a road network context. In addition, the model has been calibrated and validated for flow dynamics at different types of intersections including signalized intersections and non-signalized cross intersections (i.e. stop sign, yield sign, and unprotected left turns) but not for roundabouts [10].

1.4.3.1 CA-based Studies on Roundabout Traffic Operations

After the introduction of CA models in traffic modeling, they have been used in several studies in this field including modeling of traffic at roundabouts [36, 79, 17]. There are some studies that compared the efficiency of single or multi-lane roundabouts and cross intersections (i.e. signalized and stop-controlled intersections) using CA traffic modeling [20]. Chimdessa et al. [20] compared the efficiency of a double-lane roundabout with a signalized intersection. This study suggests that although for very low traffic arrival rates the three kinds of intersections perform similarly in terms of throughput and queue length, when the arrival rate increases installing a signal improves these measures.

Matecki and Watrobski [53] used the CA model to simulate traffic on roundabout with the goal of evaluating the the effect of changing some traffic rules at a multi-lane roundabouts (without changing the structure of the site such as the number of lanes) on the capacity. Based on this research, at multi-lane roundabouts, the main cause of reduced capacity for high arrival rates is the jamming effect in the outer lane, which does not allow approaching traffic to enter the ring while inner lanes are moderately occupied. Therefore, changing traffic rules that lead to better distributed traffic between lanes can result in improved capacity. The study suggests that maximized capacity is achieved when vehicles can enter and exit the roundabout in parallel.

1.4.3.1.1 CA-based Studies on Gap Acceptance at Roundabouts

Some research used CA to study driver behavior with respect to gap acceptance [79, 17]. Wang and Ruskin [79] used a CA model to study the performance of roundabouts in three aspects: 1) overall throughput, 2) changes in queue length, delay, and vehicle density, and 3) the impact of drivers' choice of gap acceptance on throughput and the roundabout operation. They showed that the topology of the roundabout and turning rates are influencing factors on throughput, but the effect of roundabout size is not significant, and drivers' behavior has a significant impact on the operation of a roundabout.

Belz et al. [17] analyzed priority taking and priority abstaining behavior of drivers when entering a single-lane roundabout. This study suggested that a percentage of drivers (depending on the volume) always show priority taking behavior and do not comply with the accepted and safe critical gap. This behavior leads to capacity reduction, higher delay, and longer queue length at the roundabout due to the jamming effect it produces.

1.4.3.1.2 CA-based Studies on Safety at Roundabouts

Echab et al. [25] used CA to analyze the probability of entering/circulating car accidents at a single-lane roundabout with respect to CA model parameters. They also conducted another study [26] to evaluate vehicle/pedestrian interference at a single-lane roundabout and the effect of crosswalk location and driver's cooperative behavior on the dynamic characteristics of pedestrian and vehicle flux.

1.4.4 Summary of Studies on them Environmental Performance of Roundabouts

There are several studies on the environmental performance of roundabouts mostly conducted using field measurements and the existing CF-based microsimulation tools.

Some of these studies have compared the performance of roundabouts against signalized or stop-controlled intersections. In some cases the existing literature shows completely contradictory results regarding the emission impacts of roundabouts and other types of intersections. This fact implies that there is a need for more research in this area as well as site-specific calibration of the utilized models for simulation testing. However, the existing simulation tools need high calibration efforts. TRANSIMS is a comprehensive CA-based package, which also has an emission module, but it can be used for regional-scale studies and not for a single intersection.

Furthermore, the sensitivity of emission has been analyzed mainly with respect to traffic conditions and site topological characteristics of the roundabout. Only one study has considered the impact of pedestrian volumes on roundabout emission through field measurement.

1.5 Summary of Literature Review

The review of the literature shows that there are several studies on vehicular emissions at signalized intersections as well as signal control strategies with environmental concerns. However, only a few of theses studies consider both operational and environmental objectives at the same time. Most of the developed multi-objective signal control systems combine different performance measures related to traffic operations such as delay, stop rate, and queue length, and do not address vehicular emissions directly. Furthermore, multi-objective signal timing optimization systems that minimize emissions and operational measures simultaneously, either do not use modal estimation of emissions and use more aggregate estimations based on average speed or have been conducted through simulation models, which makes their real-time implementation cumbersome. In addition, the operational measures considered in the existing studies are usually capacity or vehicle delay and no study uses total person delay along with environmental objectives to optimize signal timings.

The environmental performance of roundabouts has also been evaluated in a number of studies. However, the results of these studies are not consistent and there should be more attention to vehicular emissions produced at roundabouts. Most of the studies have focused on the effect of car demand on emissions and there has been less attention to the pedestrian crossing impacts on vehicles' stops and emissions. In addition, the literature shows that most studies have been performed through field measurements or existing microsimulation packages. Field measurements require devices to monitor vehicle operations or measure tailpipe emissions or both. Such devices are expensive and not always accessible. Furthermore, the collection of a sample of vehicle trajectories and associated emissions with a sufficient size could be time consuming. Simulation studies also need extensive calibration efforts and in some cases the integration of an emission package with a traffic simulation tool is needed, which requires additional calibration effort.

The objective of this dissertation is two-fold; first, it develops two real-time signal control strategies that minimize the weighted combinations of emission with total vehicle delay and total person delay, respectively at the presence of buses at intersections. Then, the Pareto Frontier of the optimal solutions is presented. The results of the real-time signal control system can therefore, guide traffic engineers during the decision making process on the most suitable signal timing plan for a specific site based on priorities related to mobility vs. air quality. The used emission model within the signal timing optimization problem accounts for average modal emission rates during acceleration, deceleration, cruising, and idling. Secondly, the environmental performance of roundabouts has been evaluated and compared against signalized intersections through a CA-based simulation along with VSP-based modal emission estimation. The impact of total traffic demand, left turn ratios, and pedestrian volume on produced emissions is investigated.

CHAPTER 2

SIGNAL TIMING OPTIMIZATION TO REDUCE EMISSIONS AND DELAY

This research is motivated by the need for signal control strategies that combine environmental objectives along with operational ones. This chapter presents the development of a signal control system to improve mobility and air quality at isolated signalized intersections, which operate at undersaturated conditions. The improvement in mobility and air quality is achieved through minimizing weighted combinations of total vehicle delay (or person delay) and emission of auto and transit vehicles. The bi-objective signal control strategy is based on the mathematical models developed by Christofa et al. [22] and Khalighi and Christofa [39], which respectively minimize total person delay and emissions at signalized intersections.

The Pareto Frontier of optimal solutions, which demonstrates the trade-offs between total vehicle delay (or person delay) and emission is presented to help decision makers select the most appropriate signal control strategy based on their priorities, which are motivated by different policies (e.g. policies related to transit ridership improvement and emission standards). After the decision maker chooses the best linear combination of delay and emission for a specific site and time period (with the help of available Pareto Frontiers that are based on historical data), the signal control strategy can be implemented within real-time systems to account for real-time traffic and transit conditions.

This chapter is organized as follows: First, the general mathematical model to minimize a linear combination of delay and emissions is presented. Then, the models

used to estimate vehicle and person delay and emissions are described. Next,the calculation of average VSP-based emission rates for different vehicle operation modes is presented. Then, the final mathematical formulation and the method to solve the optimization problem is presented. The test site and performed experiments are described next and are followed by a discussion on the results. Finally, the summary of findings and future work are presented.

2.1 Mathematical Model

A mathematical formulation is developed to minimize a linear combination of total vehicle delay (or person delay) and emission of auto and transit vehicles at an undersaturated signalized intersection. The optimization problem is solved for several combinations of total delay and emissions using weights for the two terms in the objective function (i.e. in each optimization problem the weights are constant while they vary across different problems). The weight for each term varies from 0 to 1 and the sum of delay and emission weights is equal to 1 (i.e. when the weight of delay is zero, only emissions are minimized and vice versa). Decision variables are the signal's phases' duration that are optimized in each cycle. Furthermore, the optimization problem is constrained to constant cycle length, minimum and maximum green times for each phase (to ensure that no phase is skipped), and minimum green time for each lane group (to ensure undersaturated condition). Additional constraints are also defined in the reformulated mathematical program to address non-linearity issues, which are described later.

The signal control system operates as follows: Assuming fixed weights for delay and emission, λ_d and λ_e, the optimal green times are obtained to minimize the weighted combination of delay and emission for only auto vehicles. The signal control system operates on these signal timings as long as there is no transit at the intersection. When one or more transit vehicles in same or conflicting lane groups (i.e. lane

groups that are served by different phases) arrive at the intersection, that cycle is optimized based on the real-time information on transit arrival times and passenger occupancy along with fixed auto arrivals and passenger occupancy used for the entire period. Therefore, in the optimization of this specific cycle, both auto and transit vehicles are considered. Then, next cycles operate on the fixed, initially optimized signal timings, until the next transit vehicle arrives. The general formulation of the signal timing optimization problem is as follows:

$$Min \;\; \lambda_d \left[\sum_{j=1}^{J} \left(D_{j,T} + \hat{D}_{j,T+1} \right) + \sum_{b=1}^{b_{max}} d_{b,T} \right] + \lambda_e \left[\sum_{j=1}^{J} \left(E_{j,T} + \hat{E}_{j,T+1} \right) + \sum_{b=1}^{b_{max}} e_{b,T} \right] \tag{2.1}$$

s.t.

$$\sum_{i=1}^{I} g_{i,T} + \sum_{i=1}^{I} y_i = C \tag{2.2}$$

$$g_{i,T} \geq g_{i,min} \quad \forall i \in I \tag{2.3}$$

$$g_{i,T} \leq g_{i,max} \quad \forall i \in I \tag{2.4}$$

$$G_j^e(g_{i,T}) \geq \frac{q_j}{s_j} C \quad \forall j \in J \tag{2.5}$$

where:

λ_d: the weight of delay in the objective function,

λ_e: the weight of emission in the objective function,

$D_{j,T}$: total auto delay in cycle T,

$\hat{D}_{j,T+1}$: total auto delay in cycle $T+1$,

$E_{j,T}$: total auto emission in cycle T,

$\hat{E}_{j,T+1}$: total auto emission in cycle $T+1$,

$d_{b,T}$: delay of bus b,

$e_{b,T}$: emission of bus b,

b_{max}: number of buses considered in the optimization of cycle T,

C: cycle length,

$g_{i,min}/g_{i,max}$: minimum and maximum green times of phase i,

$g_{i,T}$: green time of phase i in cycle T,

y_i: yellow time of phase i,

q_j: arrival flow rate of lane group j,

s_j: saturation flow rate of lane group j,

I: number of phases, and

J: the number of lane groups at the intersection.

The mathematical formulation of the proposed signal timing optimization and models to estimate delay and emissions are based on three models developed by Christofa et al. [22], Shabihkhani and Gonzales [66], and Khalighi and Christofa [39]. Christofa et al. developed a mathematical model based on queuing theory to estimate and minimize person delay of auto and transit vehicles. Shabihkhani and Gonzales developed a model to estimate modal operation times and emissions of auto vehicles by accounting for deceleration/acceleration modes. Khalighi and Christofa developed a model to estimate and minimize modal emissions of auto and transit vehicles using VSP-based emission rates. The models developed by Shabihkhani and Gonzales [66] and Khalighi and Christofa [39] assume that each vehicle stop at the intersection is a full stop. In this dissertation, an integration of all the aforementioned models is used with some modifications to the emission models to account for partial vehicle stops, which happen when an existing queue of vehicles at the intersection is dissipating.

Figure 2.1 demonstrates a queuing diagram for undersaturated condition for a lane group j with constant auto arrival rate of q_j and saturation flow rate of s_j. In this example, the signal operates on six phases and phases 4 and 5 serve lane group j. As shown in the figure changing phase durations of cycle T affects delay and operation times of three groups of auto vehicles: 1) vehicles in the residual queue of cycle $T-1$,

which are served in cycle T; 2) vehicles that arrive in cycle T, either served in cycle T or cycle $T+1$; and 3) vehicles that arrive in cycle $T+1$ and are served in the same cycle. Therefore, in order to optimize phase durations in cycle T, delay and operation times of auto vehicles in both cycles T and $T+1$ are considered while the only decision variables are the phase durations of cycle T. Thus, the estimated delay and operation times of all vehicles considered in the optimization of cycle T are based on variable phase durations of cycle T and fixed phase durations of cycles $T-1$ and $T+1$. Furthermore, since information on transit vehicles is assumed to be known a cycle in advance, only transit vehicles that arrive or are served in cycle T are considered in the optimization of this cycle.

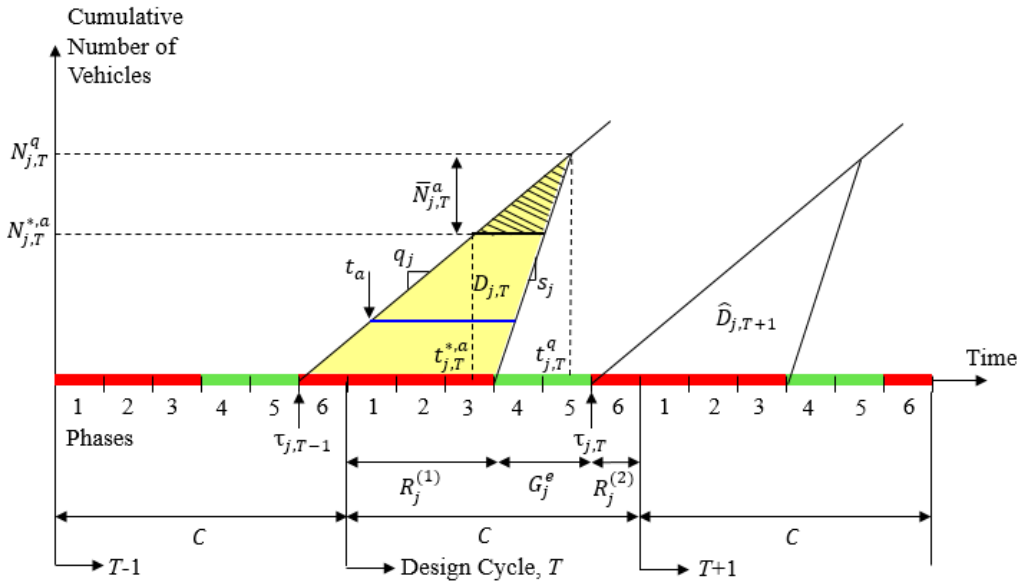

Figure 2.1: Queuing diagram of lane group j for auto arrivals at undersaturated traffic conditions

Assumptions made to estimate vehicle/person delay and emissions for a designed cycle T include:

- constant cruising speed and acceleration/deceleration rates,
- constant signal cycle length, phase sequence, and yellow times,

- deterministic vehicle arrival rates,
- fixed and known capacity for each approach, and
- known transit arrivals and passenger occupancy a cycle in advance,
- mixed-use lanes for autos and transit vehicles.

Three components that consist each cycle are $R_j^{(1)}$, $R_j^{(2)}$, and G_j^e shown in Figure 2.1 and are defined as functions of the cycle's green and yellow times as follows:

$$R_j^{(1)}\left(g_{i,T}\right) = \sum_{i=1}^{k_j-1} g_{i,T} + \sum_{i=1}^{k_j-1} y_i \tag{2.6}$$

$$G_j^e\left(g_{i,T}\right) = \sum_{i=k_j}^{l_j} g_{i,T} + \sum_{i=k_j}^{l_j-1} y_i \tag{2.7}$$

$$R_j^{(2)}\left(g_{i,T}\right) = \sum_{i=l_j+1}^{I} g_{i,T} + \sum_{i=l_j}^{I} y_i \tag{2.8}$$

Queues for lane group j in cycles $T-1$ and T start being formed at times $\tau_{j,T-1}$ and $\tau_{j,T}$, respectively, which are defined as follows:

$$\tau_{j,T-1} = (T-1)C - R_j^{(2)}(g_{i,T-1}) \tag{2.9}$$

$$\tau_{j,T} = TC - R_j^{(2)}(g_{i,T}) \tag{2.10}$$

where:

k_j: the first phase that serves lane group j, and

l_j: the last phase that serves lane group j.

The next two subsections present the estimation of delay and operation times of auto and transit vehicles.

2.1.1 Auto Vehicles

The person delay and operation times of all auto vehicles in a cycle are estimated collectively.

2.1.1.1 Auto Delay / Auto Person Delay

Auto delay and auto person delay are estimated based on queuing theory using the model developed by Christofa et al. [22]. The horizontal axis in a queuing diagram (Figure 2.1) represents time and the vertical axis represents the cumulative number of vehicles in a queue that is formed at the intersection due to red signal. In each cycle, T, auto vehicles arrive at the intersection at flow rate of their lane group, q_j, and if the signal is green they can pass through the intersection without stopping. Otherwise, they have to stop and they form a queue of length $N^q_{j,T}$. When the signal turns green, vehicles start leaving the intersection at a saturation flow rate of s_j. Therefore, the queue starts dissipating until it is cleared completely in the same cycle (assumption of undersaturated conditions) and vehicles arrive after that during the green time of lane group j pass the intersection without stopping. A similar process of queue formation and dissipation occurs in all cycles and lane groups.

For the estimation of delay, the time spent in deceleration/acceleration are not considered. It is assumed that when a vehicle arrives at the back of the queue, it stops instantaneously and when the queue in front of the vehicle is cleared, it instantly reaches cruising speed. Therefore, the delay of any individual vehicle spent in queue is equal to the time from the moment it arrives at the back of the queue until it leaves the intersection. Delay of a vehicle that arrives at t_a is shown by the blue horizontal line in Figure 2.1. Total delay of all $N^q_{j,T}$ auto vehicles that stop in cycle T is collectively estimated, which is equal to the area of the yellow triangle in cycle T, and is denoted by $D_{j,T}$. Total vehicle delay of lane group j in cycle $T+1$ is

estimated similarly and is denoted by $\hat{D}_{j,T+1}$. Total auto delay of all lane groups in cycles T and $T+1$ is calculated using equations (2.11) and (2.12), respectively.

$$\sum_{j=1}^{J} D_{j,T} = \sum_{j=1}^{J} \left[\frac{1}{2} \left(\frac{q_j}{1 - \frac{q_j}{s_j}} \right) \left(R_j^{(2)}(g_{i,T-1}) + R_j^{(1)}(g_{i,T}) \right)^2 \right] \tag{2.11}$$

$$\sum_{j=1}^{J} \hat{D}_{j,T+1} = \sum_{j=1}^{J} \left[\frac{1}{2} \left(\frac{q_j}{1 - \frac{q_j}{s_j}} \right) \left(R_j^{(2)}(g_{i,T}) + R_j^{(1)}(g_{inext}) \right)^2 \right] \tag{2.12}$$

where g_{inext} is the fixed duration of phase i in cycle $T+1$.

Total auto person delay in cycles T and $T+1$ is estimated by multiplying the average passenger occupancy assumed for an auto vehicle with the total auto delay. Total auto person delay across all lane groups for cycles T and $T+1$ is calculated by equations (2.13) and (2.14), respectively.

$$o_a \sum_{j=1}^{J} D_{j,T} = o_a \sum_{j=1}^{J} \left[\frac{1}{2} \left(\frac{q_j}{1 - \frac{q_j}{s_j}} \right) \left(R_j^{(2)}(g_{i,T-1}) + R_j^{(1)}(g_{i,T}) \right)^2 \right] \tag{2.13}$$

$$o_a \sum_{j=1}^{J} \hat{D}_{j,T+1} = o_a \sum_{j=1}^{J} \left[\frac{1}{2} \left(\frac{q_j}{1 - \frac{q_j}{s_j}} \right) \left(R_j^{(2)}(g_{i,T}) + R_j^{(1)}(g_{inext}) \right)^2 \right] \tag{2.14}$$

where o_a is the average passenger occupancy assumed for an auto vehicle.

2.1.1.2 Auto Operation Times

Auto vehicle operation times are estimated using the queuing diagram presented in Christofa et al. [22] along with assumptions made in Shabihkhani and Gonzales [66] to consider deceleration/acceleration times. In addition, some modifications are made to account for partial stops. Shabikhani and Gonzales [66] considered a trajectory for stopping vehicles that includes deceleration and acceleration modes rather than

assuming instantaneous vehicle stops. Figure 2.2a shows the time-space diagram of vehicles at an intersection assuming instantaneous stops and Figure 2.2b shows the magnified trajectory of a vehicle that has a full stop.

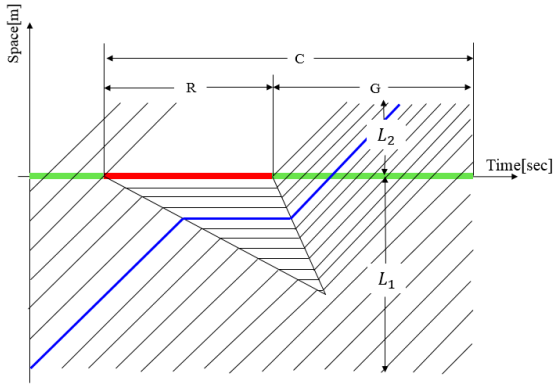

(a) Time-space diagram

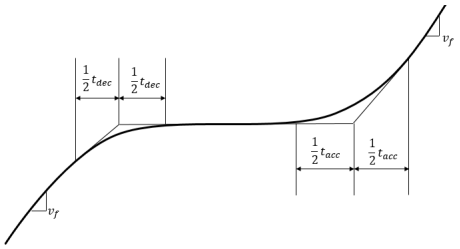

(b) A complete driving cycle of a vehicle that has a full stop

Figure 2.2: Schematic of vehicle trajectories used for estimating vehicle operation times

Shabihkhani and Gonzales [66] accounted for the acceleration mode by subtracting half of the time a vehicle needs to accelerate from a full stop to reach cruising speed from the time that the vehicle requires to travel the entire length considered upstream and downstream the intersection at cruising speed and the time that is initially considered being spent at a full stop (i.e. the length of the horizontal blue line in Figure 2.2a). The time spent in deceleration mode is accounted for similarly.

Figure 2.2b represents the driving cycle of vehicles that reach a full stop. However, vehicles that arrive at the very end of the time that the queue is being cleared do not reach a full stop; they only decelerate partially to reach the speed of queue movement. Then, they accelerate again while leaving the intersection. There are three groups of autos in terms of the amount of time they spent in idling:

- vehicles that arrive at the back of the queue and experience a complete stop. These vehicles spend some time in idling, which depends on their arrival time. This time interval is denoted by α_a ($\alpha_a = \{t_a | \tau_{j,T-1} \leq t_a < t^{*,a}_{j,T}\}$).

- vehicles that arrive at the back of the queue, but do not experience a complete stop. These vehicles do not spend any time in idling and have partial deceleration and acceleration while passing the intersection. This time interval is denoted by β_a ($\{\beta_a = t_a | t^{*,a}_{j,T} \leq t_a < t^{q}_{j,T}\}$).

- vehicles that arrive during the green time after the clearance of their lane group's queue. These vehicles pass the intersection without stopping and spend no time in idling. This time interval is denoted by γ_a ($\{\gamma_a = t_a | t^{q}_{j,T} \leq t_a < \tau_{j,T}\}$).

The last vehicle at the back of the queue in cycle T arrives at time $t^q_{j,T}$. The maximum length of queue in cycle T is denoted by $N^q_{j,T}$ and is calculated as follows:

$$N^q_{j,T} = \Big(\frac{q_j}{1 - \frac{q_j}{s_j}}\Big)\Big[R^{(2)}_j(g_{i,T-1}) + R^{(1)}_j(g_{i,T})\Big] \tag{2.15}$$

The last vehicle in queue that experiences a complete stop arrives at time $t^{*,a}_{j,T}$. Although this vehicle reaches a full stop, it does not spend any time idling because once it reaches a complete stop, the queue in front of it starts moving and the vehicle starts accelerating again. Therefore, the entire horizontal length corresponding to the arrival time of this vehicle, shown in Figure 2.1, is considered as half of deceleration and acceleration. The number of vehicles that arrive by $t^{*,a}_{j,T}$ is denoted by $N^{*,a}_{j,T}$ and is calculated by equation (2.16).

$$N^{*,a}_{j,T} = \Big(\frac{q_j}{1 - \frac{q_j}{s_j}}\Big)\Big[R^{(2)}_j(g_{i,T-1}) + R^{(1)}_j(g_{i,T}) - \big(\frac{v^a_f}{2\alpha^a_{acc}} + \frac{v^a_f}{2\alpha^a_{dec}}\big)\Big] \tag{2.16}$$

$t^{*,a}_{j,T}$ and $t^{q}_{j,T}$ are calculated by equations (2.17) and (2.18).

$$\begin{aligned} t^{*,a}_{j,T} &= \tau_{j,T-1} + \frac{N^{*,a}_{j,T}}{q_j} \\ &= (T-1)C - R^{(2)}(g_{i,T-1}) + \Big(\frac{1}{1-\frac{q_j}{s_j}}\Big)\Big[R^{(2)}_j(g_{i,T-1}) + R^{(1)}_j(g_{i,T}) - \big(\frac{v^a_f}{2\alpha^a_{acc}} + \frac{v^a_f}{2\alpha^a_{dec}}\big)\Big] \end{aligned} \tag{2.17}$$

$$t^{q}_{j,T} = \tau_{j,T-1} + \frac{N^{q}_{j,T}}{q_j} = (T-1)C - R^{(2)}(g_{i,T-1}) + \Big(\frac{1}{1-\frac{q_j}{s_j}}\Big)\Big[R^{(2)}_j(g_{i,T-1}) + R^{(1)}_j(g_{i,T})\Big] \tag{2.18}$$

where v^a_f, α^a_{acc}, and α^a_{dec} are respectively, free flow speed, acceleration rate, and deceleration rate of auto vehicles. The rest of this subsection presents the estimation of operation times for autos arriving in each of the three described time intervals in cycle T. The vehicle operation time in cycle $T+1$ can be calculated similarly.

2.1.1.2.1 Acceleration/Deceleration Time

Total auto acceleration/deceleration time of lane group j is equal to the sum of the times spent in these modes by all autos in each time interval arriving in that lane group.

$$T^a_{acc/dec,j,T} = t^{\alpha_a}_{acc/dec,j,T} + t^{\beta_a}_{acc/dec,j,T} + t^{\gamma_a}_{acc/dec,j,T} \tag{2.19}$$

where $T^a_{acc/dec,j,T}$ is the total acceleration/deceleration time of all autos of lane group j in cycle T and $t^{\alpha_a}_{acc/dec,j,T}$, $t^{\beta_a}_{acc/dec,j,T}$, and $t^{\gamma_a}_{acc/dec,j,T}$ are the total acceleration/deceleration time of autos in lane group j that arrive in time intervals α_a, β_a, and γ_a of cycle T, respectively.

Each auto in time interval α_a experiences a complete acceleration/deceleration cycle. Therefore, the total acceleration/deceleration time of vehicles in this time

interval for lane group j is estimated collectively for all autos in that lane group by equation 2.20.

$$t^{\alpha_a}_{acc/dec,j,T} = N^{*,a}_{j,T} . \frac{v^a_f}{\alpha^a_{acc/dec}} \tag{2.20}$$

Vehicles arriving in time interval β_a have a partial deceleration and acceleration while passing the intersection. The acceleration/deceleration time of an auto in this interval depends on its arrival time at the back of the queue. However, it is not necessary to know the acceleration/deceleration time of individual vehicles. Instead, the aggregate time spent in these modes by all autos is estimated. The first vehicle belonging to interval β_a arrives at $t^{*,a}_{j,T}$. Autos arriving after $t^{*,a}_{j,T}$ do not spend any time idling. Therefore, the whole area of the dashed triangle in Figure 2.1 is considered as half of acceleration/deceleration time of vehicles in interval β_a. Therefore, half of the sum of the acceleration and deceleration times of autos that arrive after $t^{*,a}_{j,T}$ is equal to the area of the dashed triangle in Figure 2.1. However, this area is not split equally between acceleration and deceleration time. It is split based on acceleration/deceleration rates since those define the time spent accelerating/decelerating. The time allocated to acceleration/deceleration has an inverse linear relationship with the corresponding rates (i.e., the higher the acceleration/deceleration is, the shorter the time spent in this mode is).

$$t^{\beta_a}_{acc,j,T} = \frac{\alpha^a_{dec}}{\alpha^a_{acc} + \alpha^a_{dec}} \Big(\frac{q_j}{1 - \frac{q_j}{s_j}} \Big) \Big(\frac{v^a_f}{2\alpha^a_{acc}} + \frac{v^a_f}{2\alpha^a_{dec}} \Big)^2 \tag{2.21}$$

$$t^{\beta_a}_{dec,j,T} = \frac{\alpha^a_{acc}}{\alpha^a_{acc} + \alpha^a_{dec}} \Big(\frac{q_j}{1 - \frac{q_j}{s_j}} \Big) \Big(\frac{v^a_f}{2\alpha^a_{acc}} + \frac{v^a_f}{2\alpha^a_{dec}} \Big)^2 \tag{2.22}$$

Vehicles in interval γ_a pass the intersection at cruising speed without stopping and their acceleration/deceleration time is equal to zero.

$$t^{\gamma_a}_{acc/dec,j,T} = 0 \tag{2.23}$$

2.1.1.2.2 Idling Time

The total idling time of all autos in lane group j is equal to the sum of the idling time of vehicles in each time interval in that lane group:

$$T^a_{id,j,T} = t^{\alpha_a}_{id,j,T} + t^{\beta_a}_{id,j,T} + t^{\gamma_a}_{id,j,T} \tag{2.24}$$

where $T^a_{id,j,T}$ is the total idling time of autos in cycle T and $t^{\alpha_a}_{id,j,T}$, $t^{\beta_a}_{id,j,T}$, and $t^{\gamma_a}_{id,j,T}$ are respectively the idling time of autos in intervals α_a, β_a, and γ_a of lane group j in cycle T. The aggregate idling times of the three time intervals are calculated by equations (2.25) and (2.26).

$$t^{\alpha_a}_{id,j,T} = \frac{1}{2} N^{*,a}_{j,T} \left(R^{(2)}_j(g_{i,T-1}) + R^{(1)}_j(g_{i,T}) - \frac{v^a_f}{2\alpha^a_{acc}} - \frac{v^a_f}{2\alpha^a_{dec}} \right) \tag{2.25}$$

The first part of the above equation is the delay of all autos of lane group j in cycle T, which arrive in time interval α_a and the second part is half of the total acceleration/deceleration time of these vehicles, which should be subtracted from the total delay as described earlier.

Vehicles, which arrive in intervals β_a and γ_a do not spent any time idling.

$$t^{\beta_a}_{id,j,T} = t^{\gamma_a}_{id,j,T} = 0 \tag{2.26}$$

2.1.1.2.3 Cruising Time

Total auto cruising time in lane group j is the sum of the cruising times of autos arriving in each time interval in that lane group.

$$T^a_{cr,j,T} = t^{\alpha_a}_{cr,j,T} + t^{\beta_a}_{cr,j,T} + t^{\gamma_a}_{cr,j,T} \tag{2.27}$$

where $T^{a}_{cr,j,T}$ is the total cruising time of auto vehicles in cycle T and $t^{\alpha_a}_{cr,j,T}$, $t^{\beta_a}_{cr,j,T}$, and $t^{\gamma_a}_{cr,j,T}$ are respectively the cruising time of vehicles in intervals α_a, β_a, and γ_a.

To estimate the cruising time certain lengths upstream and downstream of the intersection (length L_1 and L_2 in figure 2.2a) are considered to ensure that vehicles that stop at the intersection experience a complete driving cycle (i.e., deceleration, idling, acceleration, and cruising). The lengths L_1 and L_2 considered in this study are respectively 150 m and 80 m. The sum of these lengths minus the length that is traveled in acceleration/deceleration is considered to be traveled at cruising speed. Equations (2.28) to (2.31) calculate the cruising times for vehicles that arrive in each interval.

The cruising time of any vehicle arriving in interval α_a is the time needed to travel lengths L_1 and L_2 at cruising minus half of the time for a complete deceleration/acceleration. Total cruising time of autos in this interval is estimated as follows:

$$t^{\alpha_a}_{cr,j,T} = N^{*,a}_{j,T}\left(\frac{L_1+L_2}{v^a_f} - \frac{v^a_f}{2\alpha^a_{acc}} - \frac{v^a_f}{2\alpha^a_{dec}}\right) \tag{2.28}$$

Total cruising time of auto vehicles in time interval β_a is estimated using equation 2.30. The second term in equation (2.30) is half of the aggregate deceleration/acceleration time calculated by equations 2.21 and 2.22 and $\bar{N}^{a}_{j,T}$ is the number of autos arriving in this interval and calculated by equation (2.29).

$$\bar{N}_{j,T} = N^{q}_{j,T} - N^{*,a}_{j,T} \tag{2.29}$$

$$t^{\beta_a}_{cr,j,T} = \bar{N}^{a}_{j,T}\left(\frac{L_1+L_2}{v^a_f}\right) - \frac{t^{\beta,a}_{acc,j,T} + t^{\beta,a}_{dec,j,T}}{2} \tag{2.30}$$

Autos that arrive in interval γ_a travel the entire L_1 and L_2 lengths at cruising speed without stopping. Total cruising time of these vehicles is estimated by equation 2.31 where the second term represents the number of autos that arrive in this time interval.

$$t_{cr,j,T}^{\gamma_a} = \big(\frac{L_1 + L_2}{v_f^a}\big)\big(q_j C - N_{j,T}^q\big) \tag{2.31}$$

2.1.1.3 Auto Part of the Objective Function

The auto part of the objective function consists of the sum of the total vehicle delay (or person delay) and emissions for auto vehicles in cycles T and $T+1$. Equation 2.32 shows the linear combination of auto person delay and emissions in the objective function.

$$\sum_{j=1}^{J}\Bigg[\lambda_d o_a\Big[D_{j,T} + D_{j,T+1}\Big] + \lambda_e\Big[e_{acc}^a\big(T_{acc,T}^a + T_{acc,T+1}^a\big) + e_{dec}^a\big(T_{dec,T}^a + T_{dec,T+1}^a\big) + e_{id}^a\big(T_{id,T}^a + T_{id,T+1}^a\big) + e_{cr}^a\big(T_{cr,T}^a + T_{cr,T+1}^a\big)\Big]\Bigg] \tag{2.32}$$

where e_a^m is the emission rate of an auto vehicle in mode m where $m \in \{acc, dec, id, cr\}$.

2.1.2 Transit Vehicles

Similar to autos, a transit vehicle's delay and operation times depend on its arrival time during the cycle. However, the delay and operation times should be estimated for each individual transit vehicle and cannot be estimated collectively. There are four cases in terms of transit arrival times for transit vehicles that belong to a lane group j:

- transit vehicles that are served in cycle T and experience a complete stop. The time interval corresponding to the arrival time of these vehicles is denoted as α_b:

$$\alpha_b = \{t_b | t_b \leq t_{j,T}^{*,b}\} \tag{2.33}$$

- transit vehicles that are served in cycle T and experience a partial stop. The time interval corresponding to the arrival time of these vehicles is denoted as β_b:

$$\beta_b = \{t_b | t^{*,b}_{j,T} < t_b \leq t^q_{j,T}\} \tag{2.34}$$

- transit vehicles that are served in cycle T and pass the intersection without stopping. The time interval corresponding to the arrival time of these vehicles is denoted as γ_b:

$$\gamma_b = \{t_b | t^q_{j,T} < t_b \leq \tau_{j,T}\} \tag{2.35}$$

- transit vehicles that arrive in cycle T, but are served in cycle $T+1$. The time interval corresponding to the arrival time of these vehicles is denoted as δ_b:

$$\delta_b = \{t_b | t_b > \tau_{j,T}\} \tag{2.36}$$

where t_b is the arrival time of the transit vehicle b and $t^{*,b}_{j,T}$ is the arrival time of the last transit vehicle in cycle T and lane group j that experiences a complete stop. $t^{*,b}_{j,T}$ is calculated as follows:

$$t^{*,b}_{j,T} = (T-1)C - R^{(2)}(g_{i,T-1}) + \Big(\frac{1}{1-\frac{q_j}{s_j}}\Big)\Big[R^{(2)}_j(g_{i,T-1}) + R^{(1)}_j(g_{i,T}) - \big(\frac{v^b_f}{2\alpha^b_{acc}} + \frac{v^b_f}{2\alpha^b_{dec}}\big)\Big] \tag{2.37}$$

where v^b_f, α^b_{dec}, and α^b_{acc} are cruising speed, deceleration rate, and acceleration rate of transit vehicles, respectively. Figure 2.3 shows the queuing diagram of lane group j and the times mentioned above, which determine the case a transit vehicle falls into. Next two subsections present the estimation of transit delay (or person delay) and operation times.

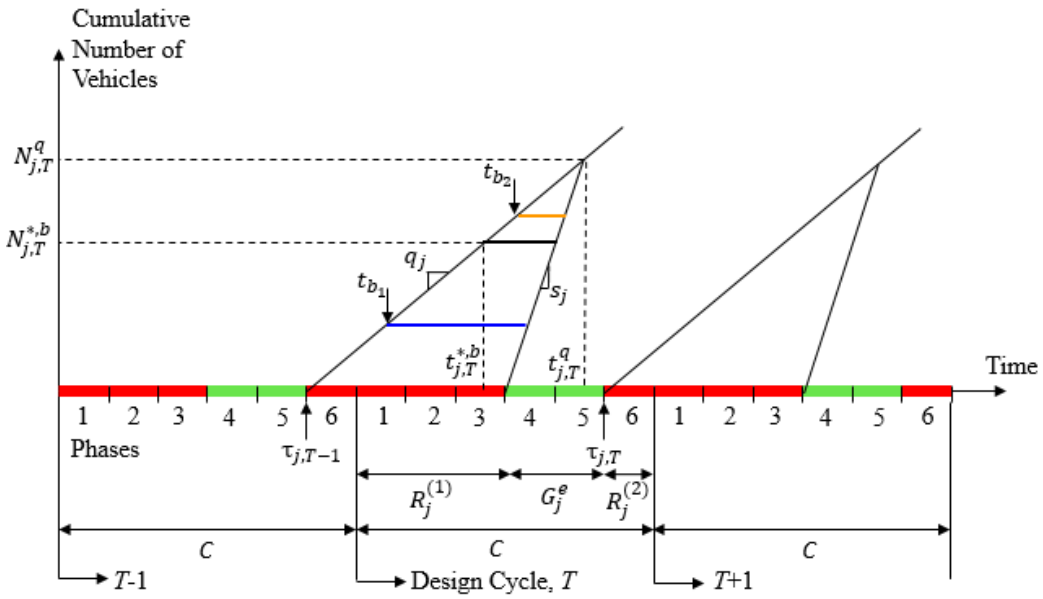

Figure 2.3: Queuing diagram of lane group j for transit arrivals at undersaturated traffic conditions

2.1.2.1 Transit Delay / Person Delay

Similar to autos, the delay of transit vehicles depends on their arrival time at the back of the queue and is calculated by equations (2.38) to (2.40) for transit vehicles of the four described cases.

Delay of a transit vehicle arriving in time intervals α_b and β_b is the same and is estimated by Equation (2.38).

$$d_{b,T}^{\alpha_b} = d_{b,T}^{\beta_b} = \left[(T-1)C + R_j^{(1)}(g_{i,T}) + \frac{q_j}{s_j}(t_b - \tau_{j,T-1}) - t_b\right] \tag{2.38}$$

Any transit vehicle that arrives in time interval γ_b passes the intersection without stopping and its delay is equal to zero.

$$d_{b,T}^{\gamma_b} = 0 \tag{2.39}$$

Any transit vehicle that arrives after the green time in cycle T is served in the next cycle and its delay is estimated by equation (2.40).

$$d_{b,T}^{\delta_b} = \left[TC + R_j^{(1)}(g_{inext}) + \frac{q_j}{s_j}(t_b - \tau_{j,T}) - t_b\right] \tag{2.40}$$

The person delay of a transit vehicle is calculated by multiplying the delay of the vehicle by the average transit passenger occupancy, o_b.

2.1.2.2 Transit Vehicle Operation Times

This subsection presents the estimation of transit vehicle operation times for each of the four cases described earlier.

2.1.2.2.1 Acceleration/Deceleration Time

A transit vehicle that arrives during time intervals α_b and δ_b experiences a complete acceleration and deceleration cycle. Therefore, its deceleration time is equal to the time it needs to reach a complete stop from a cruising speed and its acceleration time is equal to the time it needs to reach the cruising speed from a complete stop and is calculated as follows:

$$t_{b,acc/dec}^{\alpha_b} = t_{b,acc/dec}^{\delta_b} = \frac{v_f^b}{\alpha_{acc/dec}^b} \tag{2.41}$$

A transit vehicle that arrives in time interval β_b experiences a partial stop. Therefore, the total length of the orange line shown in Figure 2.3 is considered as half of the sum of acceleration/deceleration times and is split between them based on the acceleration/deceleration rates as was the case for autos.

$$t_{b,acc/dec}^{\beta_b} = 2\left[\frac{\alpha_{dec/acc}^b}{\alpha_{acc}^b + \alpha_{dec}^b}\Big((T-1)C + R_j^{(1)}(g_{i,T}) + \frac{q_j}{s_j}(t_b - \tau_{j,T-1}) - t_b\Big)\right] \tag{2.42}$$

Finally, a transit vehicle that arrives in time interval γ_b passes the intersection without stopping and its acceleration/deceleration time is zero.

$$t_{b,acc/dec}^{\gamma_b} = 0. \tag{2.43}$$

2.1.2.2.2 Idling Time

The idling time of a transit vehicle that arrives in intervals α_b and δ_b is equal to the length of the horizontal line, which corresponds to its arrival time (i.e. horizontal lines correspond to t_{b_1} and t_{b_2} as shown in Figure 2.3) minus half of the time needed for a complete acceleration/deceleration mode. A transit vehicle that arrives in case β_b has only a partial stop and its idling time is zero. Finally, any transit vehicle that arrives in case γ_b passes the intersection without stopping and its idling time is zero. The idling time of a transit vehicle in each of the four cases is calculated by equations (2.44) to (2.46).

$$t_{b,id}^{\alpha_b} = (T-1)C + R_j^{(1)}(g_{i,T}) + \frac{q_j}{s_j}(t_b - \tau_{j,T-1}) - t_b - \big(\frac{v_f^b}{2\alpha_{acc}^b} + \frac{v_f^b}{2\alpha_{dec}^b}\big) \tag{2.44}$$

$$t_{b,id}^{\beta_b} = t_{b,id}^{\gamma_b} = 0 \tag{2.45}$$

$$t_{b,id}^{\delta_b} = TC + R_j^{(1)}(g_{inext}) + \frac{q_j}{s_j}(t_b - \tau_{j,T}) - t_b - \big(\frac{t_{b,acc}^{\delta_b} + t_{b,dec}^{\delta_b}}{2}\big) \tag{2.46}$$

2.1.2.2.3 Cruising Time

The cruising time of a transit vehicle that arrives in any of the four time intervals is estimated by subtracting half of the acceleration/deceleration times from the time

needed by a transit vehicle to pass the considered lengths L_1 and L_2 at cruising speed. Equations (2.47) to (2.49) are used to estimate transit cruising times.

$$t_{b,cr}^{\alpha_b} = t_{b,cr}^{\delta_b} = \frac{L_1 + L_2}{v_f^b} - \left(\frac{v_f^b}{2\alpha_{acc}^b} + \frac{v_f^b}{2\alpha_{dec}^b}\right) \tag{2.47}$$

$$t_{b,cr}^{\beta_b} = \frac{L_1 + L_2}{v_f^b} - \frac{t_{b,acc}^{\beta_b} + t_{b,dec}^{\beta_b}}{2} \tag{2.48}$$

$$t_{b,cr}^{\gamma_b} = \frac{L_1 + L_2}{v_f^b} \tag{2.49}$$

2.1.2.3 Transit Part of the Objective Function

To add up the delay (or person delay) and emission of transit vehicles in the objective function, four binary variables are defined for each transit vehicle. The binary variables are denoted by ω_b^k, where $k \in \{\alpha_b, \beta_b, \gamma_b, \delta_b\}$. If a transit vehicle arrives in time interval k, ω_b^k will be one. Otherwise, ω_b^k will be zero. The transit part of the objective function when minimizing a combination of person delay and emission is as follows:

$$\sum_{b=1}^{b_{max}} \sum_{k\in\{\alpha_b,\beta_b,\gamma_b,\delta_b\}} \Bigg[\lambda_d o_b d_b^k + \lambda_e \Big[e_{acc}^b(\omega_b^k.t_{b,acc}^k) + e_{dec}^b(\omega_b^k.t_{b,dec}^k) + e_{id}^b(\omega_b^k.t_{b,id}^k) + e_{cr}^b(\omega_b^k.t_{b,cr}^k)\Big]\Bigg]$$

where:

e_m^b: emission rate of transit vehicle b in mode m where $m \in \{acc, dec, id, cr\}$ [gr/sec].

2.1.3 Mathematical Program Formulation

Now that vehicle delay and operation time are estimated, the optimization problem can be rewritten as follows with the additional constraints for each transit vehicle to determine the time interval it falls into.

$$Min \quad \sum_{j=1}^{J}\left[\lambda_d o_a\left[D_{j,T}+\hat{D}_{j,T+1}\right]+\lambda_e\left[e^a_{acc}(T^a_{acc,T}+T^a_{acc,T+1})+\right.\right.$$
$$\left.\left.e^a_{dec}(T^a_{dec,T}+T^a_{dec,T+1})+e^a_{id}(T^a_{id,T}+T^a_{id,T+1})+e^a_{cr}(T^a_{cr,T}+T^a_{cr,T+1})\right]\right]+$$
$$\sum_{b=1}^{b_{max}}\sum_{k\in\{\alpha_b,\beta_b,\gamma_b,\delta_b\}}\left[\lambda_d o_b\omega^k_b d^k_b+\lambda_e\left[e^b_{acc}(\omega^k_b.t^k_{b,acc})+e^b_{dec}(\omega^k_b.t^k_{b,dec})+e^b_{id}(\omega^k_b.t^k_{b,id})+e^b_{cr}(\omega^k_b.t^k_{b,cr})\right]\right] \tag{2.50}$$

Constrained to:

$$\sum_{i=1}^{I} g_{i,T}+\sum_{i=1}^{I} y_i = C \tag{2.51}$$

$$g_{i,T} \geq g_{i,min} \tag{2.52}$$

$$g_{i,T} \leq g_{i,max} \tag{2.53}$$

$$G^e_j(g_{i,T}) \geq \frac{q_j}{s_j}C \quad \forall j \tag{2.54}$$

$$t^{\alpha_b}_{b,id} \geq -(1-\omega^{\alpha_b}_b)M_1 \tag{2.55}$$

$$t^{\alpha_b}_{b,id} \leq \omega^{\alpha_b}_b M_1 \tag{2.56}$$

$$d^{\alpha_b}_b \geq -(1-\omega^{\alpha_b}_b-\omega^{\beta_b}_b)M_2 \tag{2.57}$$

$$d^{\alpha_b}_b \leq (\omega^{\alpha_b}_b+\omega^{\beta_b}_b)M_2 \tag{2.58}$$

$$(1-\omega_b^{\delta_b})t_b \leq \tau_{j,T} \tag{2.59}$$

$$(1-\omega_b^{\delta_b})M_3 + \omega_b^{\delta_b}t_b \geq \tau_{j,T} \tag{2.60}$$

$$\omega_b^{\alpha_b} + \omega_b^{\beta_b} + \omega_b^{\gamma_b} + \omega_b^{\delta_b} = 1 \tag{2.61}$$

$$\omega_b^{\alpha_b},\ \omega_b^{\beta_b},\ \omega_b^{\gamma_b},\ \omega_b^{\sigma_b} \in \{0,1\} \tag{2.62}$$

where M_1, M_2, and M_3 are large values. This optimization problem is a Mixed Integer Non-Linear Program (MINLP) since it has both continuous, $g_{i,T}$, and integer variables, ω_b^k. In addition, the objective function has bilinearities due to the multiplication of continuous and integer variables. To deal with bilinearities the method developed by Floudas [27] and used by Christofa et al. [22] is used.

Four continuous variables, $g_{i,b}^{\alpha_b}$, $g_{i,b}^{\beta_b}$, $g_{i,b}^{\gamma_b}$, and $g_{i,b}^{\delta_b}$ are introduced for each phase and each transit vehicle. The original continuous variables are redefined based on the new continuous variables as follows:

$$g_{i,T} = g_{i,b}^{\alpha_b} + g_{i,b}^{\beta_b} + g_{i,b}^{\gamma_b} + g_{i,b}^{\delta_b} \tag{2.63}$$

where:

$$g_{i,b}^{\beta_b} = g_{i,b}^{\gamma_b} = g_{i,b}^{\delta_b} = 0 \qquad if\ t_b \in \alpha_b, \tag{2.64}$$

$$g_{i,b}^{\alpha_b} = g_{i,b}^{\gamma_b} = g_{i,b}^{\delta_b} = 0 \qquad if\ t_b \in \beta_b, \tag{2.65}$$

$$g_{i,b}^{\alpha_b} = g_{i,b}^{\beta_b} = g_{i,b}^{\delta_b} = 0 \qquad if\ t_b \in \gamma_b, \tag{2.66}$$

$$g_{i,b}^{\alpha_b} = g_{i,b}^{\beta_b} = g_{i,b}^{\gamma_b} = 0 \qquad if\ t_b \in \delta_b. \tag{2.67}$$

Now each term in the transit part of the objective function, which consists of a multiplication of an integer variable and a term that is a function of continuous

variables can be rewritten using the new continuous variables. For example, the transit person delay term is rewritten as follows:

$$\sum_{b=1}^{bmax} o_b\Big[\omega_b^{\alpha_b} d_b^{\alpha_b} + \omega_b^{\beta_b} d_b^{\beta_b} + \omega_b^{\gamma_b} d_b^{\gamma_b} + \omega_b^{\delta_b} d_b^{\delta_b}\Big] =$$

$$o_b\Bigg[(\omega_b^{\alpha_b} + \omega_b^{\beta_b})\left((T-1)C + \sum_{i=1}^{k_j-1} y_i + \frac{q_j}{s_j}(t_b - \tau_{j,T-1}) - t_b\right) + \omega_b^{\gamma_b}\left(TC + R_j^{(1)}(g_{i,next}) + \right.$$

$$\left.\frac{q_j}{s_j}\left(t_b - (T-1)C - \sum_{i=1}^{l_j-1} y_i\right) - t_b\right) + \sum_{i=1}^{k_j-1}(g_{i,b}^{\alpha_b} + g_{i,b}^{\beta_b}) - \frac{q_j}{s_j}\sum_{i=1}^{l_j} g_{i,b}^{\gamma_b}\Bigg] \quad (2.68)$$

Equation (2.68) does not have any bilinearity. Similarly, the bilinearities in all terms of the initial objective function (equations 2.50) can be resolved. Constraints (2.52) and (2.53) should also be replaced by the following constraints:

$$g_{i,b}^k \geq \omega_b^k g_{i,min} \qquad \forall i, \forall k \in \{\alpha_b, \beta_b, \gamma_b, \delta_b\} \quad (2.69)$$

$$g_{i,b}^k \leq \omega_b^k g_{i,max} \qquad \forall i, \forall k \in \{\alpha_b, \beta_b, \gamma_b, \delta_b\} \quad (2.70)$$

2.2 Modal Emission Rates Estimation

The modal emission rates are estimated in Khalighi and Christofa [39] using Vehicle specific Power (VSP) approach and second-by-second rates presented in Frey et al. [28] and Zhai et al. [86] for gasoline cars and diesel buses, respectively. The VSP-based emission rates of CO and NO_x for second-by-second estimation of VSP values are presented in Figure 2.4 and 2.5 for gasoline cars and diesel buses. Carbon monoxide (CO) has detrimental effects on human health because it interferes with oxygen absorption by red blood cells. A primary source of CO emissions are gasoline cars. Although, new vehicle technologies and emission standards have led to significant improvements of CO emissions, there is still high CO concentration in areas with heavy

traffic congestion. Nitrogen oxides (NO_x) cause the irritation of airways, especially lungs. They also help the formation of smog components such as ground-level ozone. Diesel buses are the primary source of NO_x emission in some urban areas. In this study, we consider these two pollutants to see how different emission rates of cars and buses affect the performance of the proposed signal control system.

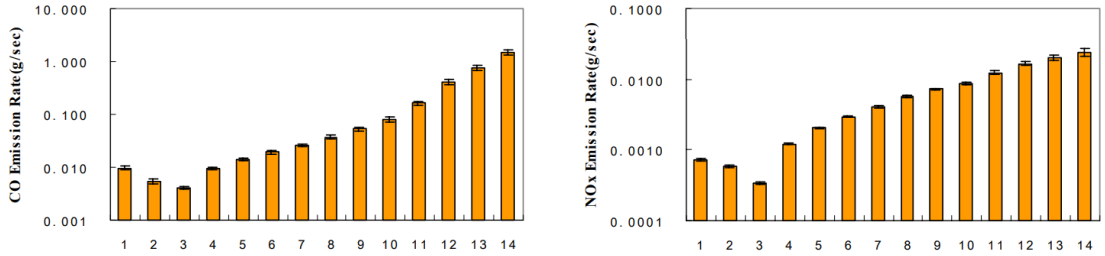

(a) (b)

Figure 2.4: Average modal emission rates of gasoline-fueled auto vehicles for 14 VSP bins for CO and NO_x [29]

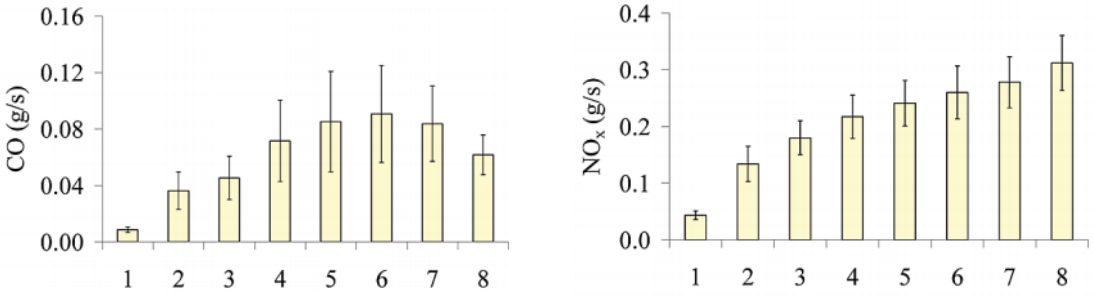

(a) (b)

Figure 2.5: Average modal emission rates of diesel-fueled transit vehicles for 8 VSP bins for CO and NO_x [86]

The detailed calculation of modal emission rates (i.e. acceleration, deceleration, cruising, and idling modes) is performed as follows:

First, the VSP value for each operation mode is calculated as a function of average speed, acceleration rate, and link's grade, which is assumed to be zero for this study.

Then, based on the calculated VSP, the associated VSP bin and the average emission rates of that bin are determined. To estimate emission rates more accurately, second by second VSP values and the resulted emission rates are estimated for the entire acceleration/deceleration time. Then, the average of the obtained rates are used for each mode. The assumptions to calculate VSP values for gasoline cars and diesel buses are as follows:

$v_f^a = 45\frac{km}{hr} = 12.5\frac{m}{s}$ $\quad$ $v_f^b = 45\frac{km}{hr} = 12.5\frac{m}{s}$

$\alpha_{acc}^a = 3\frac{m}{s^2}$ $\quad$ $\alpha_{acc}^b = 2\frac{m}{s^2}$

$\alpha_{dec}^a = 4\frac{m}{s^2}$ $\quad$ $\alpha_{dec}^b = 2\frac{m}{s^2}$

Tables 2.1 to 2.4 show second-by-second emission rates for acceleration and deceleration modes for gasoline and diesel buses. The final emission rate for each mode (i.e. acceleration and deceleration) is the average of the rates presented in each table. Second-by-second emission rates of idling and cruising modes are assumed to be constant during the entire time spent in these modes. Tables 2.5 and 2.6 present the calculated emission rates for each operation mode (i.e. acceleration, deceleration, idling, and cruising) for auto and transit vehicles, respectively.

Table 2.1: Calculation of average emission rates for gasoline cars for acceleration [40]

Time [*sec*]	Speed [m/s]	Average Speed [m/s]	VSP [kw/ton]	VSP mode	NO_x [mg/s]	CO [mg/s]
$[0-1]$	$[0-3]$	1.5	5.15	5	1.7	11.0
$[1-2]$	$[3-6]$	4.5	15.47	8	4.2	29.2
$[2-3]$	$[6-9]$	7.5	25.77	11	7.6	113.8
$[3-4]$	$[9-12]$	10.5	36.39	13	15.5	441.8
$[4-4.17]$	[12.12.5]	12.25	42.60	14	17.9	882.3
Average					7.7	178.3

Table 2.2: Calculation of average emission rates for gasoline cars for deceleration [40]

Time [*sec*]	Speed [m/s]	Avg Speed [m/s]	VSP [kw/ton]	VSP mode	NO_x [mg/s]	CO [mg/s]
$[0-1]$	$[12.5-8.5]$	10.5	-44.46	1	0.9	7.8
$[1-2]$	$[8.5-4.5]$	6.5	-27.66	1	0.9	7.8
$[2-3]$	$[4.5-0.5]$	2.5	-10.67	1	0.9	7.8
$[3-3.13]$	$[0.5-0]$	0.25	-1.07	2	0.6	3.9
Average					0.9	7.6

Table 2.3: Calculation of average emission rates for diesel buses for acceleration [40]

Time [*sec*]	Speed [m/s]	Avg Speed [m/s]	VSP [kw/ton]	VSP mode	NO_x [mg/s]	CO [mg/s]
$[0-1]$	$[0-2]$	1.00	2.09	2	133	35.0
$[1-2]$	$[2-4]$	3.00	6.28	4	220	73.0
$[2-3]$	$[4-6]$	5.00	10.49	6	255	95.0
$[3-4]$	$[6-8]$	7.00	14.72	8	320	60.0
$[4-5]$	$[8-10]$	9.00	18.98	8	320	60.0
$[5-6]$	$[10-12]$	11.00	23.29	8	320	60.0
$[6-6.25]$	$[12-12.5]$	12.25	26.01	8	320	60.0
Average					263.6	63.6

Table 2.4: Calculation of average emission rates for diesel buses for deceleration [40]

Time [*sec*]	Speed [m/s]	Avg Speed [m/s]	VSP [kw/ton]	VSP mode	NO_x [mg/s]	CO [mg/s]
$[0-1]$	$[12.5-10.5]$	11.5	-21.62	1	45.0	8.6
$[1-2]$	$[10.5-8.5]$	9.5	-17.95	1	45.0	8.6
$[2-3]$	$[8.5-6.5]$	7.5	-14.22	1	45.0	8.6
$[3-4]$	$[6.5-4.5]$	5.5	-10.45	1	45.0	8.6
$[4-5]$	$[4.5-2.5]$	3.5	-6.67	1	45.0	8.6
$[5-6]$	$[2.5-0.5]$	1.5	-2.86	1	45.0	8.6
$[6-6.25]$	$[0.5-0]$	0.25	-0.48	1	45.0	8.6
Average					45.0	8.6

Table 2.5: Modal emission rates for gasoline cars [40]

operating mode	NO_x [mg/s]	CO [mg/s]
Acceleration	7.7	178.3
Deceleration	0.9	7.6
Cruising	1.2	8.3
Idling	0.3	3.3

Table 2.6: Modal emission rates for diesel buses [40]

operating mode	NO_x[mg/s]	CO[mg/s]
Acceleration	263.5	63.6
Deceleration	45.0	8.6
Cruising	133.3	37.1
Idling	45.0	8.6

2.3 Test Site

To evaluate the performance of the proposed signal control system, real-world data of the intersection of Mesogion and Katechaki Avenues in Athens, Greece is used. This intersection serves 9 conflicting transit routes and transit vehicles travel in the same lanes as general traffic. The signal operates on a 6-phase cycle and its flow ratio during morning peak hour is $Y = 0.9$, which is close to saturation considering the cycle length of $C = 120$ seconds and lost time of $L = 14$ seconds. Figure 2.6 illustrates the intersection's layout and bus routes that travel through the intersection and figure 2.7 shows the phasing setting of the traffic signal.

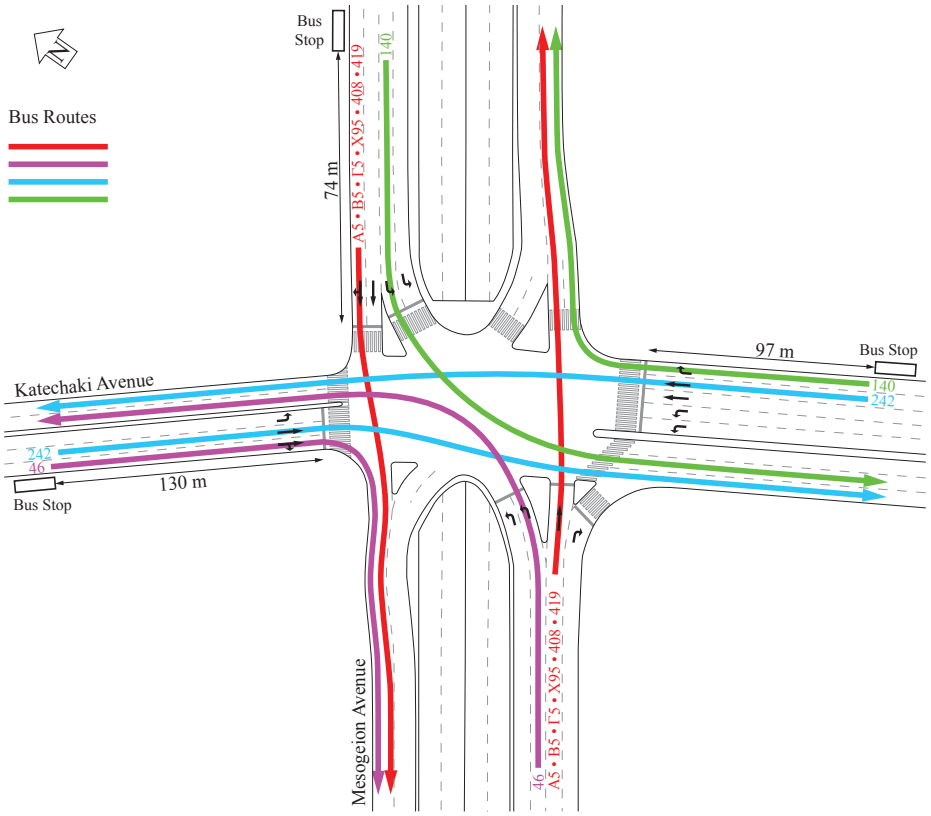

Figure 2.6: Layout of the intersection of Mesogion and Katechaki Avenues, (Source: [22])

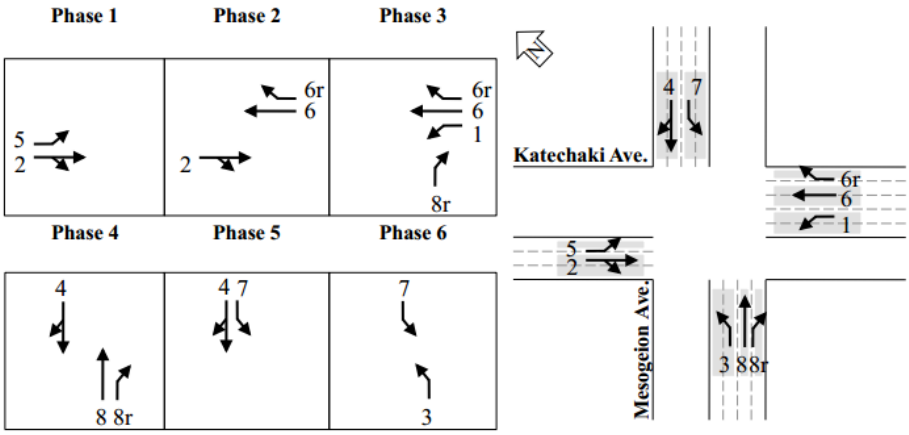

Figure 2.7: Lane group and phasing of the intersection of Mesogion and Katechaki Avenues, (Source: [22])

2.4 Evaluation Tests

The performance of the proposed signal control system has been evaluated through deterministic arrival tests. For deterministic tests, auto arrival and passenger occupancy are assumed to be known and constant. Information of transit arrivals and passenger occupancy are also assumed to be available a cycle in advance. In real-world implementation, the information of transit arrivals could be provided by detectors installed at certain distances upstream the intersection. However, in this study the arrival times of transit vehicles vary across the optimization cycle T to investigate the performance of the system for different transit arrivals. Additionally, average passenger occupancy of 1.25 and 30 passengers per vehicle is assumed for autos and transit vehicles, respectively.

Two sets of evaluation tests are performed to minimize: 1) weighted combinations of vehicle delay and emission, and 2) weighted combinations of person delay and emission. Three scenarios with no bus, one bus, two buses, and three buses in conflicting lane groups are performed for both combination of the objectives. The optimization is performed for different combinations of weighting factors, λ_d and λ_e, each varying between 0 and 1 while the sum of the weights is equal to 1. Furthermore, some scenarios are performed for three levels of general traffic demand resulting in intersection flow ratios of 0.4, 0.6, and 0.9 to investigate the impact of demand on the performance of the system. After optimizing cycle T, the trade-off between total delay (and person delay), bus delay, and emissions in two consecutive cycles T and $T + 1$ is presented.

2.5 Results

This section presents the results of the scenarios mentioned above. Insights are provided by studying the trade-off between total vehicle delay (or person delay) and

emissions and the relationship between bus delay and emissions across Pareto Optimal solutions in each designed scenario.

2.5.1 Minimizing Combination of Vehicle Delay and Emissions

Figure 2.8 shows the trade-off between vehicle delay and NO_x emissions at intersection flow ratios of 0.4, 0.6, and 0.9 when there is no bus at the intersection. According to Figure 2.8a, as λ_d varies from 0 to 1, delay decreases by only 35 sec (0.016 sec/veh) and NO_x emission increases by only 12 mg (0.005 mg/veh). This suggests that auto vehicle delay and NO_x emissions are not highly conflicting, which is due to the relatively low NO_x emission rates of auto vehicles.

At the higher intersection flow ratio of 0.6 shown in Figure 2.8b, as λ_d varies from 0 to 1, delay decreases by 49 sec (0.14 sec/veh) and NO_x emission increases by 17 mg (0.004 mg/veh). Changes in delay and emissions are lower compared to the case for intersection flow ratio of 0.4. This was expected because as the intersection flow ratio increases, the flexibility of the signal control system to adjust signal timings decreases. Figure 2.8c shows that due to the high traffic demand the system is not able to change signal timings.

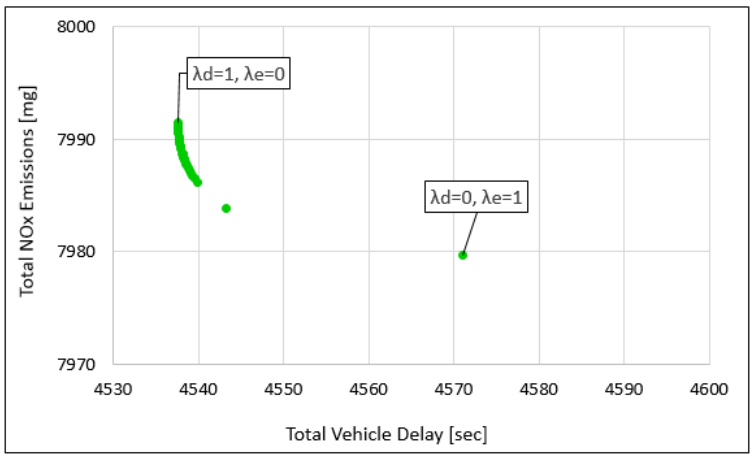

(a) Intersection flow ratio = 0.4

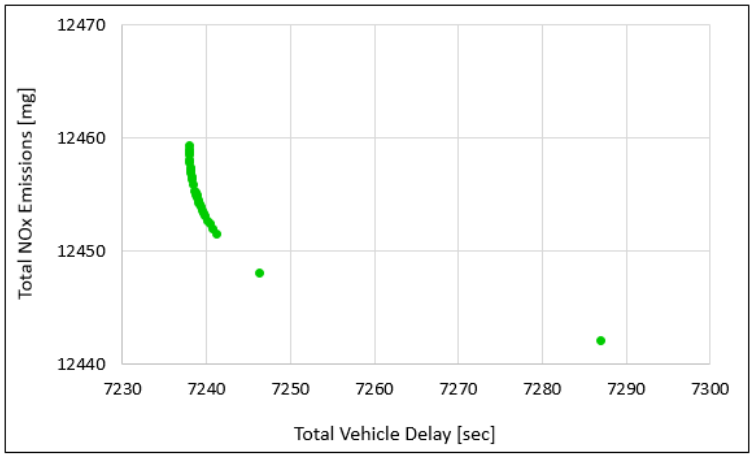

(b) Intersection flow ratio = 0.6

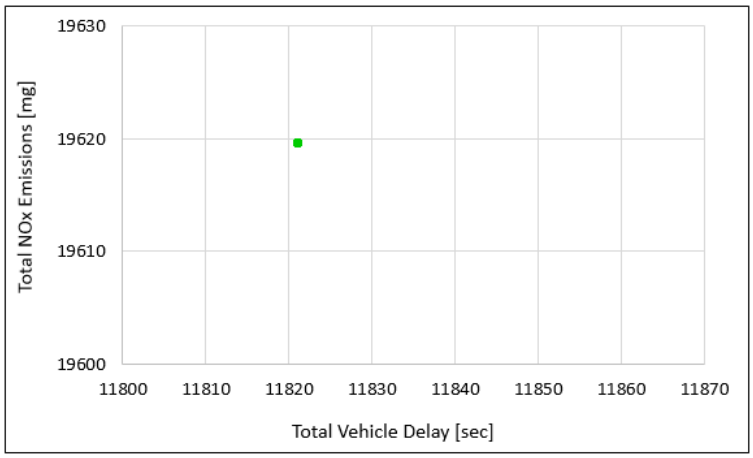

(c) Intersection flow ratio = 0.9

Figure 2.8: Trade-off between total vehicle delay and NO_x emission when there is no bus at the intersection.

Figure 2.9 shows the trade-off between vehicle delay and CO emission across Pareto optimal solutions for intersection flow ratios of 0.4, 0.6, ad 0.9 when there is no bus at the intersection. Gasoline cars have high CO emission rates particularly, during acceleration. Thus, CO emission is expected to be more conflicting with auto delay compared to NO_x emission. Figure 2.9a shows that as λ_d varies from 0 to 1 at the intersection flow ratio of 0.4, auto delay decreases by 135 sec (0.06 sec/veh), which is a higher change compared to the case when NO_x emission was included in the objective function. CO emission also increases by 720 mg (0.32 gr/veh) as λ_d varies from 0 to 1. Therefore, when CO emission levels are a concern at a specific site, the proposed signal control system can be implemented with appropriate weighting factors to reduce CO emission while keeping a balance between delay increase and emission reductions.

At higher intersection flow ratios, the system has lower flexibility to adjust signal timings. The average changes in auto delay and CO emissions per vehicle at the intersection flow ratio of 0.6 (Figure 2.9b) are respectively, 0.016 sec/veh and 0.216 mg/veh, which are lower than those changes for the intersection flow ratios of 0.4. However, because of the higher number of vehicles, the total changes in delay and emissions can be still significant. Total auto delay decreases by 53 sec and total CO emission increases by 710 mg as λ_d increases from 0 to 1. At the intersection flow ration of 0.9 shown in Figure 2.9c the congested traffic conditions does not allow the system to adjust signal timings. It should be noted that the range of axes are different in the two subfigures (and any other figure in this section) because of considerably different delay and emission produced in each scenario.

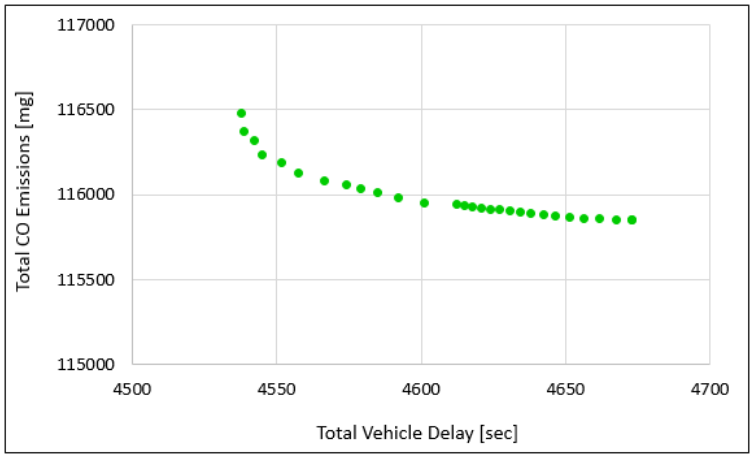

(a) Intersection flow ratio = 0.4

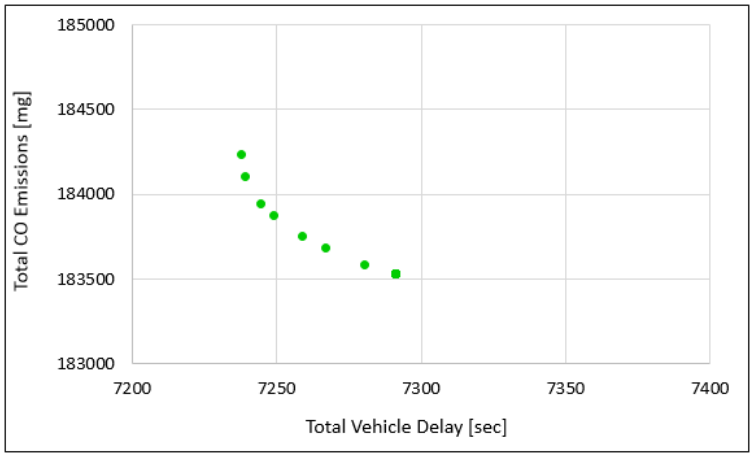

(b) Intersection flow ratio = 0.6

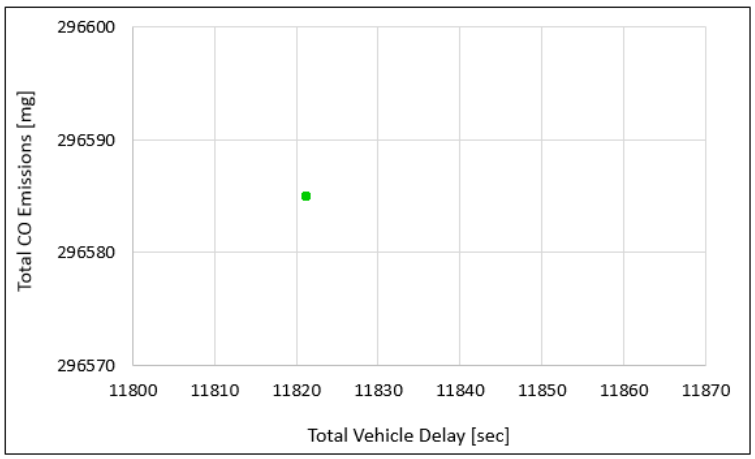

(c) Intersection flow ratio = 0.9

Figure 2.9: Trade-off between total vehicle delay and CO emission when there is no bus at the intersection.

2.5.1.1 Scenarios with One Transit Vehicle at the Intersection

When a transit vehicle is present at the intersection, it may be provided with priority over general traffic or not, depending on the emission rates, weighting factors, and intersection flow ratio. For example, diesel buses have significantly higher NO_x emission rates than gasoline cars. Therefore, when a combination of vehicle delay and NO_x emission with a high emission weight is optimized, the signal control system is likely to give priority to the transit vehicle to reduce total emission at the intersection. Unlike NO_x, the CO emission rate for diesel buses during acceleration is significantly lower than gasoline cars. Thus, when a combination of vehicle delay and CO emissions is optimized, a transit vehicle present at the intersection does not necessarily get priority because it does not produce higher emissions than an auto vehicle.

Figure 2.10 shows the Pareto Frontier of optimal solutions when weighted combinations of total vehicle delay and total NO_x emissions are minimized. In these scenarios a transit vehicle arriving in lane group 8 is considered in the optimization. As mentioned earlier, NO_x emission rates of diesel buses are significantly higher than those of gasoline cars. Therefore, we expect to observe major impacts on emissions in these scenarios.

The tests show that the largest changes in delay and emissions as weighting factors varies between 0 and 1 occurs when the bus arrives in the first red time period of the lane group, $R_8^{(1)}$, before optimizing the signal timings. This is expected because when the transit vehicle does not arrive in red duration or at the back of a queue, it can be served without stopping and the signal timings do not need to be changed to provide priority to the transit vehicle. In addition, lane group 8 is served by phases 5 and 6 and phase 6 is the last phase of the signal. Therefore, there is only one red duration ($R_8^{(1)}$) for this lane group. The curves with different colors represent different transit arrival times during $R_8^{(1)}$.

Figures 2.10a to 2.10c correspond to intersection flow ratios of 0.4, 0.6, and 0.9, respectively. At an intersection flow ratio of 0.4 (Figure 2.10a), when the bus arrives at time 0 sec, increasing λ_e from 0 to 1 leads to 1400 mg (0.62 mg/veh) reduction in NO_x emission at the price of 560 sec (0.26 sec/veh) increase in total delay. Similar changes are observed for the transit arrivals at times 10 sec, 20 sec, 30 sec, 40 sec, and 50 sec.

At an intersection flow ratio of 0.6 (Figure 2.10b), delay increases up to 570 sec (0.17 sec/veh) and NO_x emission decreases up to 1030 mg (0.31 mg/veh) as λ_e varies from 0 to 1. At intersection flow ratio of 0.9 (Figure 2.10c), delay increases up to 290 sec (0.06) and emission decreases up to 430 mg (0.09 mg/veh) as λ_e varies from 0 to 1. Thus, lower trade-off can be observed between delay and emissions as the intersection flow ratio increases.

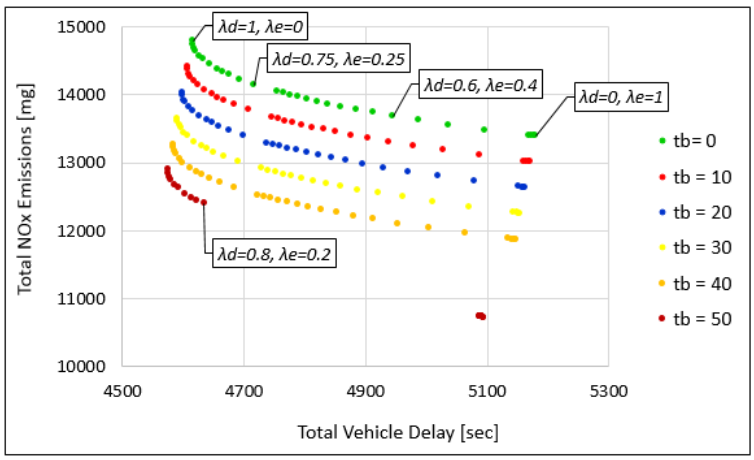

(a) Intersection flow ratio = 0.4

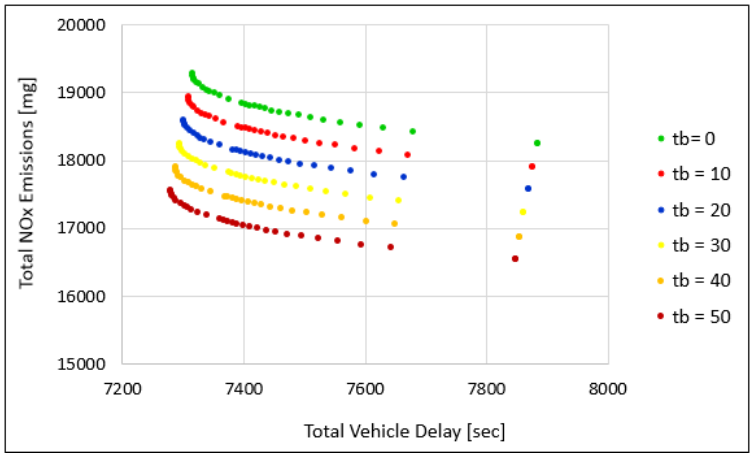

(b) Intersection flow ratio = 0.6

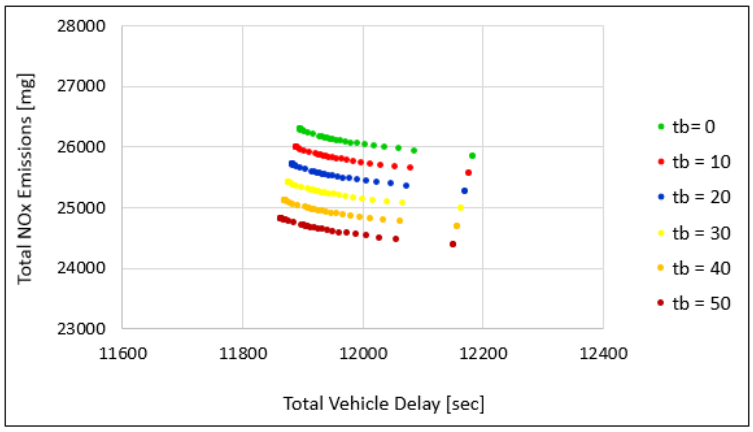

(c) Intersection flow ratio = 0.9

Figure 2.10: Trade-off between total vehicle delay and NO_x emission when a bus arrives in lane group 8.

Figure 2.11 shows the relationship between transit delay and total emissions across Pareto optimal solutions for different intersection flow ratios. It is shown that transit delay and total NO_x emissions have a direct relationship for all intersection flow ratios. This is due to the fact that improvements in NO_x emissions can be achieved through prioritizing transit vehicles because of their higher emission rates. As a result, when site conditions or emission standards necessitates implementing a signal timing plan to reduce emissions, the proposed signal control system with appropriate weighting factors can be used to improve total emissions and transit operations at the same time.

At intersection flow ratio of 0.4 (Figure 2.11) and for transit arrivals at times 0 sec, 10 sec, 20 sec, 30 sec, and 40 sec, transit delay decreases up to 38 sec as λ_e varies from 0 to 1. When the transit vehicle arrives at time 50 sec and intersection flow ratio of 0.4, if a weight higher than 0.2 is given to the emission ($\lambda_e > 0.2$), the transit vehicle can be served without a stop and its delay will be zero. At intersection flow ratio of 0.6 and 0.9 (shown in Figures 2.11b and 2.11c, respectively), the system is not flexible enough to give priority to the transit vehicles that arrives at time 50 sec for any emission weight. As a result, delay of this transit vehicle is always non-zero. The lower flexibility of the system at higher intersection flow ratios is also shown by the lower changes in transit delay and emissions across Pareto optimal solutions. At intersection flow ratio of 0.9 (Figure 2.11c), transit delay decrease by only 14 sec as λ_e varies from 0 to 1.

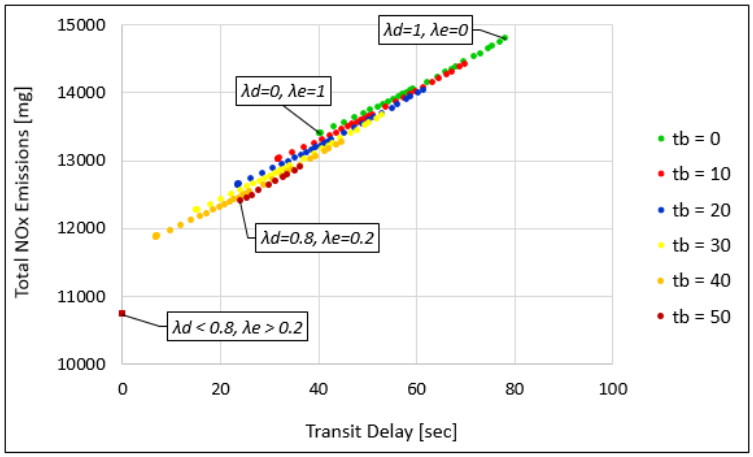

(a) Intersection flow ratio = 0.4

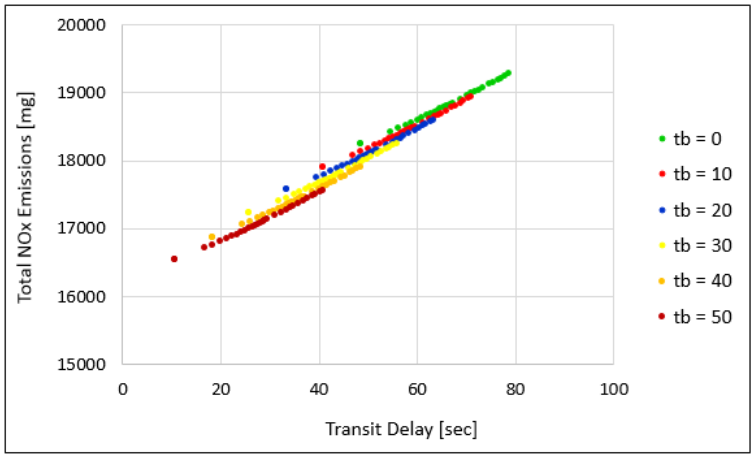

(b) Intersection flow ratio = 0.6

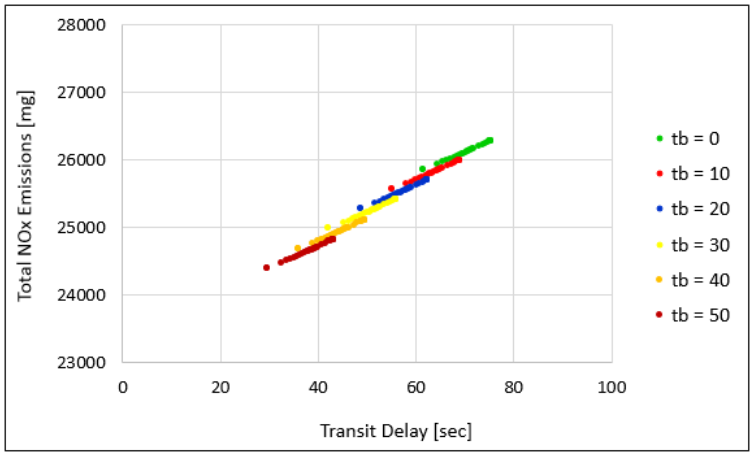

(c) Intersection flow ratio = 0.9

Figure 2.11: The relationship between transit delay and total NO_x emission for varying weight factors.

As shown earlier in Figures 2.8a and 2.9 the performance of the system also depends on the considered pollutant and the emission rates used in the objective function. Figure 2.12 shows the trade-off between vehicle delay and CO emissions for varying weights in the objective function. As mentioned earlier, diesel buses have significantly higher NO_x emission rates compared to gasoline cars, but this is not true for CO emission rates. As a result, we expect to see lower changes in total vehicle delay (i.e. higher trade-off between delay and emissions) when a combination of CO emissions and vehicle delay is used as the objective function compared to the combination of NO_x emissions and vehicle delay. At an intersection flow ratio of 0.4, which has the highest flexibility to change signal timings, changing λ_d from 0 to 1 results in only 50 sec decrease in total delay (0.023 sec/veh) and 160 mg (0.07 mg/veh) increase in CO emission. This delay reduction is considerably lower than the 560 sec (0.26 sec/veh) delay reduction in Figure 2.10a when a combination of NO_x and vehicle delay was optimized.

At an intersection flow ratio of 0.6 (Figure 2.12b), delay decreases by 63 sec (0.018 sec/veh) and CO emission increases by 417 mg (0.12 mg/veh) as λ_d varies from 0 to 1. Although total changes of delay a and CO emission are higher compared to the case for intersection flow ratio of 0.4, the average changes per vehicle are lower as expected due to the lower flexibility of the system. Finally, at the intersection flow ratio of 0.9, the system cannot make any changes in signal timings and consequent delays and emissions with the use of different weighting factors.

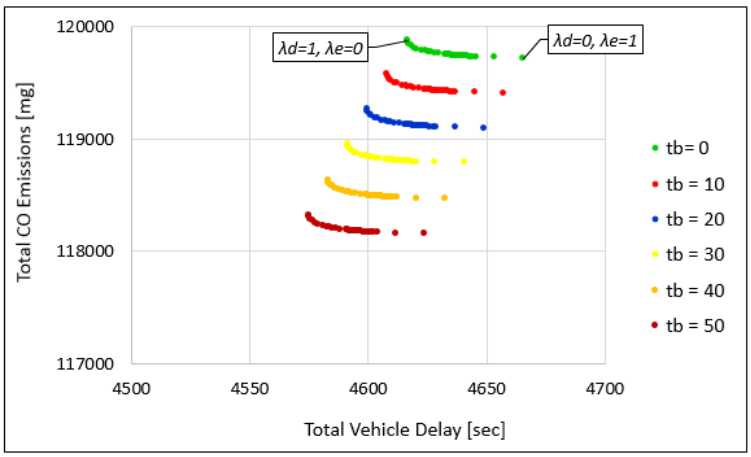

(a) Intersection flow ratio = 0.4

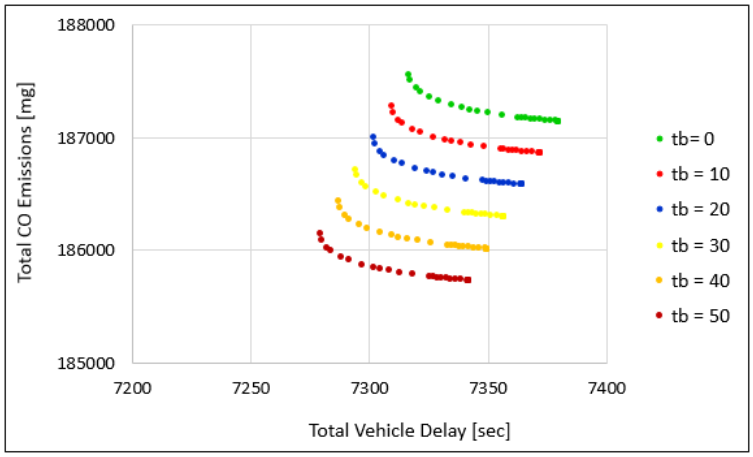

(b) Intersection flow ratio = 0.6

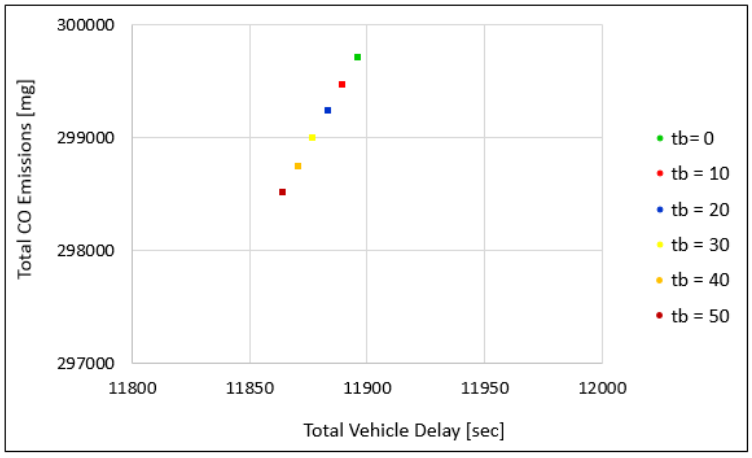

(c) Intersection flow ratio = 0.9

Figure 2.12: Trade-off between total vehicle delay and CO emission when a bus arrives in lane group 8.

Figure 2.13 shows the relationship between total CO emission and transit delay with varying weighting factors. Unlike NO_x, transit delay has an inverse relationship with CO emissions. This implies that when the combination of CO emissions and vehicle delay is minimized, transit vehicles do not have priority over auto vehicles. As expected due to auto and transit CO emission rates, the improvement in CO emissions is mostly achieved through improving the operation of auto vehicles. Therefore, decision makers should pay careful attention to the pollutant and emissions rates used in the objective of a signal control system to correctly address the air pollution issues.

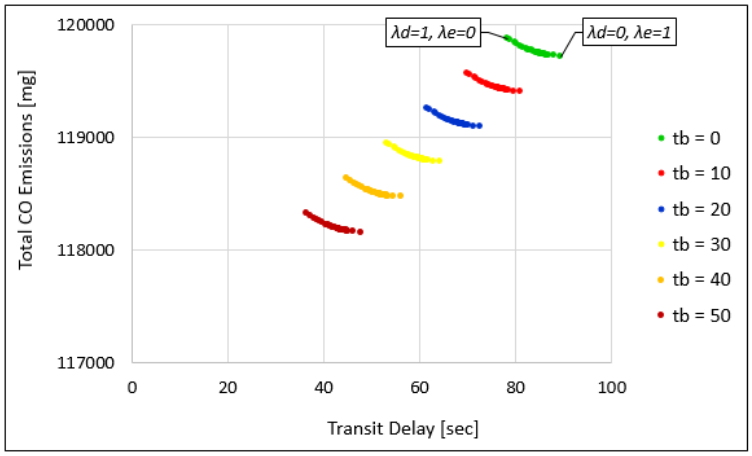

(a) Intersection flow ratio = 0.4

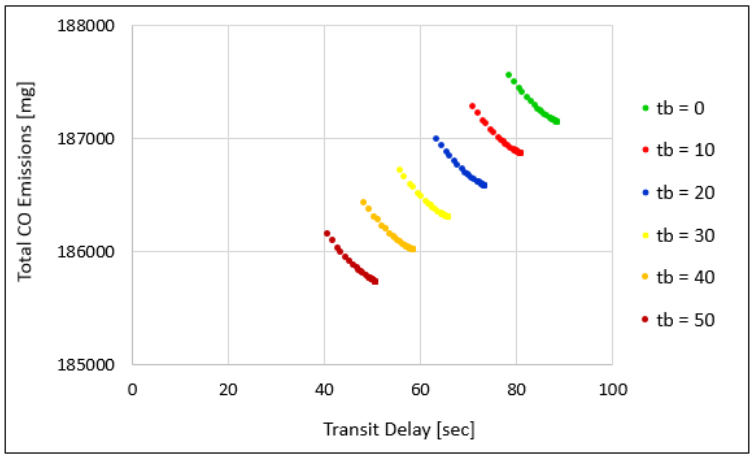

(b) Intersection flow ratio = 0.6

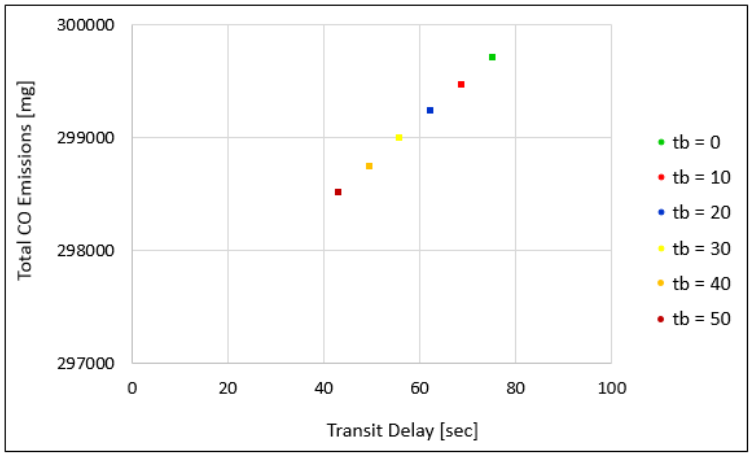

(c) Intersection flow ratio = 0.9

Figure 2.13: The relationship between bus delay and total CO emission for varying weighting factor.

2.5.1.2 Scenarios with Two Transit Vehicles at the Intersection

The performance of the signal control system is also evaluated when two transit vehicles are present at the intersection. Figure 2.14 shows the trade-off between total NO_x emission and vehicle delay when two transit vehicles arrive at the intersection in conflicting lane groups and the intersection flow ratio is 0.4. Transit vehicles arrive in lane groups 2 and 8 and their arrival times vary from 0 sec to 50 sec (i.e. different combinations of arrival times of the two transit vehicles are tested). Scenarios are performed only for the combination of vehicle delay and NO_x emissions since as shown in the previous section, these two objectives (i.e. total vehicle delay and total NO_c emissions) are more conflicting than the combination of vehicle delay and CO emissions.

Lane group 2 is served by phases 1 and 2 and during phases 3, 4, 5, and 6 a queue in this lane group is being formed. Therefore, at the beginning of cycle T, a queue with a certain length (that depends on the signal timings of cycle $T-1$) exists in this lane groups and a transit vehicle that arrives at the beginning of the cycle have to stop at the back of the queue until it is served during phases 1 or 2. Since the entire queue is formed in cycle $T-1$ and traffic condition is undersaturated (i.e. vehicles have at most one stop and are served within one cycle), changes in signal timings of cycle T does not affect the delay of the transit vehicle that arrives in lane group 2 at time 0 sec. Vice versa, this transit vehicle does not have any impact on the signal timings of cycle T, the trade-off between delay and emission in cycle T, or on the operation of the transit vehicle that arrives in lane group 8. As a result, Figure 2.14a shows the same trade-off between delay and NO_x emission as for the case with one transit vehicle shown in Figure 2.10a. Although total amounts of emissions and delays are higher than the values shown in Figure 2.10a (because emission and delay of the transit vehicle in lane group 2 is also added), the trade-off is exactly the same.

When the transit vehicle of lane group 2 arrives at time 10 sec or later, the queue of lane group 2 that was formed in cycle $T-1$ has been disappeared and the transit vehicle does not necessarily stop. Now, this transit vehicle is considered in the optimization of cycle T and is candidate to receive priority as well as the other transit vehicle in lane group 8. Thus, it affects the signal timings of cycle T and consequently, the trade-off between delay and emission and the operation of the other transit vehicle that arrives in lane group 8. If a transit vehicle is served without a stop, high emission that can be produced during a consequent acceleration is saved. Therefore, the system achieves the minimum emission level by giving priority to at least one of the transit vehicles. The transit vehicle that arrives in lane group 8 has a low chance to receive priority because it arrives during $R_8^{(1)}$ (considering the initial signal timings before optimization of cycle T). However, the transit vehicle in lane group 2 has a higher chance to receive priority by through extending green times of phases 1 and 2. Therefore, the system imposes higher delay to conflicting traffic (including the transit vehicle that arrives in lane group 8) to give priority to the transit vehicle of lane group 2. As the arrival time of the transit vehicle in lane group 2 increases, higher delay should be imposed to the conflicting traffic to serve this transit vehicle. As a result, a portion of the total saved emission and delay by giving priority to the transit vehicle in lane group 2 is canceled off by the higher imposed delay, stops, and consequent emissions to the conflicting traffic. Consequently, lower changes in total delay and emissions are observed as the arrival time of transit vehicle in lane group 2 increases. This is shown in Figure 2.15, too, which demonstrates the relationship between total NO_x emissions and delay of the transit vehicle in lane group 8. According to this figure, as the arrival time of the transit vehicle in lane group 2 increases, the minimum level of delay of the other transit vehicle in lane group 8 increases and total changes in its delay and emission across Pareto optimal

solutions decreases. It should be noted that delay of the transit vehicle in lane group 2 is zero when it arrives between times 10 sec and 50 sec.

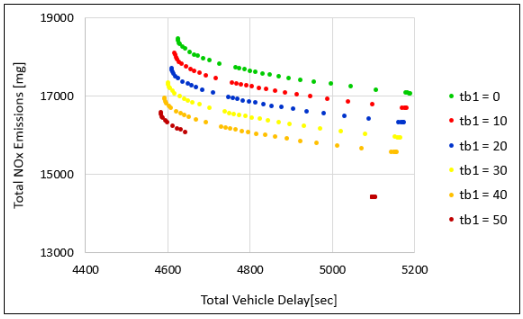

(a) $t_{b_2} = 0$ sec

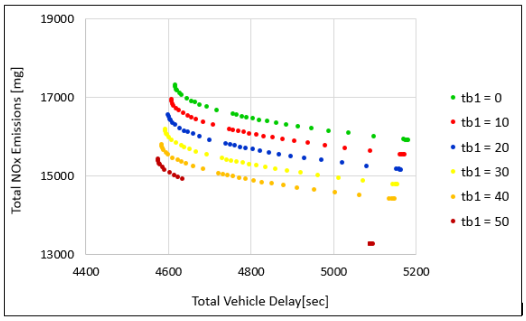

(b) $t_{b_2} = 10$ sec

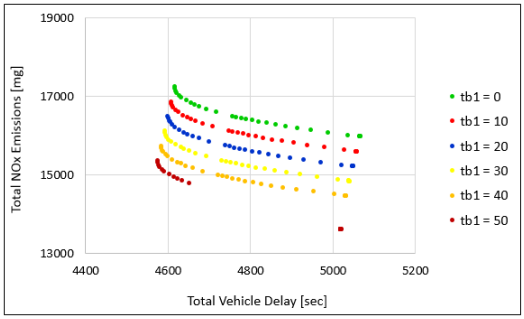

(c) $t_{b_2} = 20$ sec

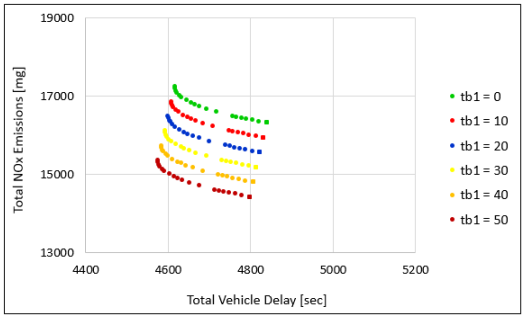

(d) $t_{b_2} = 30$ sec

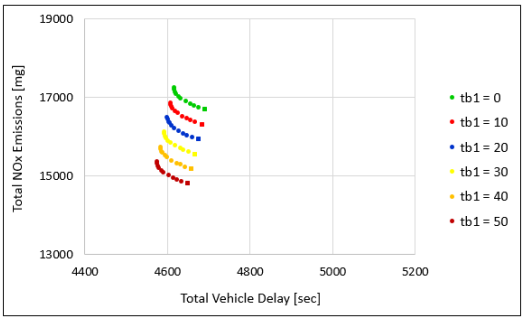

(e) $t_{b_2} = 40$ sec

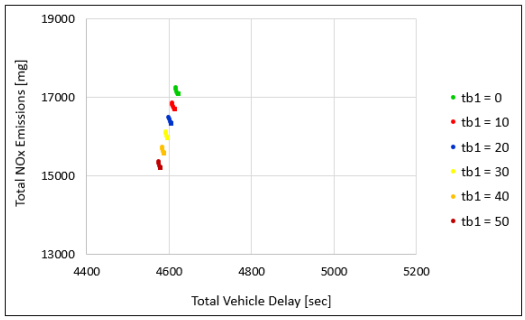

(f) $t_{b_2} = 50$ sec

Figure 2.14: Trade-off between total vehicle delay and total NO_x emission for different weighting factors when two transit vehicles are present at the intersection in lane groups 2 and 8 and the intersection flow ratio is 0.4.

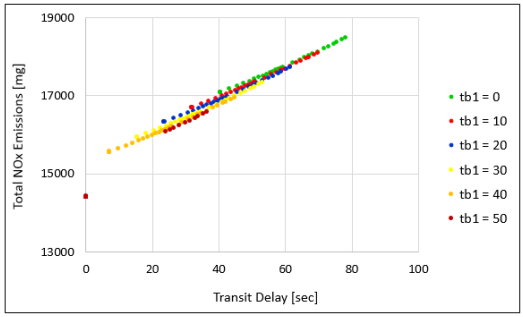

(a) $t_{b_2} = 0$ sec

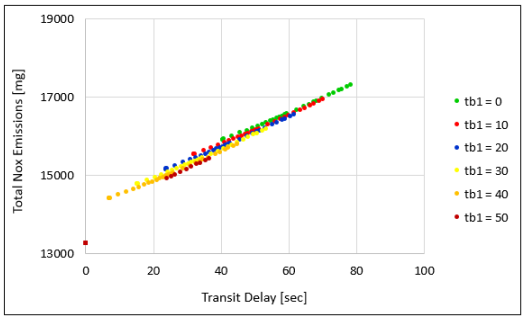

(b) $t_{b_2} = 10$ sec

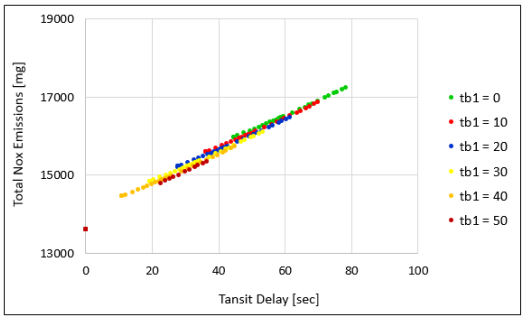

(c) $t_{b_2} = 20$ sec

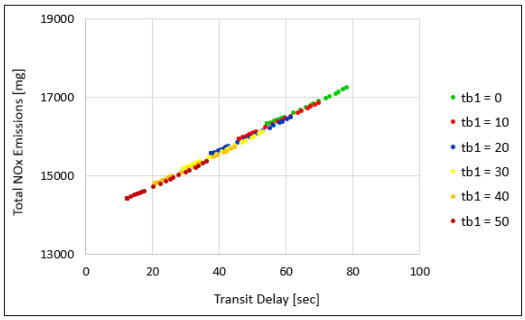

(d) $t_{b_2} = 30$ sec

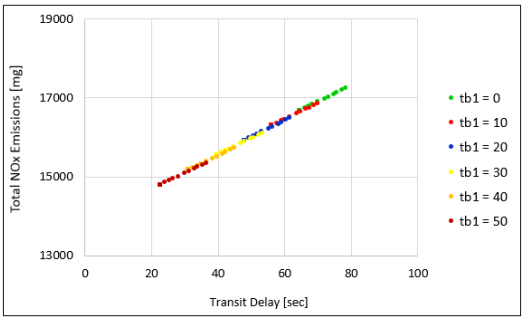

(e) $t_{b_2} = 40$ sec

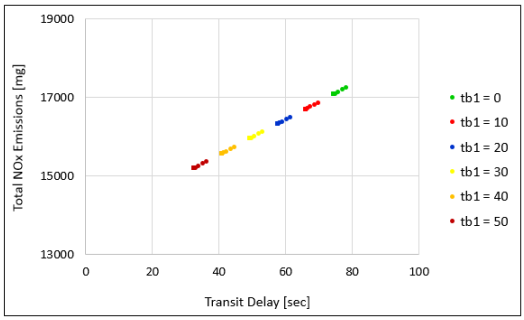

(f) $t_{b_2} = 50$ sec

Figure 2.15: The relationship between the delay of the transit vehicle that arrives in lane group 8 and total NO_x emission for varying weighting factor when two transit vehicles are present at the intersection in lane groups 2 and 8 and the intersection flow ratio is 0.4.

Figures 2.16 and 2.17 show the the results when two buses are present at the intersection and the intersection flow ratio is 0.9. As expected the changes in delay and emissions are lower compared to the case for intersection flow ratio of 0.4. For

example, when the transit vehicle in lane group 2 arrives at time 30 sec (for different arrival times of the transit vehicle in lane group 8) (Figure 2.16d), average delay per vehicle increases by 0.06 and average NO_x emissions decreases by 0.09 mg/veh. These change are lower compared to the increase of 0.16 sec/veh in average delay and the reduction of 0.38 mg/veh in average NOx emissions per vehicles at the intersection flow ratio of 0.4.

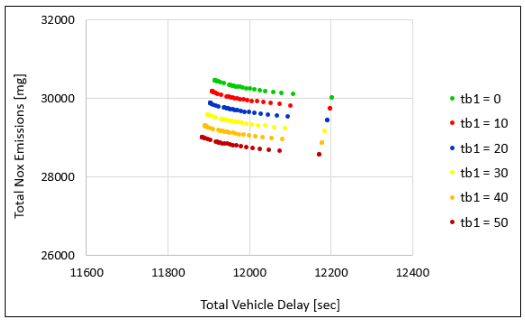

(a) $t_{b_2} = 0$ sec

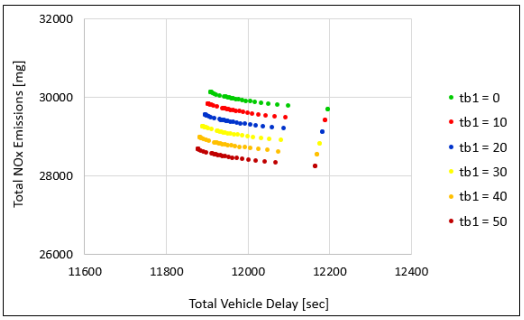

(b) $t_{b_2} = 10$ sec

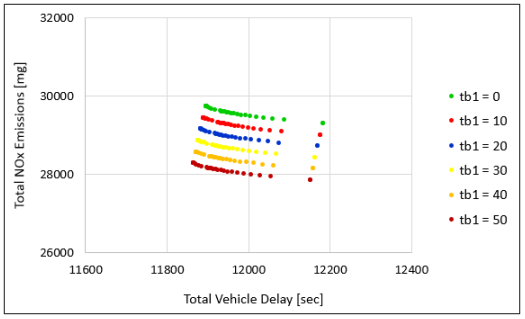

(c) $t_{b_2} = 20$ sec

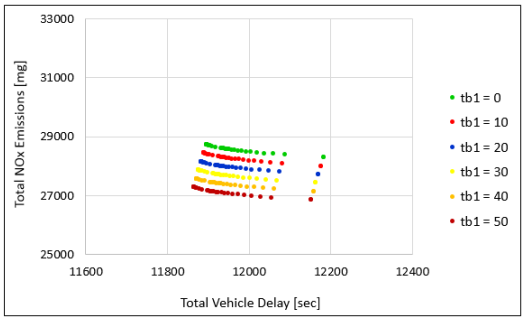

(d) $t_{b_2} = 30$ sec

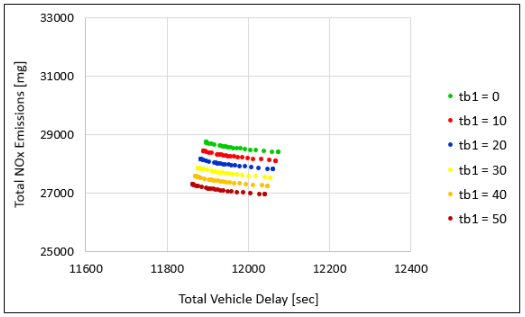

(e) $t_{b_2} = 40$ sec

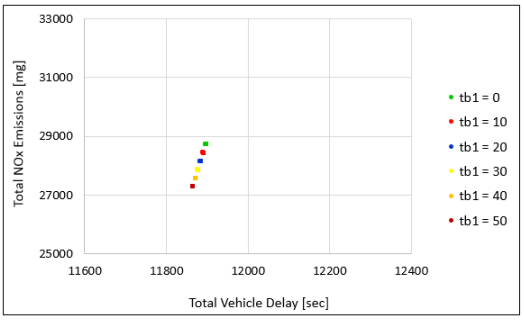

(f) $t_{b_2} = 50$ sec

Figure 2.16: Trade-off between total vehicle delay and total NO_x emission for different weighting factors when two transit vehicles are present at the intersection in lane groups 2 and 8 and the intersection flow ratio is 0.9.

Figure 2.17 shows delay of the transit vehicle in lane group 8 when another transit vehicle arrives in lane group 2 at different times. Comparing this figure with Figure 2.15 shows that at intersection flow ratio of 0.9, delay of the first transit vehicle (in lane group 8) is less affected by the presence of the second transit vehicle (in lane

group 2) compared to the case for intersection flow ratio of 0.4. This is due to the lower flexibility of the system to adjust signal timings.

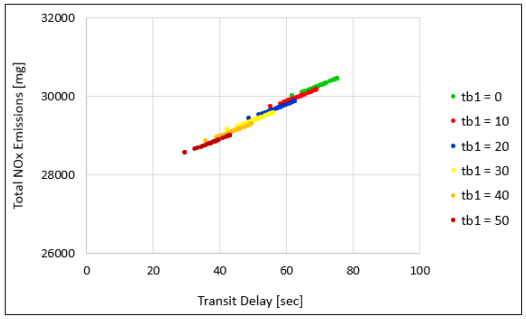

(a) $t_{b_2} = 0$ sec

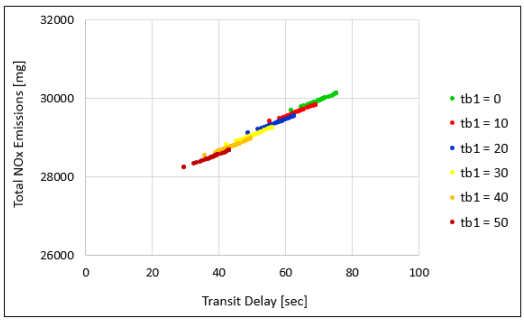

(b) $t_{b_2} = 10$ sec

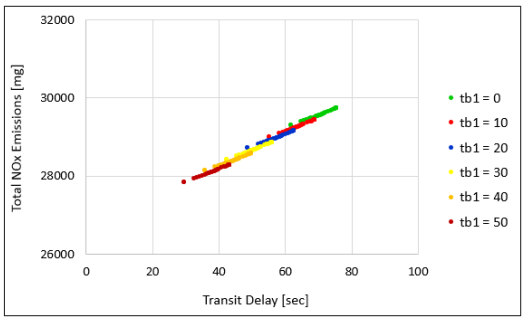

(c) $t_{b_2} = 20$ sec

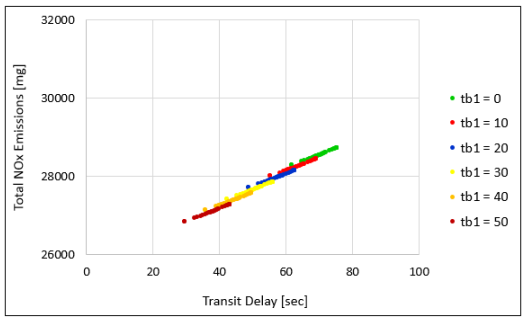

(d) $t_{b_2} = 30$ sec

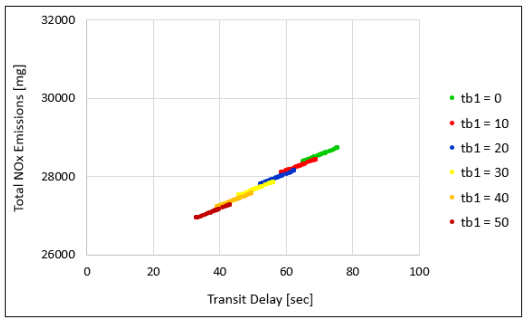

(e) $t_{b_2} = 40$ sec

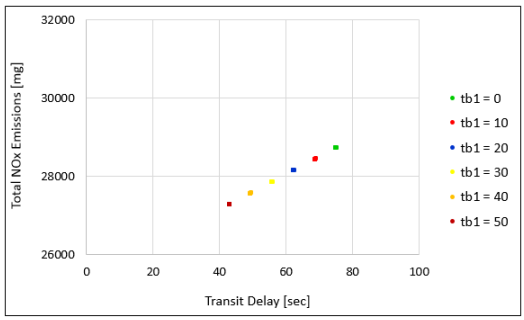

(f) $t_{b_2} = 50$ sec

Figure 2.17: The relationship between the delay of the transit vehicle that arrives in lane group 8 and total NO_x emission for varying weighting factor when two transit vehicles are present at the intersection in lane groups 2 and 8 and the intersection flow ratio is 0.9.

Figure 2.18 shows the trade-off between vehicle delay and CO emissions when two transit vehicles arrive at the intersection during cycle T and the intersection flow ratio is 0.4. The figure shows that the transit vehicle that arrives in lane group 2 has no effect on signal timings and consequently resulted vehicle delay and emissions. This was expected because transit vehicles have significantly lower CO emission rate during acceleration. Therefore, highest improvements in CO emissions is achieved through improving auto operations and presence of a transit vehicle does not have a major impact on signal timings.

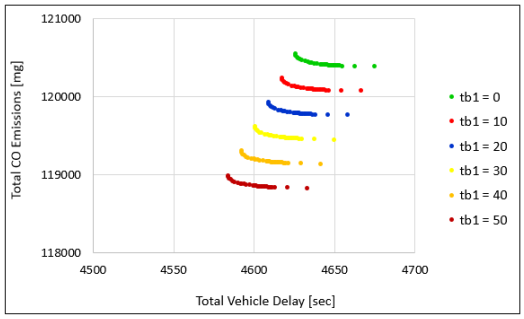

(a) $t_{b_2} = 0$ sec

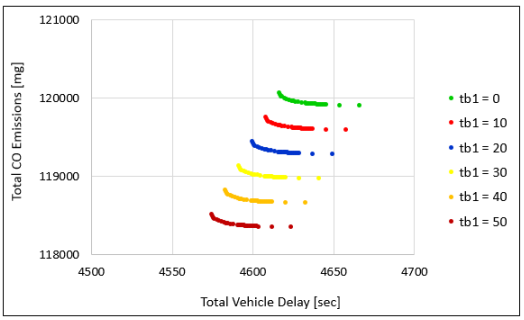

(b) $t_{b_2} = 10$ sec

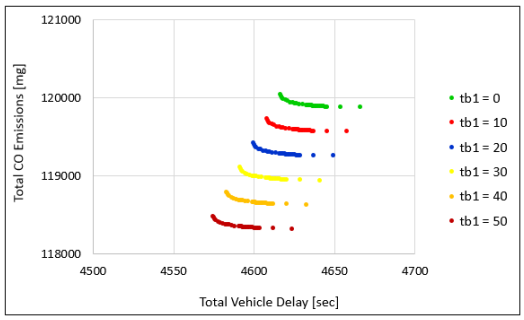

(c) $t_{b_2} = 20$ sec

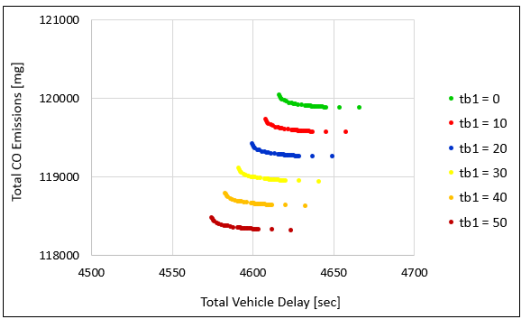

(d) $t_{b_2} = 30$ sec

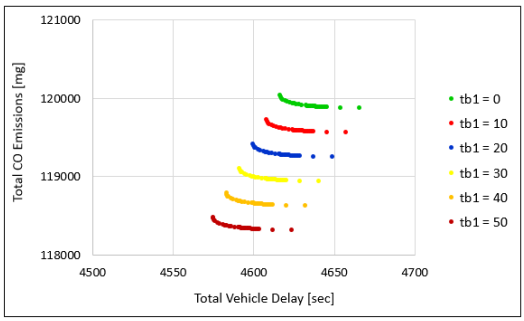

(e) $t_{b_2} = 40$ sec

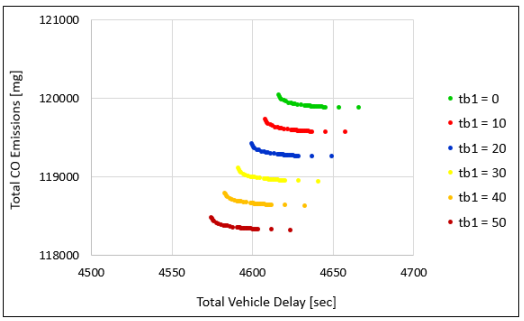

(f) $t_{b_2} = 50$ sec

Figure 2.18: Trade-off between total vehicle delay and total CO emission for different weighting factors when two transit vehicles are present at the intersection in lane groups 2 and 8 and the intersection flow ratio is 0.4.

Figure 2.19 also shows that signal timings and consequently the operation of the transit vehicle that arrives in lane group 8 is not affected by the presence of the second transit vehicles that arrives in lane group 2.

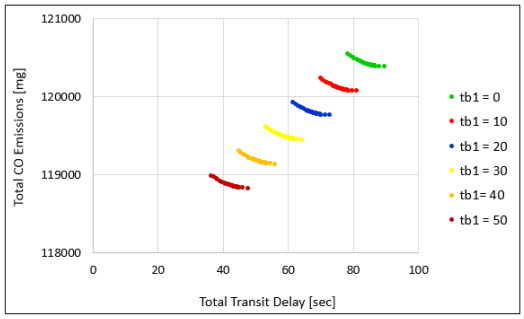

(a) $t_{b_2} = 0$ sec

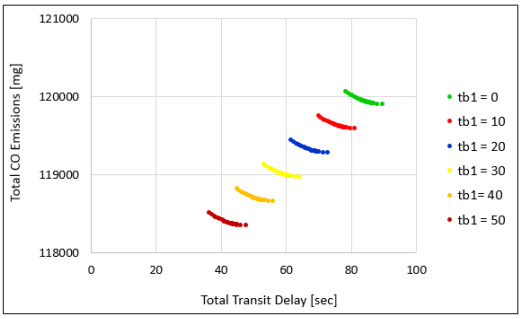

(b) $t_{b_2} = 10$ sec

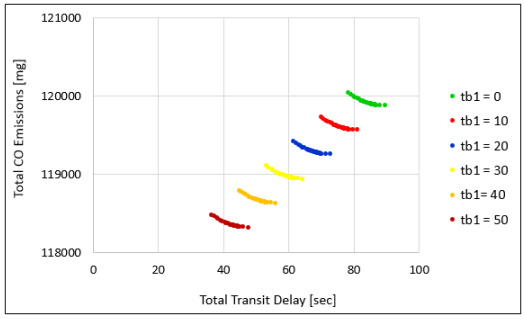

(c) $t_{b_2} = 20$ sec

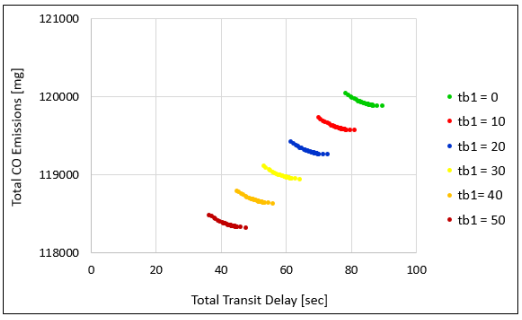

(d) $t_{b_2} = 30$ sec

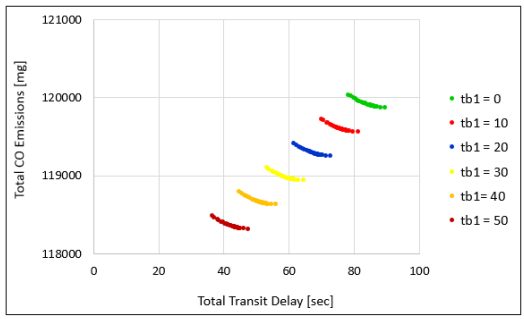

(e) $t_{b_2} = 40$ sec

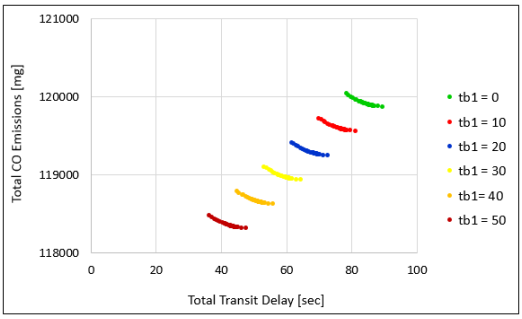

(f) $t_{b_2} = 50$ sec

Figure 2.19: The relationship between the delay of the transit vehicle that arrives in lane group 8 and total CO emission for varying weighting factor when two transit vehicles are present at the intersection in lane groups 2 and 8 and the intersection flow ratio is 0.4.

2.5.1.3 Scenarios with Three Transit Vehicles at the Intersection

It was shown earlier that when two transit vehicles in lane groups 8 and 2 respectively arrive at times 0 sec and 30 sec, they both are considered in the optimization problem

(Figure 2.20a). As a result of considering both transit vehicles in the optimization problem, the system provided priority to the transit vehicle in lane group 2 and higher delay was imposed to the transit vehicle in lane group 8 (when a high emission weight was used in the objective function). Now, we add the third transit vehicle in lane group 1, which is conflicting with lane groups 2 and 8. Therefore, transit vehicles in lane groups 8 and 2 arrives at times 0 sec and 30 sec and arrival time of the third transit vehicle varies from time 0 sec to 50 sec. Figure 2.20a shows the resulted delay and NO_x emissions across Pareto optimal solutions when combinations of these two objectives are minimized.

Figure 2.20b shows that how the presence of the third transit vehicle in lane group 1 affects the operation of transit vehicle in lane group 8. It is shown that when the third transit vehicle arrives at times 0 sec to 40 sec, it does not have any impact on the operation of the transit vehicle in lane group 8. When the third transit vehicle arrives at time 50 sec and a high emission weight is used in the objective function, the system provides priority to transit vehicles in lane groups 1 and 2. As a result, a higher delay is imposed to vehicles in other lane groups including the transit vehicle in lane group 8.

Figures 2.20a and 2.20b suggest that when a low emission weight and high delay weight is used in the objective function, adding another transit vehicle does not impact resulted delay and emissions. This is expected because, transit vehicles are treated as auto vehicle are. However, when a high emission weight and low delay weight are used in the objective function, usually, the minimized emission is achieved by prioritizing one or more transit vehicles at the price of imposing higher delay to other vehicles.

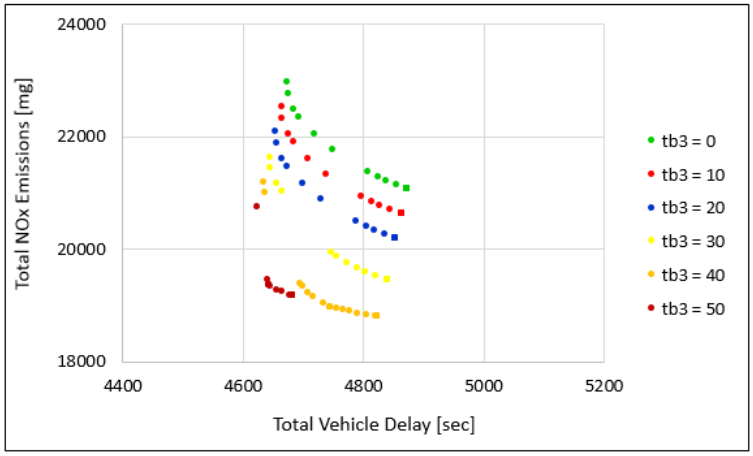

(a) Trade-off between total vehicle delay and total NO_x emissions

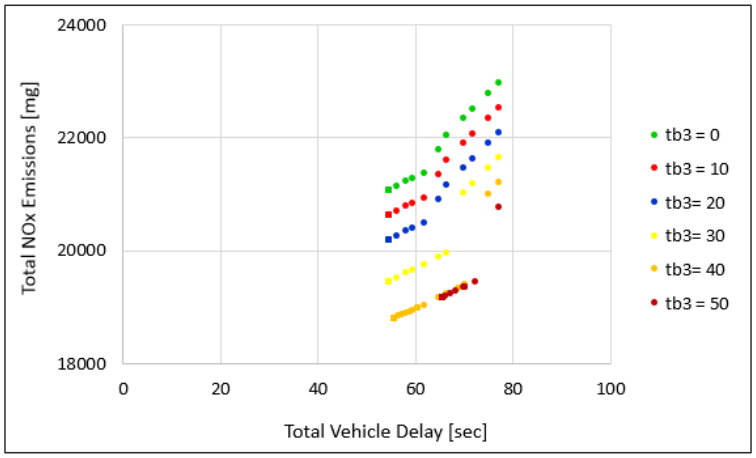

(b) Relationship between transit delay and total NO_x emissions

Figure 2.20: The impact of the signal control system on vehicle delay and NO_x emissions when there are three transit vehicles at the intersection in lane groups 1, 2, and 8 and the intersection flow ration is 0.4.

Figure 2.21a and 2.21b respectively show the trade-off between vehicle delay and CO emissions and the relationship between transit delay and CO emissions when weighted combinations of vehicle delay and CO emissions are minimized. It is shown that the presence of the third transit vehicle results in lower flexibility of the system to favor delay or emissions as weighting factors change. However, when transit vehicle of lane group 1 arrives at time 50 sec (when the signal is green based on the initial

signal timings), it does not have a significant impact on the system. Therefore, the system has higher flexibility to adjust signal timings to improve emission or delay. Consequently, higher trade-off between delay and emission is observed for this case.

Figure 2.21b shows the relationship between transit delay in lane group 8 and total CO emissions. As expected, due to lower flexibility of the system when three transit vehicles are present at the intersection, the operation of transit vehicle in lane group 8 does not change significantly across Pareto optimal solutions.

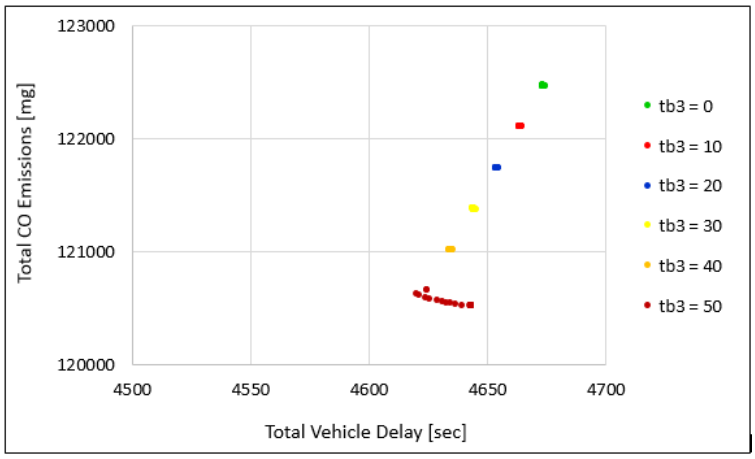

(a) Trade-off between total vehicle delay and total CO emissions

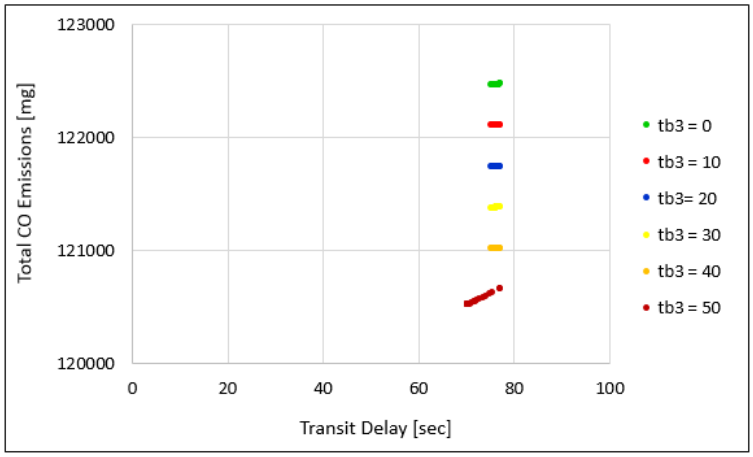

(b) Relationship between transit delay and total CO emissions

Figure 2.21: The impact of the signal control system on vehicle delay and CO emissions when there are three transit vehicles at the intersection in lane groups 1, 2, and 8 and the intersection flow ration is 0.4.

2.5.2 Minimizing Combination of Person Delay and Emissions

In the second set of optimization scenarios, a linear combination of total person delay and emission is minimized. Figures 2.22 and 2.23 show the trade-off between auto person delay and emissions when NO_x and CO are considered in the objective function, respectively. Figure 2.22a shows that at the intersection flow ratio of 0.4, total person delay decreases by 42 sec (0.016 sec/person) and total NO_x emission increases by 12 mg (0.005 mg/veh) as λ_d varies from 0 to 1. At the intersection flow ratio of 0.6, there is a reduction of 0.014 sec/person and an increase of 0.005 mg/veh as λ_d varies from 0 to 1. Changes in average person delay and emission becomes lower as the intersection flow ratio increases, which is due to the lower flexibility of the system to adjust signal timings. The low changes and values of emissions and delay are also due to the low NO_x emission rates of gasoline cars. At the intersection flow ratio of 0.9, changing weighting factors does not have any impact on signal timings and consequent delays and emissions (Figure 2.22c).

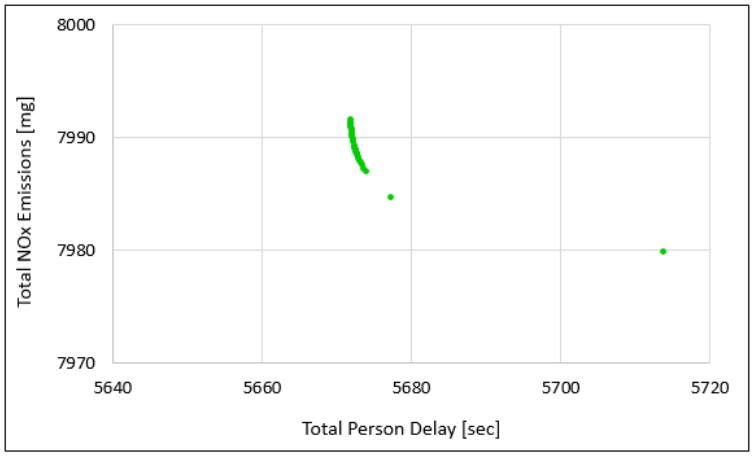

(a) Intersection flow ratio = 0.4

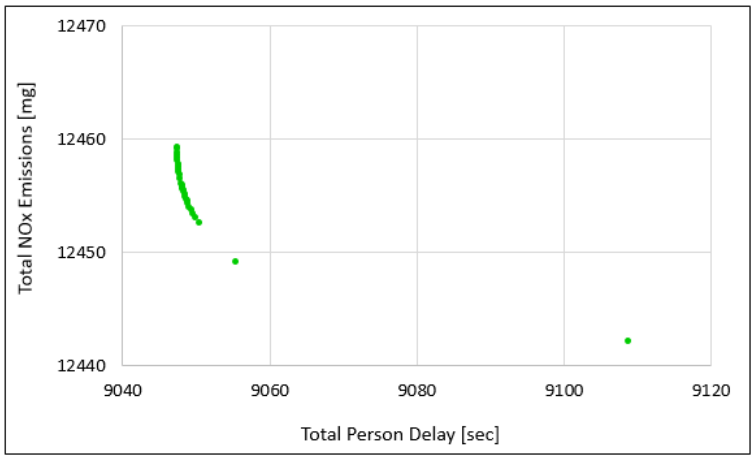

(b) Intersection flow ratio = 0.6

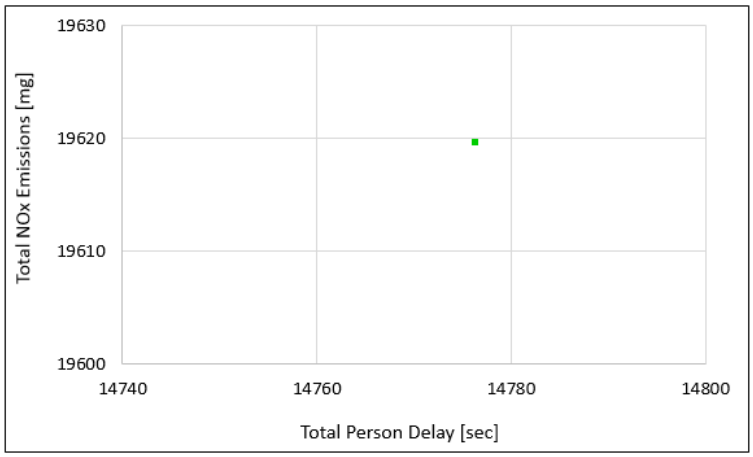

(c) Intersection flow ratio = 0.9

Figure 2.22: Trade-off between total person delay and NO_x emission when there is no transit vehicle at the intersection.

Figure 2.23 shows more significant trade-offs between person delay and emissions when CO emission is considered in the objective function compared to the case for NO_x emissions. The reason is that CO emission rates of gasoline cars is higher than their NO_x emission rates. Figure 2.23 shows that at the intersection flow ratios of 0.4 and 0.6 changes in person delay are respectively, 0.06 sec/person and 0.02 sec/person and changes in CO emission are respectively, 0.32 mg/veh and 0.21 mg/veh. Figure 2.23c shows that all weighting factors result in the same solution at the intersection flow ratio of 0.9.

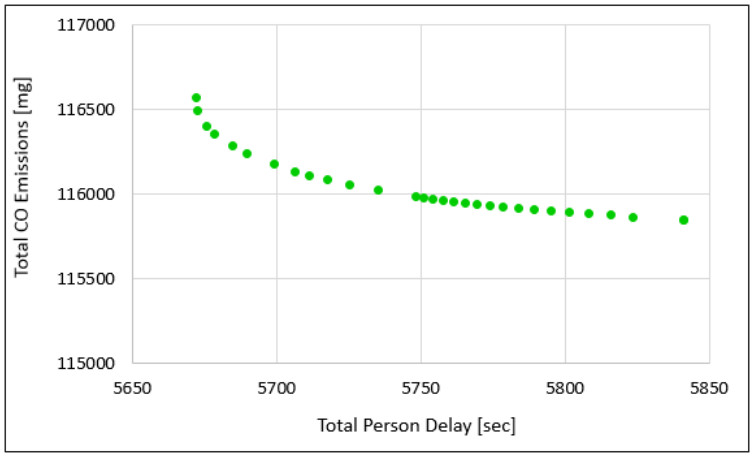

(a) Intersection flow ratio = 0.4

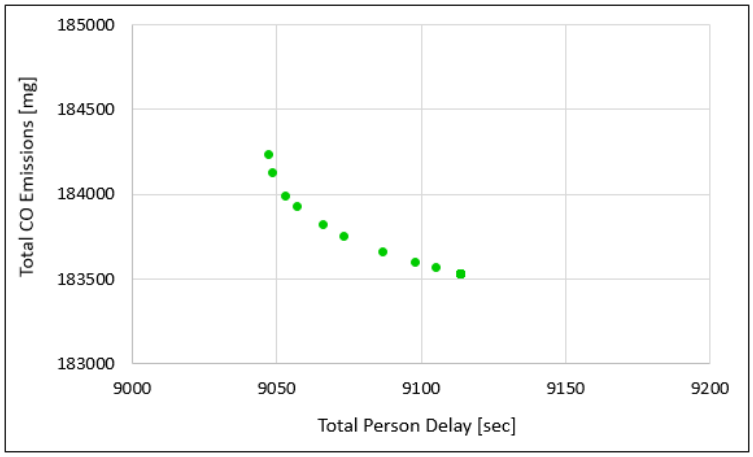

(b) Intersection flow ratio = 0.6

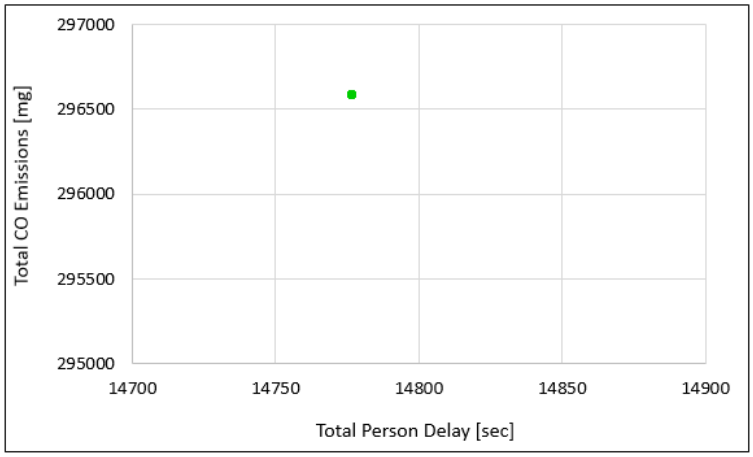

(c) Intersection flow ratio = 0.9

Figure 2.23: Trade-off between total person delay and CO emission when there is no transit vehicle at the intersection.

2.5.2.1 Scenarios with One Transit Vehicle at the Intersection

Transit vehicles have higher passenger occupancy and emission rates compared to auto vehicles. As a result, if the general traffic conditions allow, for a high delay weight in the objective function, transit vehicles get priority due to their higher passenger occupancy and for high emission weights they get priority due to their higher emission rates.

Figure 2.24a shows the trade-off between total person delay and NO_x emissions for different transit arrival times in lane group 8 and intersection flow ratio of 0.4. As expected the change in person delay and emissions is lower (around 40 sec (0.01 sec/person) decrease in person delay and 270 mg (0.12 mg/veh) increase in NO_x emission) when λ_d varies from 0 to 1 compared to the case with a combination of vehicle delay and emission as the objective function. This means that the current two objective are less conflicting than the combination of vehicle delay and NO_x emissions. At the intersection flow ratio of 0.6 (Figure 2.24b), changes in person delay and emissions across Pareto optimal solutions are respectively, 108 sec (0.03 sec/person) and 355 mg (0.11 mg/veh) and at the intersection flow ratio of 0.9 (Figure 2.24c), these changes are respectively 44 sec (0.006 sec/person) and 168 mg (0.03 mg/veh).

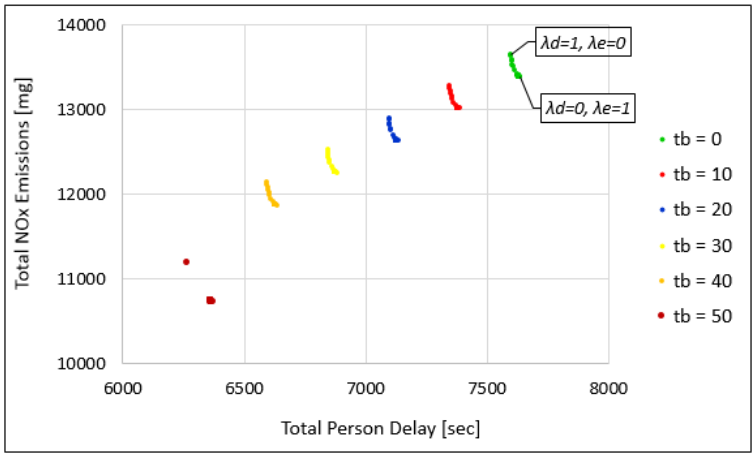

(a) Intersection flow ratio = 0.4

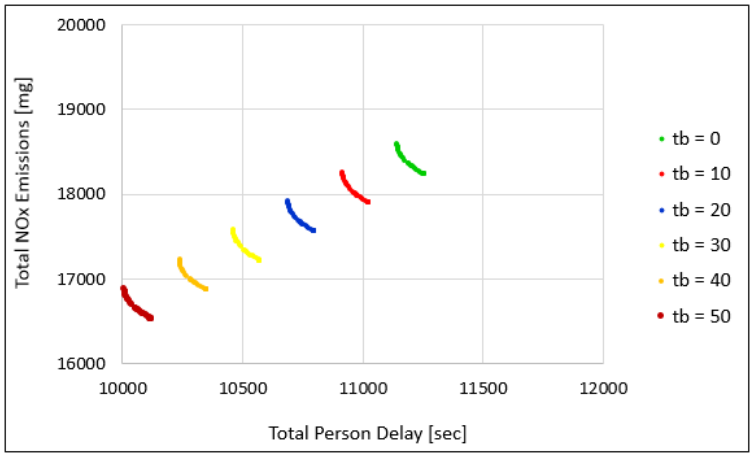

(b) Intersection flow ratio = 0.6

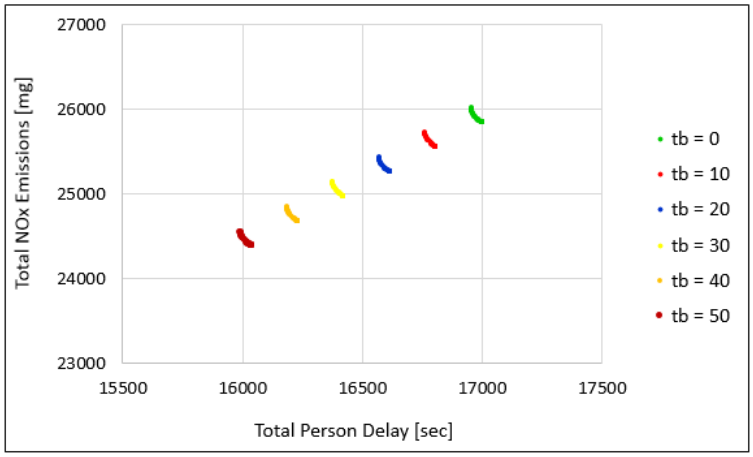

(c) Intersection flow ratio = 0.9

Figure 2.24: Trade-off between total person delay and NO_x emission when a transit vehicle arrives in lane group 8.

Figure 2.25 shows the relationship between transit person delay and total NOx emissions. Since a major improvement in NO_x emissions is achieved by improving the operation of transit vehicles, transit person delay has a direct relationship with emissions. Thus, increasing the weight of emissions in the objective function leads to the improvement of both emissions and transit person delay. Figure 2.25a shows that at the intersection flow ratio of 0.4, 0.6, and 0.9, changing the emission weight from 0 to 1 results in up to respectively, 240 sec, 355 sec, and 175 sec improvement in transit person delay.

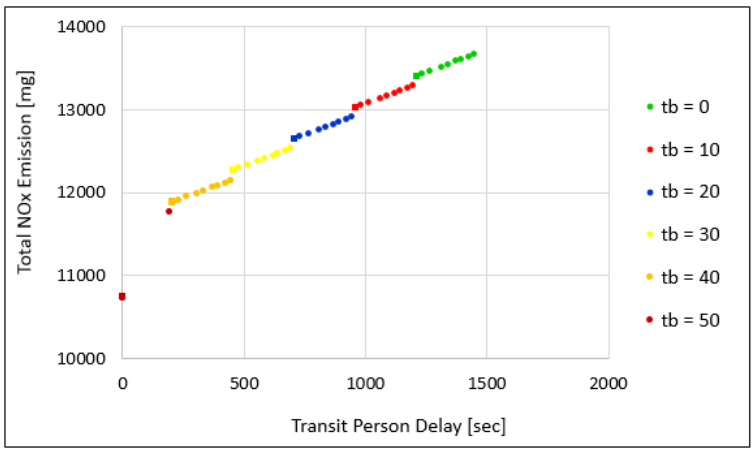

(a) Intersection flow ratio = 0.4

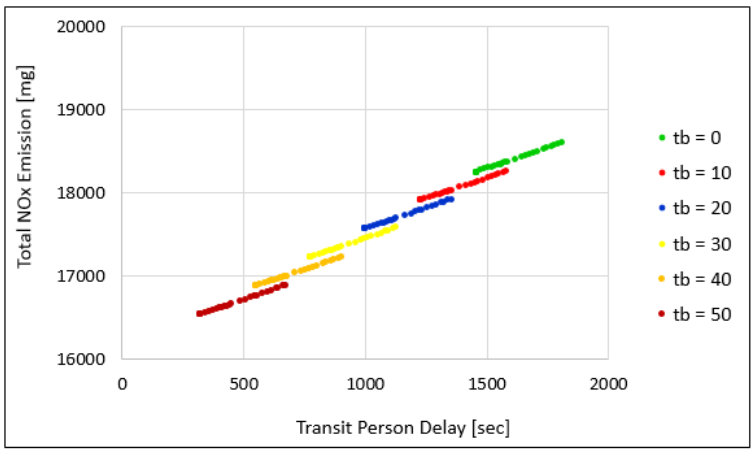

(b) Intersection flow ratio = 0.6

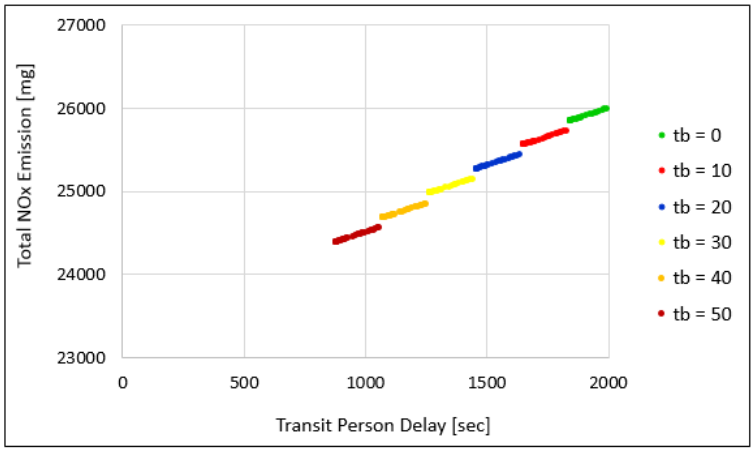

(c) Intersection flow ratio = 0.9

Figure 2.25: The relationship between transit person delay and total NO_x emission for varying weight factors.

Figure 2.26 shows the resulted person delay and emissions across the Pareto optimal solutions when a combination of total person delay and CO emission is optimized. Transit vehicles have higher passenger occupancy than auto vehicles and if the traffic conditions allow, they may receive priority when a high delay weight, λ_d, is used in the objective function. Figure 2.26a shows that as λ_d varies from 0 to 1, total person delay decreases by 805 sec (0.29 sec/veh) and total CO emission increases by 2320 mg (1.03 mg/veh). The higher change in emissions compared to 160 mg (0.07 mg/veh) change in Figure 2.12a means that the two objectives person delay and CO emissions are more conflicting than vehicle delay and CO emissions, which is due to the higher passenger occupancy of transit vehicles.

As the intersection flow ratio increases (Figures 2.26b and 2.26c) lower changes in person delay and CO emissions are observed. In addition, at the intersection flow ratio of 0.9 when a combination of vehicle delay and CO emission was optimized, all weighting factors resulted in the same solution (Figure 2.12c). However, Figure 2.26c shows that when a combination of person delay and CO emission is optimized, the signal timings can be adjusted to some extent to favor one of the objectives over the other. According to this figure, an improvement of 1260 mg (0.25 mg/veh) in CO emissions can be achieved at the price of 80 sec (0.013 sec/person) increase in person delay.

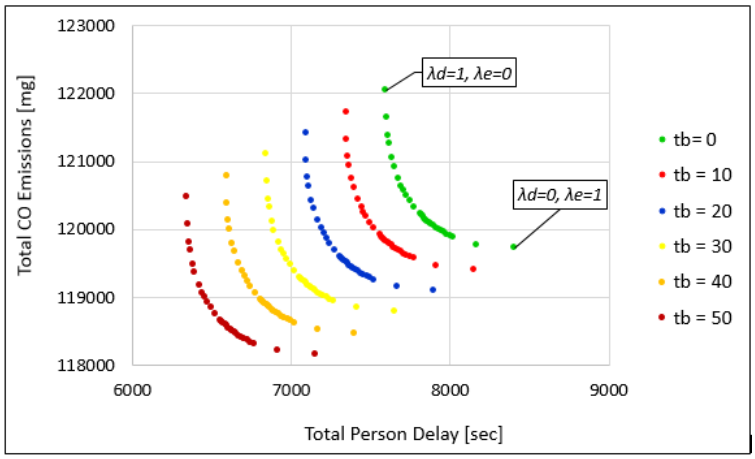

(a) Intersection flow ratio = 0.4

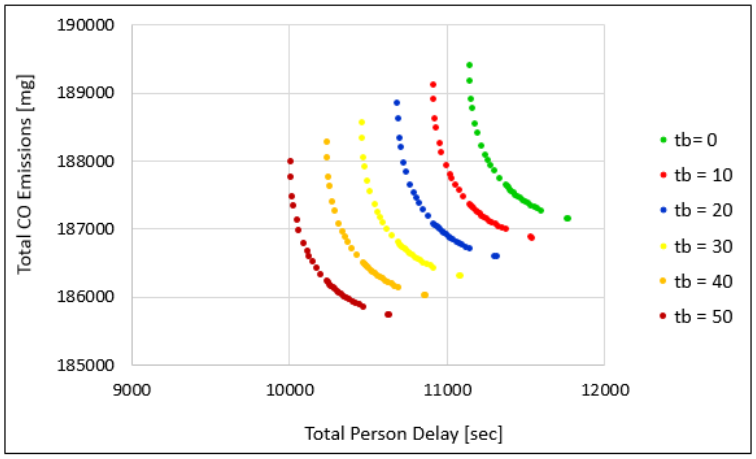

(b) Intersection flow ratio = 0.6

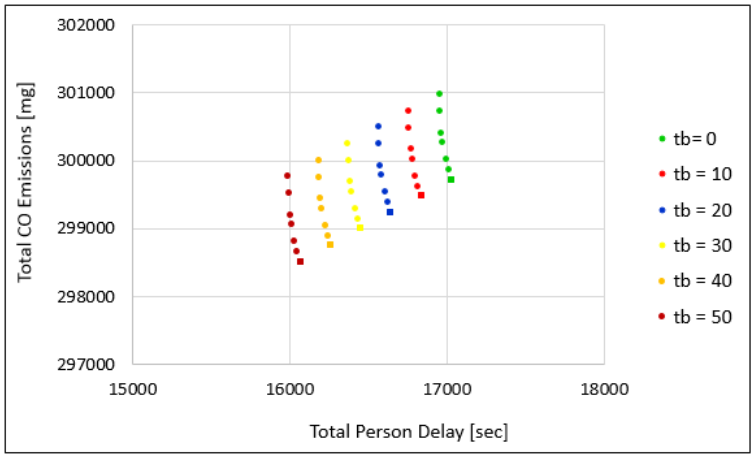

(c) Intersection flow ratio = 0.9

Figure 2.26: Trade-off between total person delay and CO emission when a transit vehicle arrives in lane group 8.

Figure 2.27 shows the relationship between transit person delay and total CO emissions across Pareto optimal solutions when a transit vehicle arrives in lane group 8. Figure shows that when a higher weight is given to CO emission, transit person delay increases. As mentioned earlier, improving CO emission in achieved through improving auto operations. Therefore, depending on the general traffic condition and the lane group that a transit vehicle arrives in, transit operation may be improved or not. To prevent high delays imposed to transit vehicles, a penalty can be considered for the solutions that worsen transit operation.

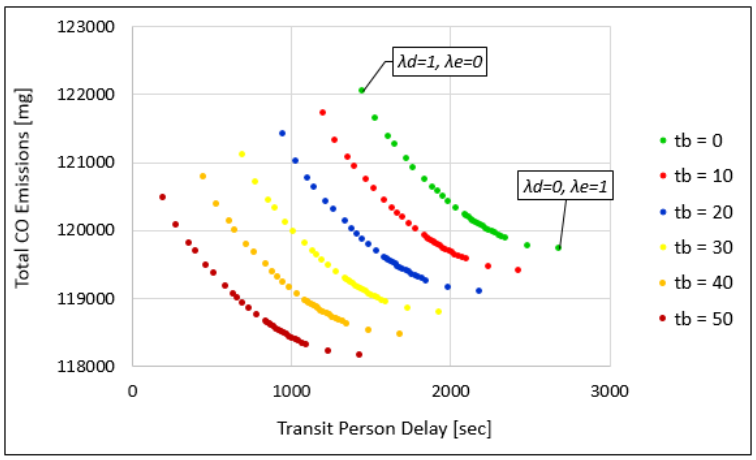

(a) Intersection flow ratio = 0.4

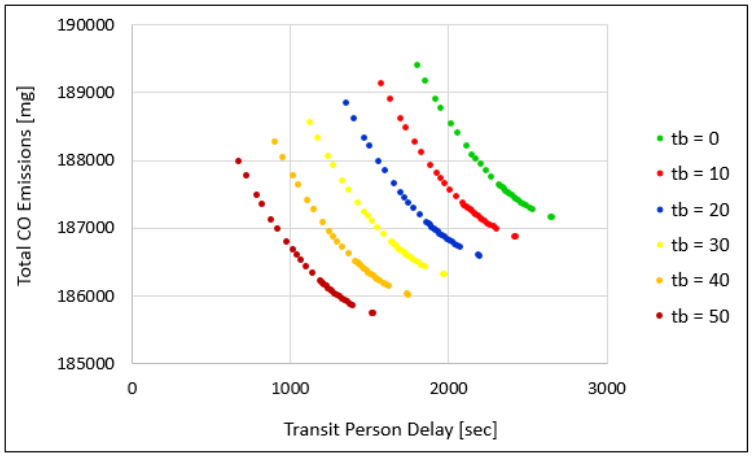

(b) Intersection flow ratio = 0.6

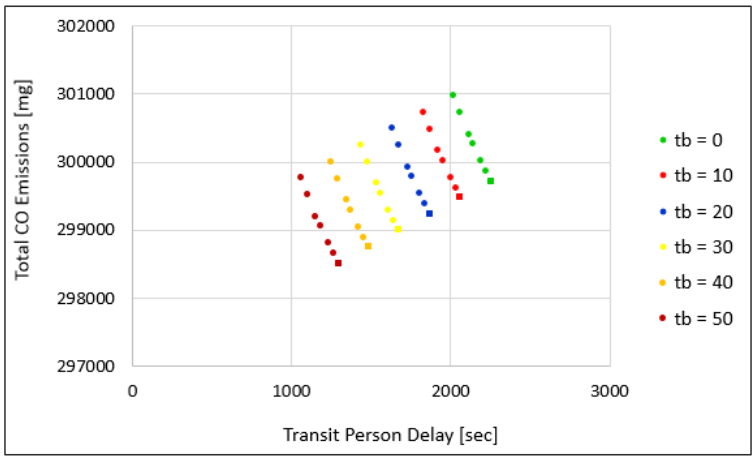

(c) Intersection flow ratio = 0.9

Figure 2.27: The relationship between transit person delay and total CO emission for varying weight factors.

2.5.2.2 Scenarios with Two Buses at the Intersection

Figure 2.28 shows total person delay and NO_x emissions across Pareto optimal solutions when two transit vehicles in conflicting lane groups 2 and 8 arrive at the intersection. Different combinations of arrival times 0 sec, 10 sec, 20 sec, 30 sec, 40 sec, and 50 sec for each transit vehicle are tested. As mentioned earlier, the two objectives total person delay and NOx emissions are not as conflicting as vehicle delay and NO_x emissions. As a result, changing weighting factors has small impacts on resulted person delay and emissions. If the transit vehicle in lane group 2 arrives at time 0 sec, it is not considered in the optimization of cycle T and it does not have any impact on the optimized signal timings. When this transit vehicle arrives at time 10 sec (Figure 2.28b), it is served during green time (based on the initial signal timings) and again it does not have any impact on signal timings, but since it does not have to stop, the total person delays and emissions are lower compared to Figure 2.28a. When the transit vehicle in lane group 2 arrives at times 20 sec or later, depending on the signal timings it may have to stop or not. Therefore, both transit vehicles in lane groups 2 and 8 are candidates to receive priority. When a high weight is given to the delay term in the objective function, the most improvement in total person delay can be achieved by giving priority to both transit vehicles due to their high passenger occupancy. Similarly, when a high weight is given to the emissions, the highest improvement is achieved by giving priority to the transit vehicles due to their high emission rates. Therefore, when two transit vehicles are candidate to receive priority, but they are in conflicting lane groups, the flexibility of the system to adjust signal timings is low. This is the reason of low changes in person delay and emissions in Figures 2.28c to 2.28f.

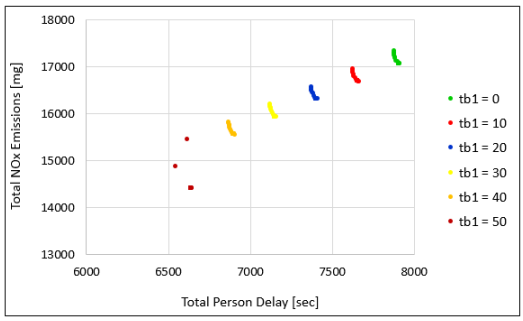

(a) $t_{b_2} = 0$ sec

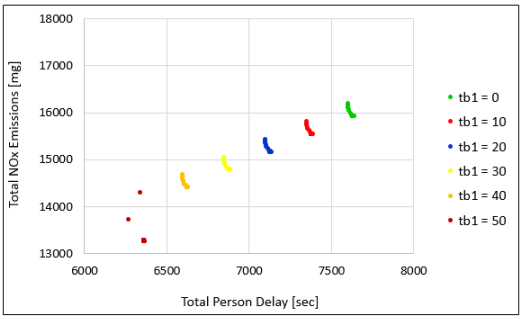

(b) $t_{b_2} = 10$ sec

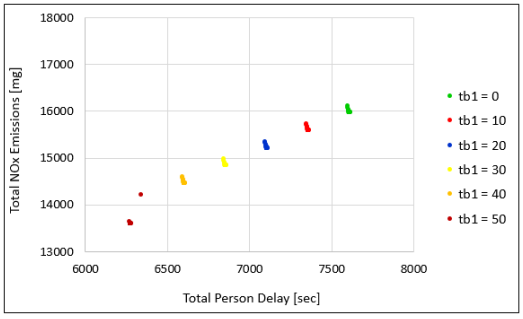

(c) $t_{b_2} = 20$ sec

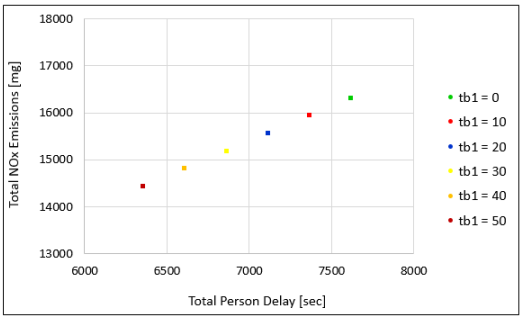

(d) $t_{b_2} = 30$ sec

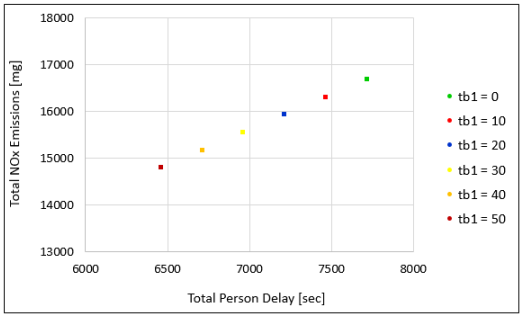

(e) $t_{b_2} = 40$ sec

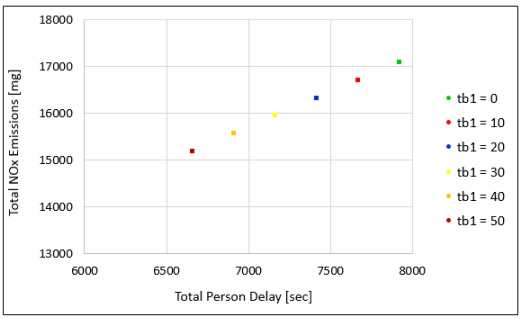

(f) $t_{b_2} = 50$ sec

Figure 2.28: Trade-off between total person delay and total NO_x emission for different weighting factors when two transit vehicles are present at the intersection in lane groups 2 and 8 and the intersection flow ratio is 0.4.

Figure 2.29 shows the relationship between total NO_x emissions and person delay of the transit vehicle that arrives in lane group 8 across Pareto optimal solutions. Figure shows that transit person delay has a direct relationship with total NO_x emissions, which is expected since improvement in total emission can be achieved through

giving priority to transit vehicles. However, in Figures 2.29c to 2.29f corresponding to times 20 sec to 50 sec, considering a second transit vehicle in the optimization, limits the ability of the system to change signal timings and having any impact on transit operations.

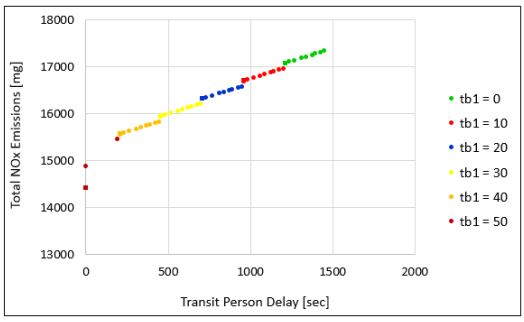

(a) $t_{b_2} = 0$ sec

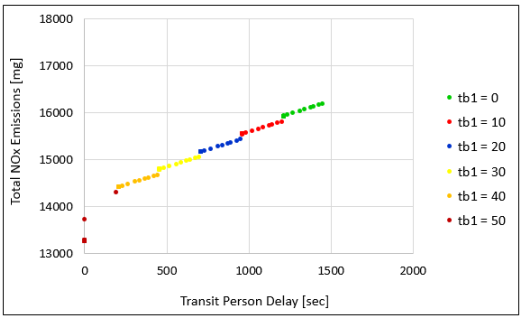

(b) $t_{b_2} = 10$ sec

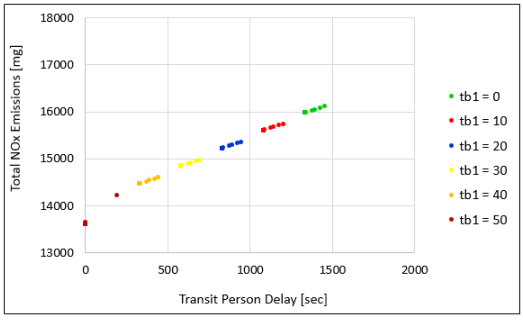

(c) $t_{b_2} = 20$ sec

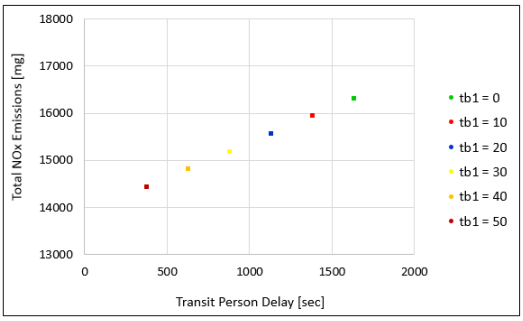

(d) $t_{b_2} = 30$ sec

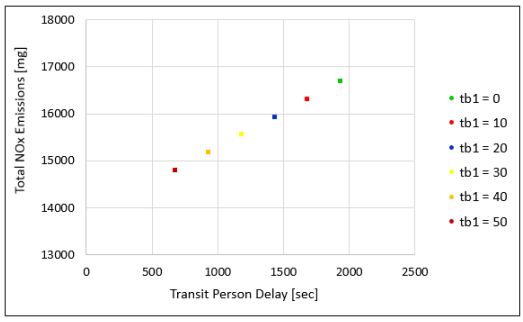

(e) $t_{b_2} = 40$ sec

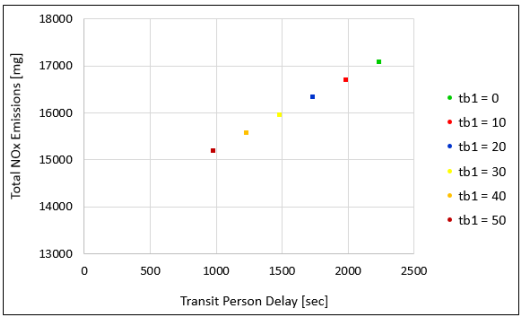

(f) $t_{b_2} = 50$ sec

Figure 2.29: The relationship between the person delay of the transit vehicle that arrives in lane group 8 and total NO_x emission for varying weighting factor when two transit vehicles are present at the intersection in lane groups 2 and 8 and the intersection flow ratio is 0.4.

Figure 2.30 shows changes in person delay and emissions across Pareto optimal solutions when a combination of person delay and CO emissions is optimized. Also, the intersection flow ratio is 0.4 and two transit vehicles arrive at the intersection in conflicting lane groups 2 and 8. As described earlier, when the transit vehicle in lane group 2 arrives at times 0 sec and 10 sec, it does not affect signal timings. However, when this transit vehicle arrives at times later than 20 sec, it imposes some delay to conflicting traffic to receive priority. Comparison of Figure 2.30 with Figure 2.28 suggests that when buses are present at the intersection, the combination of person delay and CO emissions are more conflicting than person delay and NO_x emissions. The reason is that a when CO emission is consider in the objective function, a high weight of emission does not necessarily lead to prioritizing transit vehicles while a high delay weight leads to prioritizing transit vehicles due to their higher passenger occupancy. However, when NO_x emission is considered in the objective function, both high emission or delay weight lead to prioritizing transit vehicles if the general traffic conditions allow. For example, at Figure 2.30d shows that when the transit vehicle in lane group 2 arrives at time 30 sec and as λ_d varies form 0 to 1, total person delay decreases up to 790 sec while when NO_x emission is considered in the objective function 2.30d, there is no trade-off between person delay and emissions.

Figure 2.31 shows the relationship between total CO emissions and the transit vehicle that arrives in lane group 8. As expected CO emissions and transit person delay have an inverse relationship since high emission improvements can be achieved through improving general traffic operations. The increase in transit person delay when a high emission weight is used shows the importance of directly or indirectly (i.e. using a penalty for solutions that leads to increased transit delay) considering transit operation in the objective function.

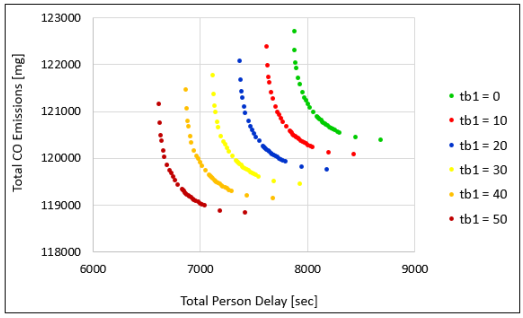

(a) $t_{b_2} = 0$ sec

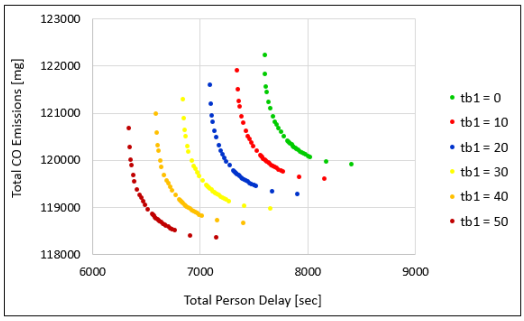

(b) $t_{b_2} = 10$ sec

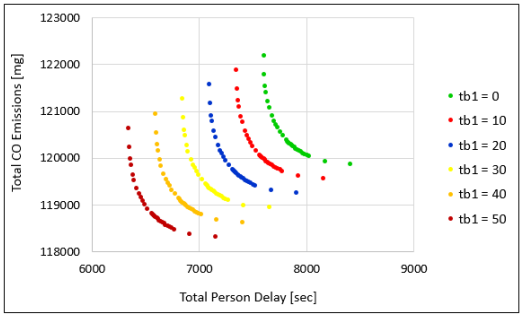

(c) $t_{b_2} = 20$ sec

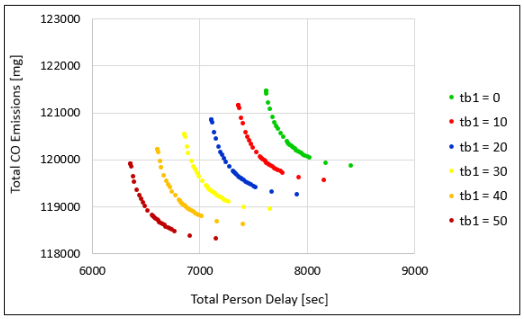

(d) $t_{b_2} = 30$ sec

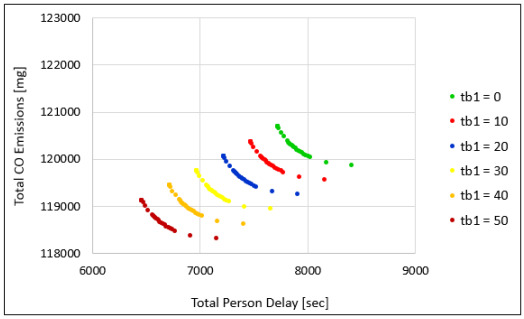

(e) $t_{b_2} = 40$ sec

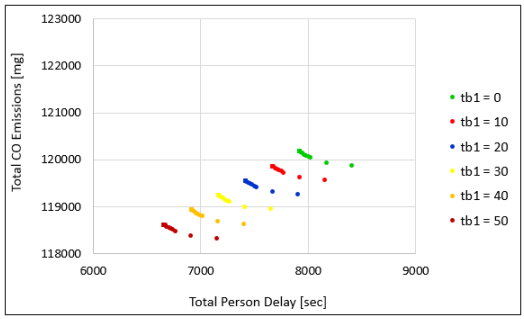

(f) $t_{b_2} = 50$ sec

Figure 2.30: Trade-off between total person delay and total CO emission for different weighting factors when two transit vehicles are present at the intersection in lane groups 2 and 8 and the intersection flow ratio is 0.4.

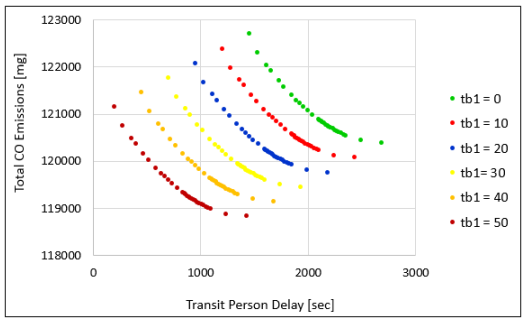

(a) $t_{b_2} = 0$ sec

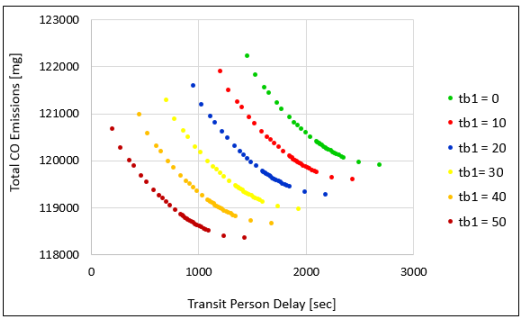

(b) $t_{b_2} = 10$ sec

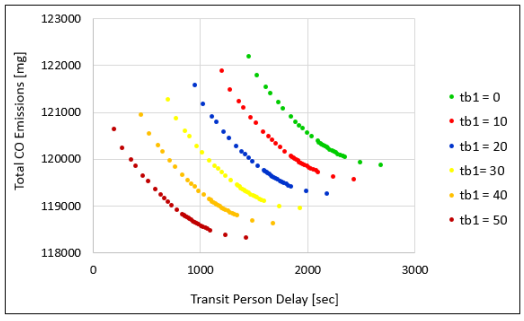

(c) $t_{b_2} = 20$ sec

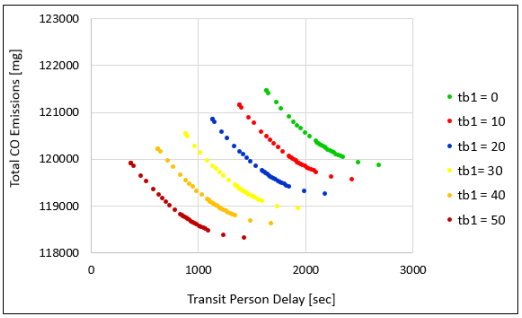

(d) $t_{b_2} = 30$ sec

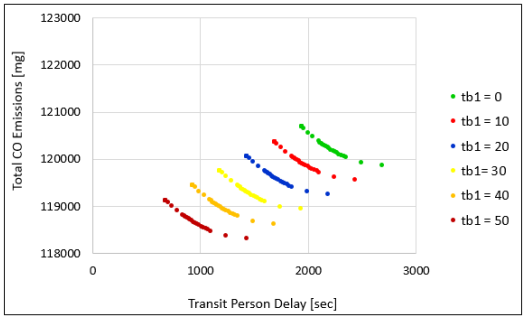

(e) $t_{b_2} = 40$ sec

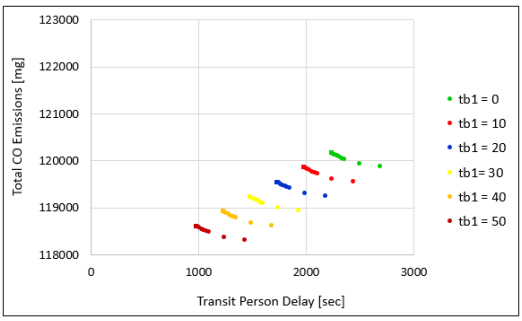

(f) $t_{b_2} = 50$ sec

Figure 2.31: The relationship between the person delay of the transit vehicle that arrives in lane group 8 and total CO emission for varying weighting factor when two transit vehicles are present at the intersection in lane groups 2 and 8 and the intersection flow ratio is 0.4.

Figure 2.32 shows the trade-off between delay and CO emissions when two transit vehicles in lane groups 2 and 8 are present at the intersection and the intersection flow ratio is 0.9.

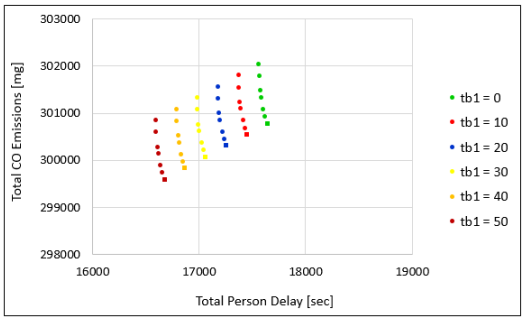

(a) $t_{b_2} = 0$ sec

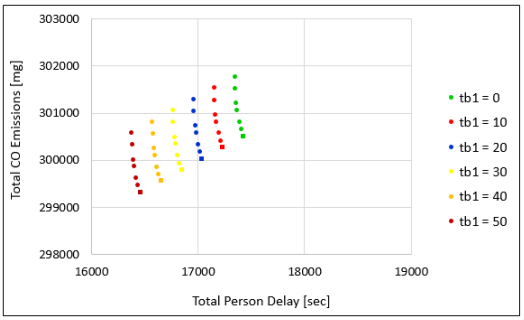

(b) $t_{b_2} = 10$ sec

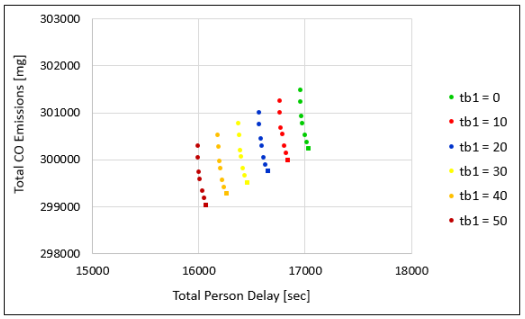

(c) $t_{b_2} = 20$ sec

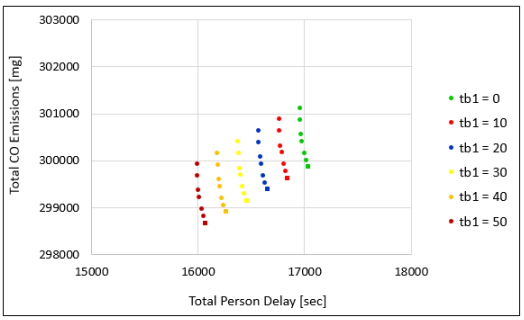

(d) $t_{b_2} = 30$ sec

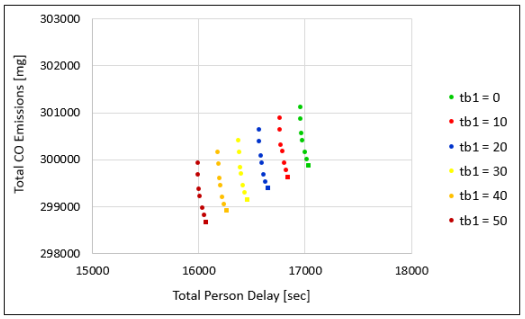

(e) $t_{b_2} = 40$ sec

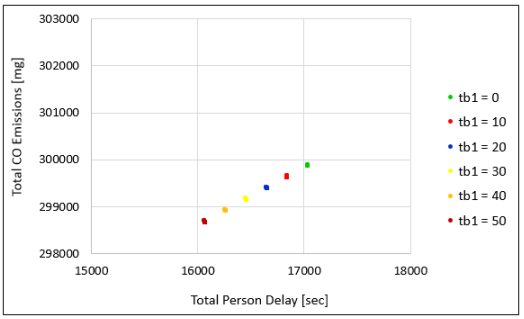

(f) $t_{b_2} = 50$ sec

Figure 2.32: Trade-off between total person delay and total CO emission for different weighting factors when two transit vehicles are present at the intersection in lane groups 2 and 8 and the intersection flow ratio is 0.9.

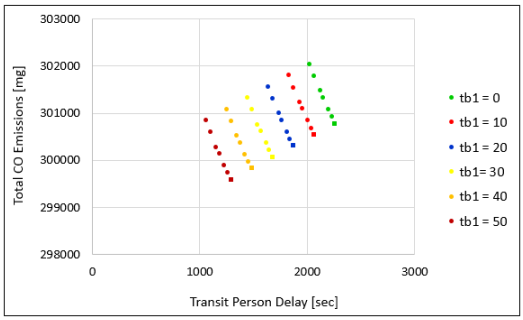

(a) $t_{b_2} = 0$ sec

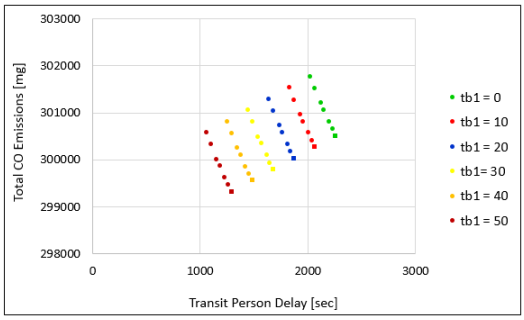

(b) $t_{b_2} = 10$ sec

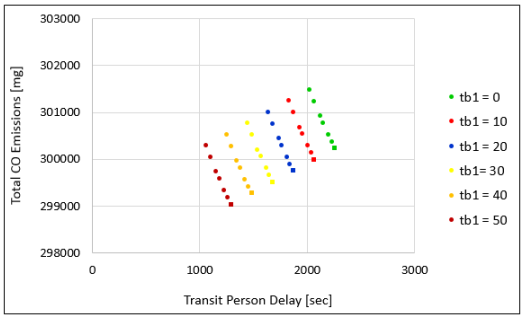

(c) $t_{b_2} = 20$ sec

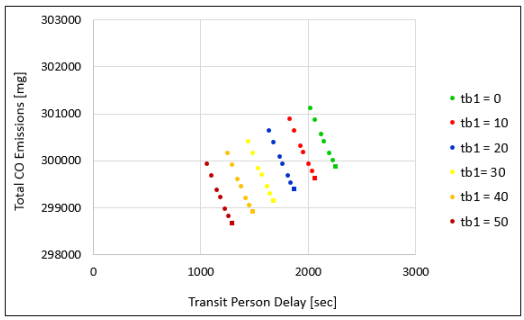

(d) $t_{b_2} = 30$ sec

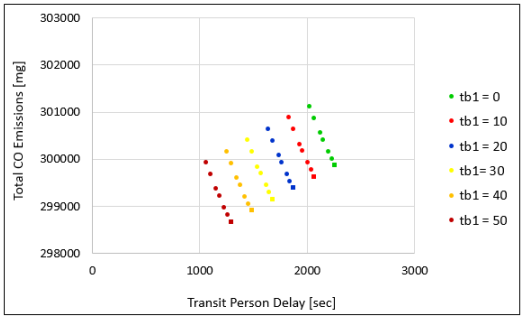

(e) $t_{b_2} = 40$ sec

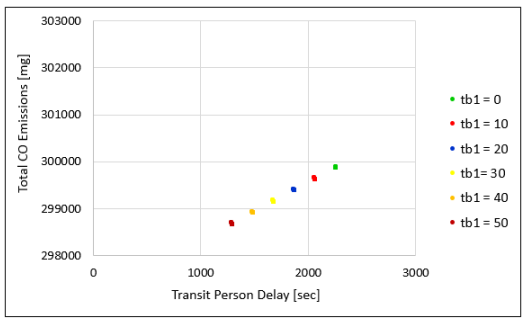

(f) $t_{b_2} = 50$ sec

Figure 2.33: The relationship between the person delay of the transit vehicle that arrives in lane group 8 and total CO emission for varying weighting factor when two transit vehicles are present at the intersection in lane groups 2 and 8 and the intersection flow ratio is 0.9.

2.5.2.3 Scenarios with Three Transit Vehicles at the Intersection

Figure 2.34 shows the trade-off between total person delay and NO_x emissions when three transit vehicles in lane groups 1, 2, and 8 arrive at the intersection during the

optimization cycle. Transit vehicles in lane groups 8 and 2 arrives at times 0 sec and 30 sec, and the arrival time of transit vehicle in lane group 1 varies from time 0 sec to 50 sec. The figure shows that the system has not any flexibility to adjust signal timings to favor person delay or emissions as the weighting factors change.

The same scenario has been performed considering CO emissions in the objective function and results are shown in Figure 2.35. In this case there is a trade-off between person delay and emissions across Pareto optimal solutions. This shows that the pair of person delay and CO emissions are more conflicting than the pair of person delay and NO_x emissions.

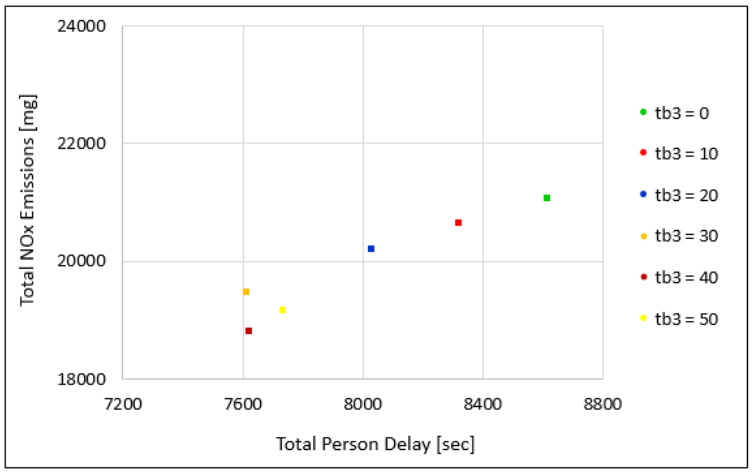

Figure 2.34: Trade-off between total person delay and total NO_x emissions when three transit vehicle are present at the intersection in lane groups 1, 2, and 8 and the intersection flow ratio is 0.4.

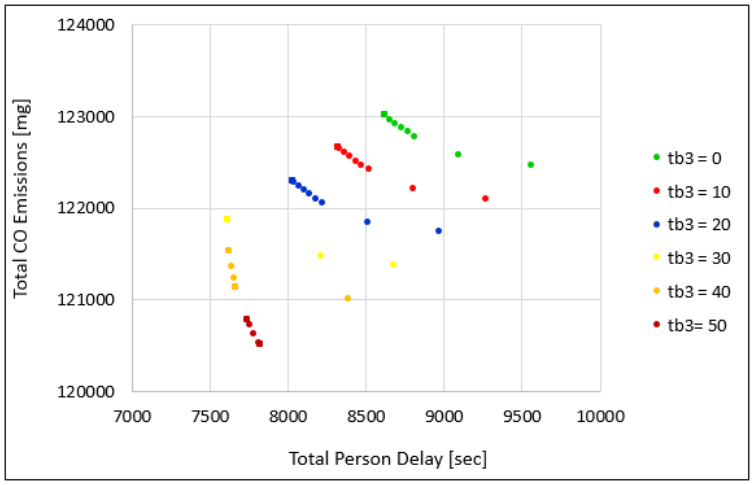

Figure 2.35: Trade-off between total person delay and total CO emissions when three transit vehicle are present at the intersection in lane groups 1, 2, and 8 and the intersection flow ratio is 0.4.

2.6 Cost Analysis

To evaluate and compare the delay and emissions associated with Pareto optimal solutions, the same unit should be used for both performance measures. Therefore, the cost of delay and emissions is evaluated across Pareto optimal solutions. Figure 2.36 shows the Pareto Frontier resulted from optimizing weighted combinations of vehicle delay and NO_x emission are minimized. To convert delay and emission to associated costs, value of time of 15 \$/hr (average value of time per person in Chicago [51]) and NO_x emission cost of 77,000 \$/ton [67] is used. As shown in the figure the rate of change in emission cost is significantly lower than the rate of change in delay cost across Pareto optimal solutions.

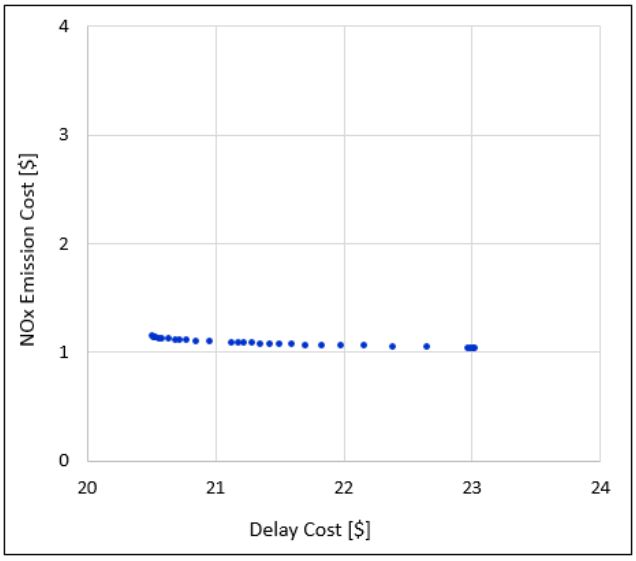

Figure 2.36: Delay and NO_x emissions cost associated with Pareto optimal solutions

2.7 Summary of Findings

Two real-time signal control systems are proposed for isolated intersections, which operate at undersaturated traffic conditions. The first signal control strategy minimizes a weighted combination of total vehicle delay and total emissions and the second signal control system minimizes a weighted combination of total person delay and emissions. Both auto and transit vehicles are considered in the developed signal control system. The impact of each individual auto and transit vehicle on optimal signal timings is significantly different due to their different passenger occupancy and emission rates for those two modes. Furthermore, this signal control system is able to deal with a situation when more than one transit vehicle arrive in conflicting routes, based on the impact they have on total delay and emissions at the intersection.

The experiments performed to evaluate the performance of the signal control strategies showed that total vehicle delay and emissions objectives or total person delay and emissions could be highly conflicting depending on the considered pollutant and emission rates used. Furthermore, the operation of transit vehicles could be

directly or inversely related to total emissions again depending on the specific pollutant considered. This study presents optimal solutions and the trade-offs between delay and emissions as well as their impact on transit operation for different combinations of the two conflicting objectives. The presented Pareto Frontiers help authorities make informed decisions regarding the appropriate choice of objective function for a specific site and meeting emission standards considering the impact on traffic and transit operations at an intersection.

The study shows that when there is no transit vehicle at the intersection and a combination of total vehicle delay and NO_x emissions is optimized, there is a low trade-off between delay and emissions due to low NO_x emission rates of autos. However, when there are transit vehicles at the intersection, these two objectives are highly conflicting and also significant improvements in NO_x emissions can be achieved by improving transit operations. On the contrary, total vehicle delay and CO emissions are more conflicting because of higher CO emission rates of auto vehicles, but the presence of transit vehicles does not have a major impact on signal timings due to low CO emission rates of transit vehicles compared to autos. Furthermore, total person delay and NO_x emissions are less conflicting than the objectives total person delay and CO emissions when transit vehicles are present at the intersection. The reason is that in the former, highest improvements can be achieved through prioritizing transit vehicles no matter what weighting factors are used. However, in the latter, transit vehicles are likely to get priority and impact signal timings if a high weight for delay is used. The study also shows that the system is less flexible to adjust signal timings at higher intersection flow ratios and lower trade-off between average delay and emission per vehicle (or per person) is observed.

Future studies will focus on extending the current signal control strategy to account for the entire range of traffic conditions from undersaturated to oversaturated

condition. Furthermore, the assumptions of constant cycle length or phase sequence will be relaxed to improve the flexibility of the system to optimize signal settings.

CHAPTER 3

ENVIRONMENTAL PERFORMANCE OF ROUNDABOUTS

The need for a simple yet adequate tool that can be used for a comprehensive evaluation of the performance of roundabouts motivates this study. A model based on Cellular Automata (CA) is developed to simulate traffic conditions at a single-lane roundabout and the corresponding signalized intersection to obtain vehicle trajectories and estimate operational measures (i.e. travel time and delay). Vehicle trajectories are also used along with VSP-based emission rates to estimate emissions at the roundabout and signalized intersection. The operational and environmental performance of single-lane roundabouts and signalized intersections under different traffic conditions (i.e. total traffic demand and left turn ratios) and pedestrian volumes are compared against each other. The conclusions of this study on the operational and environmental performance of roundabouts can assist transportation engineers make informed decisions when to replace a signalized intersection with a roundabout.

This chapter is organized as follows. First, the general CA model for traffic simulation is presented. Then, the CA model is calibrated for a roundabout and a signalized intersection with single-lane approaches. After that, the estimation of VSP-based emission rates for gasoline cars and diesel buses is presented. The next section describes the sensitivity analysis scenarios designed for evaluating the performance of roundabouts and signalized intersections under different conditions. Before presenting the results of sensitivity analysis, the CA-based models are compared with the results from the Aimsun microsimulation tool. Then, the results of sensitivity analysis are discussed and conclusions are presented.

3.1 Traffic Simulation based on Cellular Automata

The CA model is used in this study because of the following reasons:

- the model needs simple calibration,
- it reproduces individual vehicle's trajectories,
- it can account for different moving objects with different lengths by considering an appropriate cell length and number of cells for each object, and
- ideally, it can account for different cruising speed of vehicles (depending on the simulation step),

Cellular Automata (CA) is a mathematical model, first developed in 1948 by a mathematician and physicist, John Louis von Neumann to understand biological evolution and self-reproduction in biological systems [78]. After that , the concept was used in a broad range of fields. In early 1990s, it was used in traffic simulation by two German physicists Kai Nagel and Michael Schreckenberg [55]. The original Nagel-Schreckenberg model was a simple model for freeway traffic flow that could reproduce traffic jams (i.e. the model could show transition from laminar flow to start-stop waves with increasing vehicle density.)

A cellular automaton is a system that consists of cells with equal size that form a one or multi-dimensional array. Each cell can be in a state of a finite set of states and interacts with its neighboring cells. The state of a cell is updated at discrete time steps using the information of the state of the cell itself and its neighboring cells at the previous time step based on some predefined rules. Therefore, all cells can be updated in parallel as the information of the previous time step is sufficient to update a cells' state [55].

The Nagel-Schreckenberg model for traffic simulation is defined as a one-dimensional array of cells, which represents a freeway segment. Each cell has a length of 7.5 m

and can be either occupied by one vehicle or be empty. Vehicles travel at a speed that takes an integer value between 0 and v_{max}. A speed value represents the number of cells a vehicle moves forward during one time step (i.e. simulation step). The rules to update a cell's state are as follows:

1. Acceleration: If the gap in front of a vehicle (i.e. the number of empty cells between a vehicle and the preceding vehicle) is greater than the current speed and the current speed is less than v_{max}, then the speed of the vehicle will be increased by one.

$$\text{if gap} > v_t \text{ and } v_t < v_{max} \Rightarrow v_{t+1} = v_t + 1 \tag{3.1}$$

2. Deceleration (due to other vehicles): if the gap in front of a vehicle is less than its current speed, then the speed will be decreased to the available gap such that the vehicle stops behind the preceding vehicle.

$$\text{if gap} = i \text{ and } i < v_t \Rightarrow v_{t+1} = i \tag{3.2}$$

3. Randomization: if the velocity of a vehicle is greater than zero, it will be decreased by one with probability p.

4. Movement: Each vehicle moves v cells forward.

where v_t and v_{t+1} are the speed of a vehicle at time steps t and $t+1$, respectively. The randomization step is essential in simulating traffic to account for fluctuations due to human behavior or varying external conditions such as road's geometry. Figure 3.1 shows the state of a short section of three cells during 6 time steps.

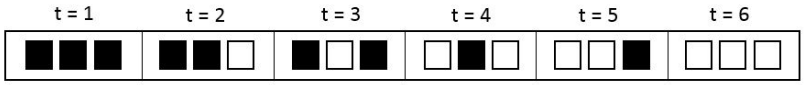

Figure 3.1: Vehicles movement in CA model

It is worth noting that in the CA model when a queue of vehicles is dissipating, each vehicle has a reaction time of one simulation step to move forward since it should see an empty cell in front at the previous simulation step to be able to move forward at the current simulation step. For example, when there is a queue at a roundabout and there is enough gap in the circular section, vehicles enter the roundabout at a headway of two simulation steps as show in figure 3.2

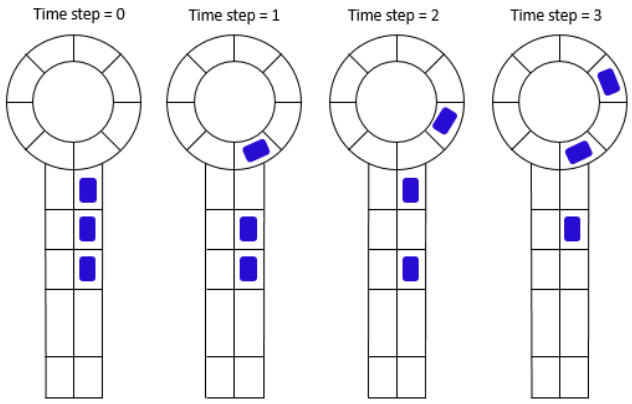

Figure 3.2: The state of the roundabout at consecutive simulation steps steps when there is a queue at the entry

3.1.1 Application of CA Model on a Roundabout with Single-Lane Approaches

The Nagel-Schreckenberg model is used in this study with the following considerations regarding roundabout's specific traffic rules: 1) Vehicles slow down while approaching the roundabout in order to reach a safe speed to enter the roundabout; 2) Vehicles stop at the entry of the roundabout if there is not sufficient gap (i.e. enough empty cells) in the circulating area; 3) Vehicles need to yield before crosswalks if a pedestrian is present at the crosswalk. Thus, if there is any pedestrian at one of the crosswalks, that corresponding cell is assumed to be occupied until the pedestrian crosses the street. Figure 3.3 illustrates the general cell structure of a single-lane roundabout.

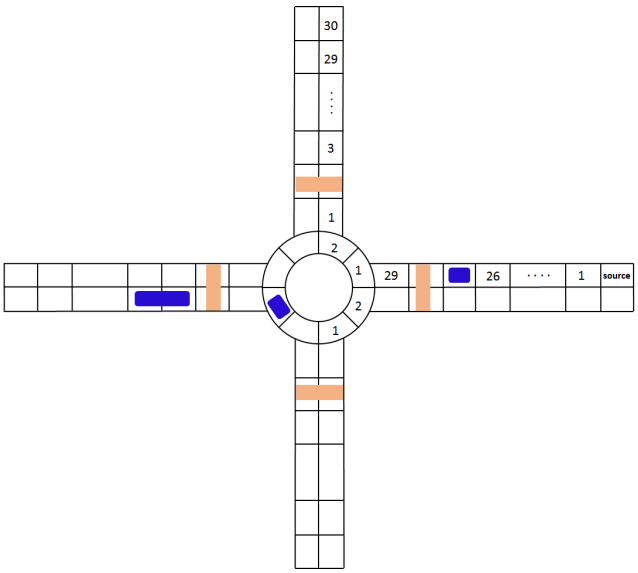

Figure 3.3: Cell structure of a single-lane roundabout

3.1.1.1 Study Site

The roundabout on the campus of the University of Massachusetts (UMass) Amherst (intersection of N. Pleasant St. and Governor's Dr.), is used as the case study. Figure 3.4 shows an aerial photo of the study site.

Figure 3.4: The roundabout at the intersection of N. Pleasant St. and Governor's Dr., Amherst, MA [5]

The real-world traffic demand and pedestrian volume data are used as the basis of the experiments. Data on traffic demand and pedestrian volume was collected using

installed cameras at the site during 8:00 AM - 10:00 AM on 10/25/2016 (Tuesday), and the peak hour demand (8:30 AM - 9:30 AM) is used in this study, which is presented in Table 3.1. Traffic and pedestrian arrivals are assumed to follow Poisson distribution with mean flow rates according to the collected data in the field. In addition, the real-world schedule of Pioneer Valley Transit Authority (PVTA) buses is used along with general traffic demand. At a signalized intersection with cycle length of 51 sec, green splits of 22.5 sec for both NB-SB and EB-WB directions and yellow time of 3 sec (optimal signal timings obtained by SYNCHRO), the real-world traffic demand results in a volume-to-capacity (v/c) ratio of 0.5.

Table 3.1: Traffic and pedestrian demand at the roundabout of N. Pleasant St. and Governor's Dr., Amherst, MA

	Traffic Demand (veh/hr)				Pedestrian Volume (Ped/hr)
	N. Pleasant St. (NB)	Eastman Ln. (WB)	N. Pleasant St. (SB)	Governor's dr. (EB)	
N. Pleasant St. (NB)		62	69	49	159
Eastman Ln. (WB)	59		89	196	168
N. Pleasant St. (SB)	116	103		250	80
Governor's dr. (EB)	38	107	74		75

An INTERSECTOR radar [7] was used to collect vehicles' real-world trajectories at the test site during a non-peak time (11:30 AM - 12:00 PM) to approximate the models' speed limits based on the real speed of non-stopping vehicles. Vehicles' speed do not necessarily follow the posted speed limits on the site. Observations show that vehicles travel at higher speeds at far distances from the roundabout and slow down when they get closer to reach a safe speed to enter the roundabout. In the CA model, the maximum speed on different segments of the approaching links is calibrated such that simulation trajectories better match real-world trajectories.

The radar was installed on a light post on the southbound direction of the N. Pleasant St. (downstream the roundabout) to capture vehicles' trajectories approach-

ing from the upstream link. The radar could detect vehicles at approximately 200 m upstream the roundabout and monitor their movement until they arrive at the roundabout (point 0 on the horizontal axis on Figure 3.5). In some cases captured trajectories continue to some distance inside the roundabout, but the speed data of radar is not very accurate for close distances where the angle between the radar and the moving object is large. Therefore, we do not use those parts of trajectories (inside the roundabout) for speed calibration.

Figure 3.5 shows representative trajectories (i.e. speed vs. distance from the roundabout) of vehicles that do not have to stop or decelerate due to a preceding car, conflicting traffic, or pedestrian. These vehicles only slow down to reach a safe speed at the entry of the roundabout. It is described in subsection 3.1.1.2 that how speed limits in the CA model are determined using the real-world trajectories. The next subsection presents the general inputs of the roundabout CA model.

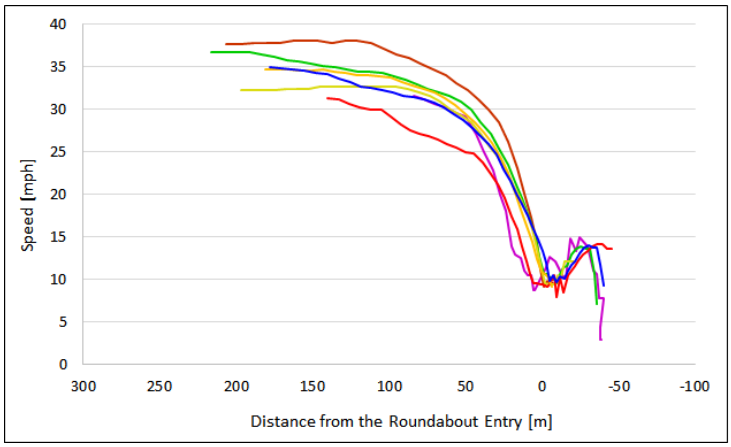

Figure 3.5: Trajectories of non-stopping vehicles (southbound direction)

3.1.1.2 General Inputs

The inputs to the model are as follows:

- **Cell length:** A length of 7.5 m is assumed for each cell as the length assumed in the Nagel-Schreckenberg model, which is the sum of 4.5 m that is the repre-

sentation of an average length of a car and 1.5 m empty space at the beginning and end of a cell. Buses have a length of 12 m and they occupy two cells.

- **Cellular structure:** The circular part of the roundabout consists of 8 cells, so each quarter consists of 2 cells as shown in figure 3.3. A length of 225 m (30 cells) has been considered in the simulation of the roundabout. This length is selected such that it covers the maximum queue length for the tested scenarios.

- **Simulation step:** One of the limitations of the CA model is related to the choice of an appropriate simulation step. The choice of the simulation step affects the speed resolution (i.e. feasible speed levels) in a CA model since vehicles should be able to travel at least one cell per simulation step. As a result, the smaller the simulation step the greater the speed values are. Usually, a simulation step of 1 second is used in CA-based traffic models for freeways. At urban intersections, the fluctuations in speed are more than at freeways due to the interactions between vehicles, pedestrians, and the geometric design of the intersections as well as the presence of control. Therefore, a smaller simulation step results in better capturing these fluctuations. On the other hand, a smaller simulation step leads to less accurate speed estimations at urban streets, which have lower speed limits than freeways. Thus, attention should be paid when selecting the simulation step. In this study, the roundabout traffic is modeled using two different simulation steps of 1 sec and 1.5 sec and the model that most accurately fits the results obtained by Aimsun microsimulation tool is used to perform the sensitivity analysis. A simulation step of 1.5 sec results in discrete speed levels of 11.2 mph, 22.4 mph, and 33.6 mph for respectively, 1, 2, and 3 cells per simulation step. We will see later this choice of simulation step leads to a reasonable gap acceptance, follow-up headway, and entry speed of vehicles at the roundabout. On the other hand, this specific simulation step has some

disadvantages such as a circulating speed inside the roundabout that is higher than the average real-world speed. A simulation step of 1 sec results in discrete speed levels of 16.8 mph and 33.6 mph for 1 and 2 cells per simulation step. A simulation step of 1 sec results in more accurate speed inside the circulating area, but higher acceleration/deceleration rates. The pros and cons of each simulation step are presented later in this section.

- **Pedestrian crossing:** Pedestrian crosswalks are located at approximately 10 m before the entry and after the exit of the roundabout. If a pedestrian is present at a crosswalk, the corresponding cell is assumed to be occupied until the pedestrian crosses the lane. According to the Highway Capacity Manual (HCM 2010), pedestrian walking speed for crossing a street is 3.5 ft/sec (1.07 m/sec) for most conditions with small number of old pedestrians. The walking distance on each crosswalk (curb to refugee island and vice versa) is 5.2 m. Therefore, a pedestrian needs 4.9 sec to cross each lane. However, the average of pedestrians' crossing times at the test site obtained from the video data (collected from 8:00 AM - 10:00 AM on 10/25/2016) were on average 4.2 seconds (the reason for lower real crossing time than the one presented in HCM 2010 is that the majority of pedestrian population at this specific test site is young college students). Therefore, in the experiments with simulation step of 1.5 sec and 1 sec, pedestrian crossing time of respectively 3 simulation steps and 4 simulation steps for crossing the crosswalks on both directions of a link is used. Gates et la. [31] showed that pedestrian groups of 5 or more are about 0.6 ft/s (0.18 m/sec) slower than individuals. However, there is no pedestrian signal at the roundabout and it was observed that the majority of pedestrians cross the street individually once they arrive at the crosswalk. Thus, the group effect on walking speed is ignored in the roundabout CA model. It is however, later

considered in the calculation of pedestrians crossing time when simulating the signalized intersection.

- **Speed limits:** The speed resolution of the CA model does not allow an accurate calibration of speed. For the roundabout CA model with a simulation step of 1.5 sec, field trajectories at the test site are used to determine the speed limits. The feasible speed levels in the CA model with simulation step of 1.5 sec are 11.2 mph, 22.4 mph, and 33.6 mph. As illustrated in figure 3.5, the maximum speed of vehicles is between 32 mph to 37 mph. Therefore, the highest speed in the CA model is assumed to be 3 cells/simulation step (33.6 mph). The lengths to impose speed limits of 2 cells/simulation step and 3 cells/simulation step are selected such that the sum square of the differences of real speeds on trajectories and the speed limit of the sections gets minimized. As a result, the maximum speed of vehicles on upstream links is 3 cells/simulation step from the beginning of the link to 47 m upstream the roundabout. Vehicles slow down to 2 cells/simulation step when they have a shorter distance of 47 m ($\approx$6 cells) to the roundabout and they again decelerate to 1 cell/simulation step at the last cell upstream the roundabout. Since vehicles trajectories within the roundabout and the exiting link are not available, video data is used to simply estimate the speed based on travel time and distance between two points for vehicles that do not slow down due to a preceding vehicle or a pedestrian. The observations showed an average speed of 15 mph inside the roundabout and 24.1 mph on the first 5 cells after the roundabout exit. Video data on exiting links was not available so the same speed limit of 33.6 mph used for far cell on upstream link is used here, too. Therefore, the CA speed limits on exiting links are 2 cells/simulation step and 3 cells/simulation step. However, the average speed inside the circular section is not close to any of speed levels (11.2 mph or 22.4 mph), which is a limitation of the CA model that can result in inaccurate

estimation of operational and environmental measures. Figure 3.6a illustrates speed limits on different section of the roundabout when the simulation step is 1.5 sec.

In the simulation models with simulation step of 1 sec, a speed limit of 16.8 mph (≈1 cell/simulation step) is used at 30 m (4 cells) upstream, 22.5 m (3 cells) downstream, and inside the junction. Distances that are further away from the intersection have a speed limit of 33.6 mph (≈2 cells/simulation step). Figure 3.6b shows the speed limit on different sections of the roundabout when the simulation step is 1 sec. In both models with either a simulation step of 1 sec or 1.5 sec, the same speed limits for cars and buses are used because at an urban intersection (where speed limits are not very high) with one-lane approaches they have to follow the same speed limits.

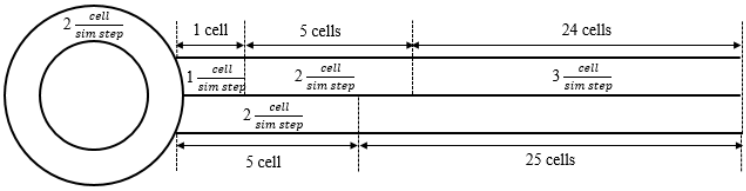

(a) Simulation step = 1.5 sec

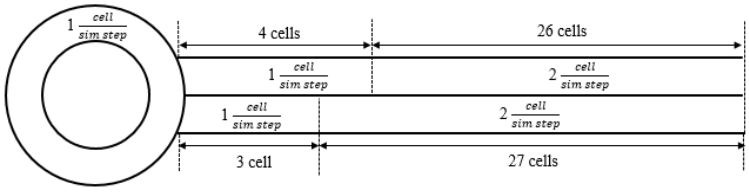

(b) Simulation step = 1 sec

Figure 3.6: Speed limits at the roundabout

- **Critical gap:** Critical gap is the minimum time interval in the circulating flow when an entering vehicle can safely enter a roundabout [83]. According to the National Cooperative Highway Research Program (NCHRP), critical gap

at single-lane roundabouts in U.S. is 4.5 sec, but it is recommended that the site-specific values are used if available [62]. A field study conducted by Abrams et al. [12] to measure the critical gap on the same roundabout modeled in this dissertation suggests a critical gap of 2.2 sec. Therefore, when a simulation step of 1.5 sec is used, the assumed critical gap is approximately 1.5 simulation steps. Considering the speed limit inside the roundabout (2 cell/simulation step) a vehicle, which is not stopped or slowed down by a preceding vehicle, travels 3 cells in 1.5 simulation steps. Therefore, a spatial interpretation of the critical gap is 3 cells (the cell right after the entry plus the cells on the previous roundabout quarter), which is verified by the video data at the roundabout of interest. In simulations with time step of 1 sec, a critical gap of 3 sec is used since, which again has an interpretation of 3 cells considering the speed limit of 1 cell/time inside the roundabout.

- **Follow-up headway:** Follow-up headway is defined as the time between the departure of the first vehicle from the roundabout entry and the departure of the next vehicle when a vehicle exists on the roundabout entry [52]. HCM 2010, HCM 2016, and NCHRP respectively present values of 3.2 sec, 2.6 sec, and 3.2 sec for follow up headway at a single-lane roundabout [52]. The follow up headway in the CA model is directly determined by the simulation step since it always takes 2 simulation steps for the second vehicle in the queue to enter the roundabout (as show in figure 3.2). Therefore, a simulation step of 1.5 sec leads to a follow up headway of 3 sec and a simulation step of 1 sec leads to a follow up headway of 2 sec.

3.1.2 CA Model for a Signalized Intersection

This section describes the CA model for a signalized intersection. Figure 3.8 demonstrates the cell structure of a signalized intersection. The inputs and assumptions of the model are as follows:

- **Cell length:** A cell length of 7.5 m is assumed as the case for the roundabout model.

- **Cellular structure:** The Cellular structure of a signalized intersection with one-lane approaches is shown in figure 3.8. There are four cells inside the intersection and a length of 225 m (30 cells) is assumed for all links.

- **Simulation step:** Simulation step of 1 sec is assumed for the simulation of the signalized intersection. Although this small simulation step results in large speed bins, it leads to the saturation headway of 2 sec, which is recommended by HCM 2010 and has a significant effect on the capacity of the intersection.

- **Pedestrian crossing:** When pedestrians arrive at the intersection wait until their opposite direction's signal turns green. Then, they cross the intersection individually or in groups (if there are more than one pedestrians waiting to cross the same street in the same direction). The crossing speed of pedestrians suggested in HCM 2010 is 3.5 ft/sec (1.07 m/sec), but pedestrian groups of 5 or more are about 0.6 ft/s (0.18 m/sec) slower than individuals [31]. Therefore, when a pedestrian group is larger than 5 pedestrians, their walking speed reduces to 2.9 ft/sec (0.89 m/sec). A width of 3.2 m is used for each lane at the intersection. Thus, individuals or groups of less than 5 pedestrians need 6 sec (6 simulation steps) and groups of more than 5 pedestrians need 7.2 sec ($\approx$ 7 simulation steps) to cross both lanes. Right and left turning vehicles should yield to pedestrians on the crosswalks on both entering and exiting links and wait until the pedestrian leaves the crosswalk before they proceed.

- **Speed limits:** The speed limits have been chosen to be as close as possible to the real-world speed limits (i.e. speed limits at a signalized intersection in an urban area). A speed limit of 16.8 mph (≈1 cells/simulation step) is used from 30 m (4 cells) upstream the intersection to the stop-bar, right after the intersection to 22.5 m (3 cells) downstream, and inside the intersection. Further distances on the links have a speed limit of 33.6 mph (≈2 cells/simulation step). Figure 3.7 shows the speed limits on different sections.

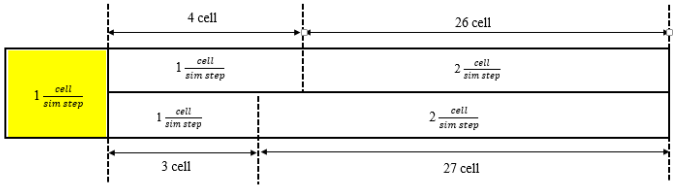

Figure 3.7: Speed limits at the signalized intersection

- **Signal Settings:** The traffic signal operates on two phases and therefore, permissive left turns. Phase 1 serves the Northbound and Southbound directions and phase 2 serves the Eastbound and Westbound directions. In addition, right turn on red is allowed. Signal settings are optimized using SYNCHRO for each designed scenario. The optimized signal timings are presented in table 3.2

Table 3.2: Optimized signal timings by SYNCHRO

	Traffic Demand (% of the base demand)								
	60%	80%	100%	120%	140%	160%	180%	200%	220%
Cycle Length [sec]	51	51	51	56	61	62	65	74	80
Duration of Phase 1 [sec]	23	23	23	27	32	32	34	38	40
Duration of Phase 2 [sec]	22	22	22	23	23	24	25	30	34
Yellow [sec]	3	3	3	3	3	3	3	3	3
Intersection Degree of Saturation	0.31	0.42	0.53	0.63	0.72	0.83	0.93	1.02	1.11

- **Critical Gap:** A critical gap of 3 sec for permissive left turns is assumed. When a vehicle is in the intersection and wants to turn left, it waits for a gap of 3 sec, which has a spatial interpretation of 3 cells (considering 1 sec for the simulation step) in the through traffic.

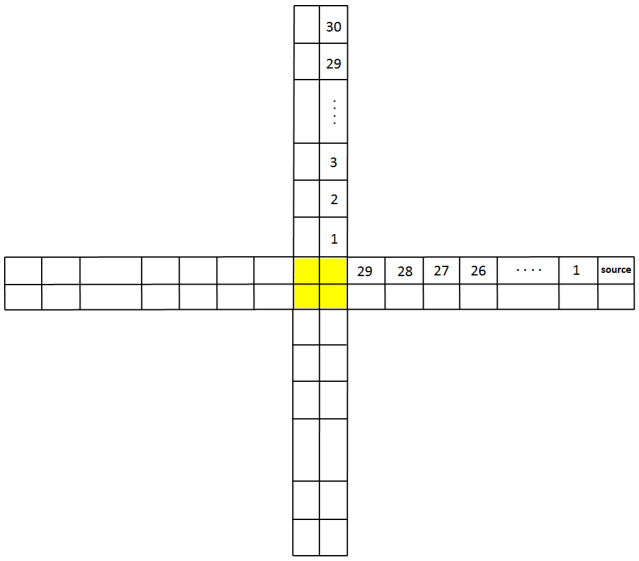

Figure 3.8: Cell structure of a signalized intersection with one-lane approches

3.2 Aimsun Models Calibration

The CA-based simulation models of roundabout and signalized intersection are evaluated by the Aimsun microsimulation tool. Amongst the two roundabout models with simulation steps of 1 sec and 1.5 sec, the model that matches the Aimsun model more is used in the sensitivity analysis experiments. Average travel times obtained from the CA models are compared to Aimsun results at different traffic demands. The simulation parameters used in Aimsun are as follows:

- simulation step: 1 sec,
- reaction time to stop: 1.35 sec,
- reaction time at traffic light: 2 sec,
- initial safety margin [1] of 3 sec,

[1] "a safety gap required between a passing yielding vehicle and the next priority vehicle. This gap is used when the yielding vehicle has just arrived at the yield sign." [1]

- final safety margin[2]: 1 sec,
- initial give-way time factor[3]: 1,
- final give-way time factor[4]: 2.

Aimsun does not have a single value for critical gap at roundabouts, but the gap acceptance behavior can be calibrated using the last four parameters described above. The Aimsun default values are used for these parameters.

3.3 Emission Rates

After simulating traffic and reproducing vehicles' trajectories, emission is estimated using the speed profile of individual vehicles. As explained in chapter 2, vehicular emission rates are significantly different across the vehicle operation modes and acceleration has the highest emission rates. In addition, it is shown that the Vehicle Specific Power (VSP) approach, which is an indicator of the vehicle's engine power is directly associated with vehicle's emission rates [14]. Therefore, we use the VSP-based emission rates along with vehicle trajectories to estimate emissions.

To calculate VSP-based emission rates, the equations presented by Frey et al. [29] and Zhai et al. [86] respectively for gasoline cars and diesel buses are used. Emission rates are estimated for the transition from one to the next simulation step. A vehicle's speed for the period from time t to $t+1$ is the average of the two speeds at these two simulation steps. Since a vehicle's speed increases up to 1 cell/simulation step (this is a rule of the CA model that vehicles cannot increase their speed more than

---

[2] "a safety gap required between a passing yielding vehicle and the next priority vehicle. This gap is used when the yielding vehicle has now been waiting for a time at the yield sign." [1]

[3] "Multiplied by the giveWayTime of the vehicle, this factor determines when the gap required by the vehicle starts to decrease linearly from the maximumGap value."[1]

[4] "Multiplied by the giveWayTime of the vehicle, this factor determines when the gap required by the vehicle has reached the minimumGap value." [1]

1 cell/simulation step), the acceleration rate will be either zero or 1 cell/(simulation step)^2, which results in an approximate acceleration rate of 4.44 m/s^2 when a simulation step of 1.5 sec is used and 7.5 m/s^2 when a simulation step of 1 sec is used. Deceleration rate gets any of the values of -1, -2, or -3 cells/(simulation step)^2 when the simulation step is 1.5 sec and -1 or -2 cells/(simulation step)^2 when the simulation step is 1 sec. These values are respectively equal to -4.44, -8.88, -13.31 m/s^2 for a simulation step of 1.5 sec and -7.5 and -15 m/s^2 for a simulation step of 1 sec. Estimated CO_2, NO_x and CO emission rates of gasoline cars and diesel buses for possible speed and acceleration/deceleration combinations for CA models with a simulation step of 1 sec or 1.5 sec are presented in Tables 3.3 to 3.6. The original emission rates for the VSP binning approach are presented by [29] and shown in Figure 2.4.

Table 3.3: Estimated emission rates of gasoline cars with a simulation step of 1.5 sec

Speed at t [cell/ time step] \ Speed at t+1 [cell/time step]	0			1			2			3		
	Emissions [gr/sec]											
	CO [$\times 10^{-3}$]	NO_x [$\times 10^{-3}$]	CO_2	CO [$\times 10^{-3}$]	NO_x [$\times 10^{-3}$]	CO_2	CO [$\times 10^{-3}$]	NO_x [$\times 10^{-3}$]	CO_2	CO [$\times 10^{-3}$]	NO_x [$\times 10^{-3}$]	CO_2
0	6.5	0.58	0.07	37.2	5.2	5.97						
1	9.9	0.88	1.75	6.5	0.58	0.07	652.8	29.1	9.71			
2	9.9	0.88	1.75	9.9	0.88	1.75	9.9	1.7	3.63	2617.2	44.4	19.31
3	9.9	0.88	1.75	9.9	0.88	1.75	9.9	0.88	1.75	9.9	1.7	3.63

Table 3.4: Estimated emission rates of diesel buses with a simultion step of 1.5 sec

Speed at t [cell/ time step] \ Speed at t+1 [cell/time step]	0			1			2			3		
	Emissions [gr/sec]											
	CO [$\times 10^{-3}$]	NO_x [$\times 10^{-3}$]	CO_2	CO [$\times 10^{-3}$]	NO_x [$\times 10^{-3}$]	CO_2	CO [$\times 10^{-3}$]	NO_x [$\times 10^{-3}$]	CO_2	CO [$\times 10^{-3}$]	NO_x [$\times 10^{-3}$]	CO_2
0	6.5	0.58	2.56	37.2	5.2	24.98						
1	9.9	0.88	2.56	6.5	0.58	6.20	652.8	29.1	29.74			
2	9.9	0.88	2.56	9.9	0.88	2.56	9.9	1.7	6.20	2617.2	44.4	29.74
3	9.9	0.88	2.56	9.9	0.88	2.56	9.9	0.88	2.56	9.9	1.7	12.56

Table 3.5: Estimated emission rates of gasoline cars with a simulation step of 1 sec

Speed at t [cell/ time step] \ Speed at t+1 [cell/time step]	0			1			2		
	Emissions [gr/sec]								
	CO [$\times 10^{-3}$]	NO_x [$\times 10^{-3}$]	CO_2	CO [$\times 10^{-3}$]	NO_x [$\times 10^{-3}$]	CO_2	CO [$\times 10^{-3}$]	NO_x [$\times 10^{-3}$]	CO_2
0	6.50	0.58	0.07	37.20	5.20	9.71			
1	9.90	0.88	1.75	6.50	0.58	3.63	2617.2	29.10	19.31
2	9.90	0.88	1.75	9.90	0.88	0.07	9.90	1.70	3.63

Table 3.6: Estimated emission rates of diesel buses with a simultion step of 1 sec

Speed at t [cell/ time step] \ Speed at t+1 [cell/time step]	0			1			2		
	Emissions [gr/sec]								
	CO [$\times 10^{-3}$]	NO_x [$\times 10^{-3}$]	CO_2	CO [$\times 10^{-3}$]	NO_x [$\times 10^{-3}$]	CO_2	CO [$\times 10^{-3}$]	NO_x [$\times 10^{-3}$]	CO_2
0	8.70	43.00	2.56	61.60	311.70	29.74			
1	8.70	43.00	2.56	36.00	134.00	6.20	61.60	311.70	29.74
2	8.70	43.00	2.56	8.70	43.00	2.56	36.00	134.00	6.20

3.4 Experiments

This section describes various scenarios designed to analyze the sensitivity of performance measures (i.e. travel time, delay, and emissions) to total traffic demand, left turning ratio, and pedestrian volume. Ten replications with different random seeds have been ran for each scenario and model to account for the stochasticity in vehicle and pedestrian arrivals.

Scenarios with Varying Traffic Demand

The first set of scenarios investigates the performance of roundabouts and signalized intersections under different levels of total traffic demand at the junction without the presence of pedestrians. The real-world traffic demand is used as the basis of these scenarios such that the demand used in each scenario is a percentage of the real-world demand. In addition, the sensitivity analysis has been performed with and without the presence of buses.

Nine scenarios with zero pedestrian volume paired with 60%, 80%, 100%, 120%, 140%, 160%, 180%, 200%, and 220% of the base traffic demand are designed. In the

first set of experiments buses are included in the simulation and in the second set they are not included. As presented in Table 3.2, traffic demand of 60% to 180% of the base demand results in undersaturated condition, traffic demand of 200% of the base demand leads to saturated condition, and Finally, a traffic demand of 220% of the base demand results in oversaturated conditions. The resulted CO, CO_2 and NO_x emissions, travel time, and delay are presented.

Scenarios with Varying Left Turn Ratio

In the second set of scenarios, the impact of left turn ratios on the performance of signalized intersections and roundabouts is analyzed. Two sets of scenarios are designed. In each set, zero right turn demand is paired with total demand of 300 vph for through and left turning traffic on each approach. In the first subset of scenarios, only the left turning ratio of Northbound and Southbound approaches changes as shown in Figure 3.9a while the left turn demand on the Eastbound and Westbound approaches is fixed and equal to zero. In the second set of scenarios, the left turning ratio on all approaches changes as shown in Figure 3.9b. In these scenarios, buses are not included in the simulations.

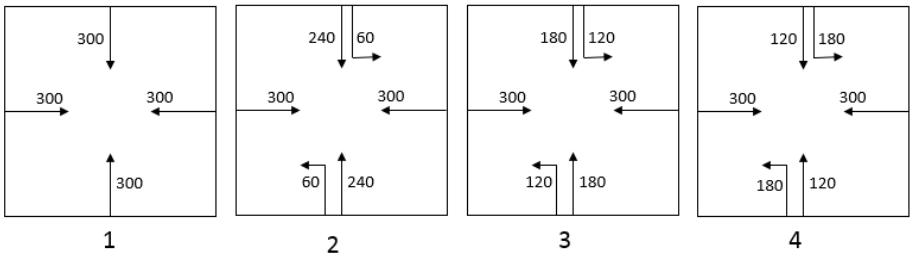

(a) Varying left turning ratio on Northbound and Southbound approaches

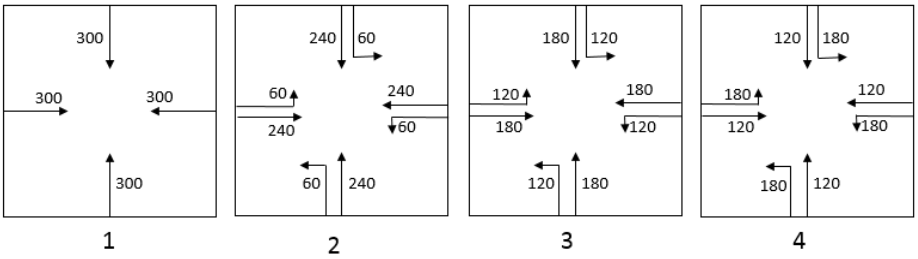

(b) Varying left turning ratio on all approaches

Figure 3.9: Scenarios for sensitivity analysis with respect to left turning ratios

Scenarios with Varying Pedestrian Volume

An important difference between signalized intersections and roundabouts is related to pedestrian crossings. At roundabouts vehicles have to yield to pedestrians present at crosswalks so higher pedestrian volumes can potentially increase the number of stops and emissions. Two sensitivity analysis experiments are performed to assess the effect of various levels of pedestrian volume on the performance of roundabouts and signalized intersections. In the first set of scenarios, buses are not included in the simulations, but in the second set, they are included. In all scenarios traffic demand is constant and equal to the real-world demand and pedestrian volume takes different percentages of 0%, 40%, 60%, 80%, 100%, 120%, 140% of the real-world volume.

3.5 Results

This section first validates the CA models of roundabout and signalized intersection using Aimsun. Then, the results of the sensitivity analyses using the CA model are presented and discussed.

3.5.1 Evaluation of the CA model

The results for CA roundabout models with simulation steps of 1.5 sec and 1 sec are presented and the simulation step, which leads to more consistent results as Aimsun results is selected to be used for the sensitivity analysis. For the signalized intersection, the results of a CA model with a simulation step of 1 sec are presented and the same model is used in the sensitivity analysis experiments.

Average travel time and delay per vehicle are the performance measures used to evaluate the CA model. It is worth noting that Aimsun considers a speed acceptance parameter for each type of vehicle that is multiplied by sections' speed limits and determines the maximum speed a vehicle can have. This parameter is used to account for the fact that vehicles do not necessarily follow the speed limits in the real-world. Speed acceptance affects travel time and delay estimated by Aimsun since the actual travel time depends on the vehicle's speed. In addition, delay is calculated as the difference between free flow and actual travel time and the speed acceptance factor is considered in the calculation of free flow travel time (i.e. speed limits are multiplied by this parameter). The value used in Aimsun is 1.1 with a deviation of 0.1 for cars. The same values are used for buses in this study.

Furthermore, CA results on the number of stops are not compared with Aimsun's results since the CA model overestimates the number of stops and this measure is more sensitive to increases in traffic demand. In the CA model, every time a vehicle decelerates from speed 1 cell/simulation step (16.8 mph), it reaches speed 0

cell/simulation step. However, in reality any deceleration from speed 16.8 mph does not necessarily lead to a complete stop.

3.5.1.1 Evaluation Tests when Buses are Considered

This subsection presents the results of evaluation experiments when buses are not included in the simulations. Figure 3.10a shows the average travel times per vehicle. At traffic demands of 60% to 120% of the base demand (i.e. undersaturated traffic conditions), travel times obtained from the CA model and Aimsun are similar with very small differences , which are not significant. However, at the traffic demands of 140% and 160% of the base demand (i.e. undersaturated traffic conditions), the CA model results in higher travel times, which are statistically significant. Again, at traffic demands of 180% to 220% of the base demand (i.e. respectively represents close to saturated, saturated, and oversaturated conditions), the CA and Aimsun models lead to travel times that are not statistically different.

In the CA model it takes at least one simulation step (1.5 sec) for a stopped vehicle to react to movement of the vehicle in front. However, as presented in section 3.2 the drivers' reaction time to stop in Aimsun is 1.35 sec, which is lower than the CA model. In addition, as described in section 3.2, the critical gap in Aimsun has an initial value, which decreases gradually as traffic demand and consequent vehicles' waiting time increase until it reaches a certain minimum value. Therefore, we expect the CA model be more sensitive to traffic demand and consequent vehicle stops. As shown in Figure 3.10a the sharp increase in the travel times of the CA model happens at a lower traffic demand compared to Aimsun, which proves the higher sensitivity of a CA model with a simulation step of 1.5 sec to vehicle stops.

Figure 3.10b shows the average delay per vehicle estimated by the CA model and Aimsun. Delay growth pattern by each model is similar to the travel time growth patterns shown in Figure 3.10a. In addition, delay estimated by Aimsun for 60%

to 120% of the base demand is higher than the delay estimated by the CA model, but the difference is very small. Due to the inconsistent patterns observed in travel time and delay of the CA model and Aimsun, we cannot use the CA model with a simulation step of 1.5 sec for traffic demands higher than 120% of the base demand.

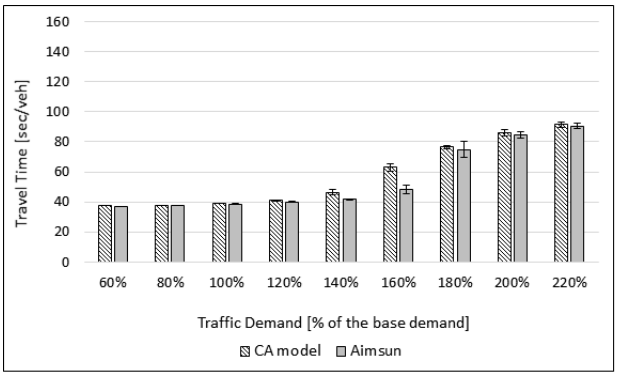

(a)

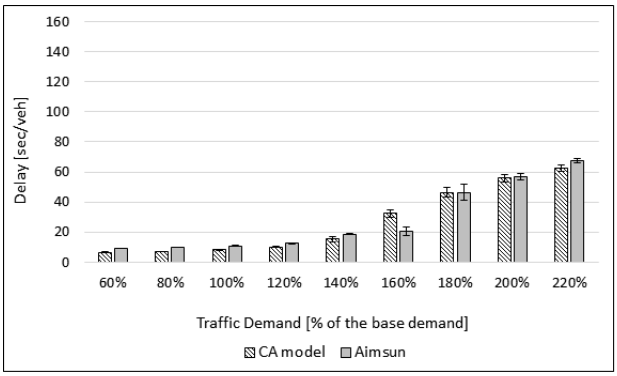

(b)

Figure 3.10: Comparison of CA and Aimsun roundabout models using simulation steps of 1.5 sec and 1 sec, respectively.

Figure 3.11 shows travel time and delay at the roundabout estimated by the CA model and Aimsun both using a simulation step of 1 sec. Figure 3.11a shows that travel times estimated by the CA model and Aimsun are similar for traffic demands lower than 180% of the base demand. When traffic conditions gets close to saturated conditions (i.e. 180% of the base demand) as well as saturated (200% of the base

demand) and oversaturated (220% of the base demand) traffic conditions, Aimsun shows a rapid increase in travel time, which is not reflected in the CA model. The reaction time to stops in the CA model (the same as the simulation step, which is 1 sec) is lower than the reaction time in Aimsun (1.35 sec). Therefore, Aimsun is more sensitive to vehicle stops compared to the CA model.

Figure 3.11b shows the average delay at the roundabout estimated by the CA model and Aimsun using a simulation step f 1 sec. For a big range of understaurated traffic conditions (i.e. 60% to 160% of the base demand), the CA model estimates lower delays than Aimsun. Although the observed differences are statistically significant, they are small and can be due to the more stochastic nature of Aimsun. At the traffic demands of 180% to 220% of the base demands, the difference between delay estimated by the CA model is much lower than Aimsun, which is expected as the corresponding travel times were lower, too.

Considering the above observations in travel time and delay, we can use the roundabout CA model for traffic demands lower than 180% of the base demand, which includes a big range of undersaturated traffic conditions. The CA model needs to be modified in order to be used for higher traffic demands. Therefore, the roundabout CA model with a simulation step of 1 sec is used to perform the sensitivity analysis for undersaturated traffic conditions.

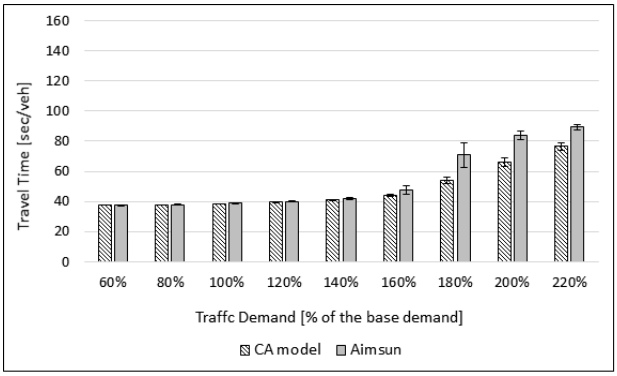

(a)

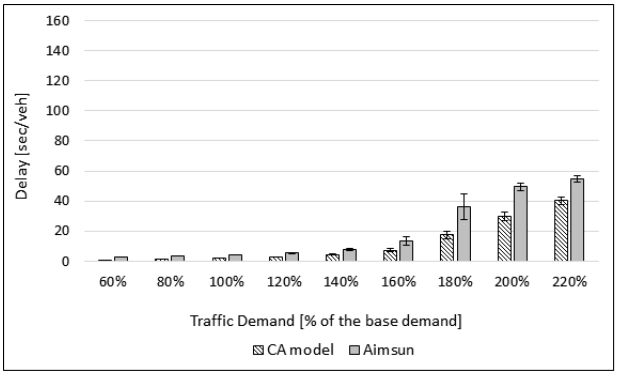

(b)

Figure 3.11: Comparison of CA and Aimsun roundabout models using a simulation step of 1 sec in both models

Figure 3.12 shows the estimated performance measures at the signalized intersection using the CA model and Aimsun. A simulation step of 1 sec is used in both models as well as the same speed limits on approaches and within the node (i.e. roundabout and signalized intersection) as described in sections 3.1.2 and 3.2. Figure 3.12a shows that at traffic demands of 60% to 140% of the base demand, travel times estimated by the CA model are very close to those estimated by Aimsun. At traffic demands of 160% and 180% of the base demand, travel times estimated by the CA model is higher than those estimated by Aimsun, but the differences are not statistically significant. Finally, at higher traffic demands, which represent saturated

and oversaturated traffic conditions, the CA model leads to statistically higher travel times compared to Aimsun. A reason for this could be related to the gap acceptance behavior of left turning vehicles. In the CA model the gap acceptance of left turning vehicles is fixed and does not depend on the traffic demand. In contrary, in Aimsun the accepted critical gap for left turning vehicles decreases over time as the waiting time of vehicle to find an enough gap increases. As a result, the increased left turn demand imposes a lower delay to other vehicles in the queue in Aimsun compared to the CA model. Although the varying gap acceptance behavior is true for the Aimsun roundabout model as well, its effect was not observed in Figure 3.11. A reason could be the lower sensitivity of roundabouts to left turning movements compared to signalized intersections, which will be shown later in this study.

Figure 3.12b shows the average delay at signalized intersection estimated by the CA model and Aimsun using a simulation step of 1 sec. At traffic demands of 60% to 140% of the base demand, the CA model estimates a lower delay than Aimsun. Similar to the case for roundabout, the differences could be due to the higher stochasticity in vehicles' speeds. At traffic demands of 160% and 180% of the base demand, estimated delay by the CA model is higher than the estimated delay by Aimsun, but the differences are not statistically significant. Finally, at the demand of 200% and 220% of the base demand (i.e. saturated and oversaturated traffic conditions), the CA model shows higher delays, which are statistically significant. Therefore, the CA model can be used for traffic demands lower than 200% of the base demand (i.e. undersaturated traffic conditions) and modifications are required to use it for saturated and oversaturated traffic conditions.

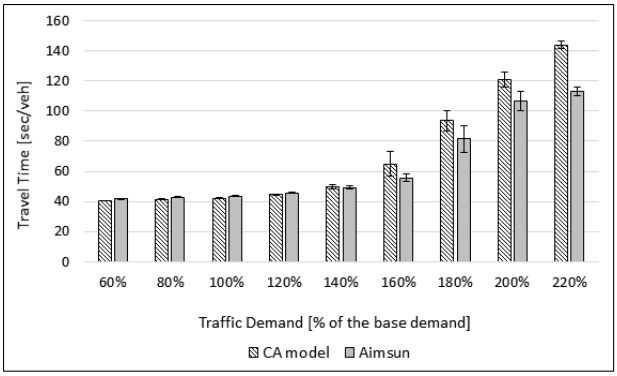

(a)

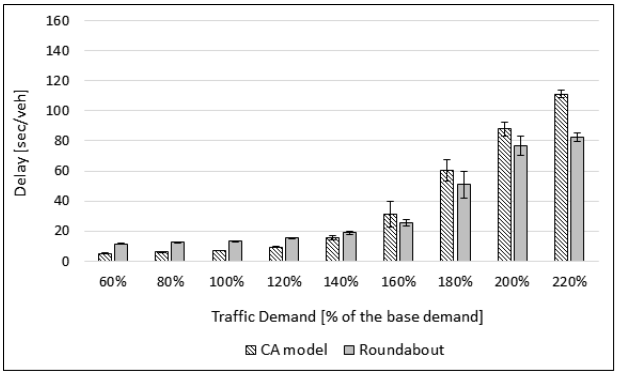

(b)

Figure 3.12: Comparison of CA and Aimsun models for the signalized intersection using a simulation step of 1 sec in both models

To sum up, when buses are not incorporated into the simulation, the CA models of roundabouts and signalized intersections can be used for undersaturated traffic conditions up to 160% and 180% of the base demand, respectively. Since the goal of this study is to compare the performance of roundabouts and signalized intersections, we use the models for traffic demands up to 160% of the base demand. The next subsection presents the results of comparisons between the CA model and Aimsun when buses are included in the simulation.

3.5.1.2 Evaluation Tests when Buses are not Considered

This subsection compares travel times and delays at the roundabout and signalized intersection estimated by the CA model and Aimsun when buses are simulated as well as cars and a simulation step of 1 sec is used. This simulation step is selected since it led to more accurate results in the previous evaluation tests. Fixed bus schedule and headways (the same as the PVTA bus schedule in Amherst) are used in all traffic demand scenarios. In addition, the effect of bus stops are ignored and there is no bus stop in the simulated network. Average travel time and delay per vehicle are presented for all traffic, cars, and buses, separately.

Figure 3.13 shows the average travel times estimated by the CA model and Aimsun when buses are included in the simulations. It is worth mentioning again that at an urban intersection as assumed in this study, buses have similar speeds as cars. The differences of buses and cars are their lower acceleration rates and higher length of buses. The combination of a simulation step of 1 sec and a cell length of 7.5 m results in an acceleration rate of 7.5 m/s^2, which is higher than 2 m/s^2 acceleration rate assumed in Aimsun. Therefore, we expect to observe shorter travel times and delays for buses estimated by the CA model.

As shown in Figure 3.13a and 3.13b, buses do not have a significant impact on the average travel time per vehicle in neither Aimsun nor the CA model. The reason is that the higher number of cars overweight the impact the lower acceleration rate and higher length of buses can have on the results. Consequently, similar pattern and values are observed for travel times whether buses are included or not in the simulations.

As shown in Figure 3.13c, the average travel times per bus are lower in the CA model than Aimsun, which is due to the higher acceleration rate of buses in the CA model. This issue will be addressed in the future works by assuming shorter cells, which leads to smaller speed bins and acceleration/deceleration rates.

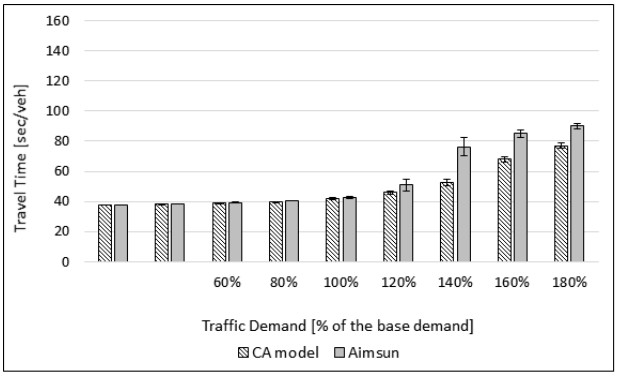

(a) Average travel time per vehicle (including cars and buses)

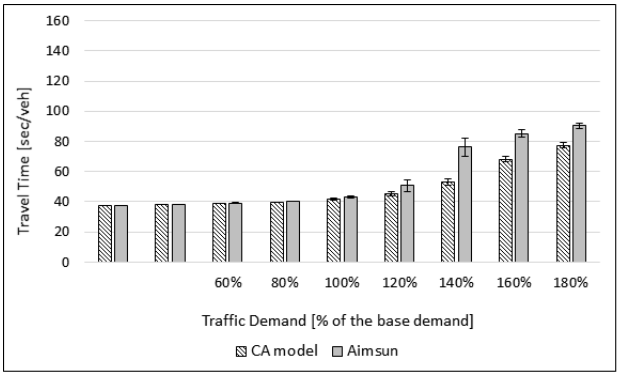

(b) Average travel time per car

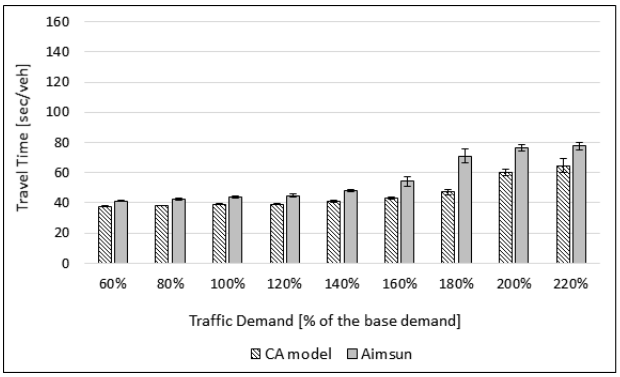

(c) Average travel time per bus

Figure 3.13: Comparison of CA and Aimsun models for the roundabout when buses are incorporated into the simulation using a simulation step of 1 sec in both models

Figure 3.14 shows average delays estimated by the CA model and Aimsun when buses are included in the simulation. Figures 3.14a and 3.14b show similar changes

in delay as for the case without buses (shown by Figure 3.11b). This shows that the presence of buses does not affect average delay of cars in neither the CA model nor Aimsun. However, the difference between average delay estimated by the CA model and Aimsun for buses is greater than the difference of average car delay estimated by the two models. This is expected as the acceleration rate of buses in Aimsun is significantly lower than the CA model.

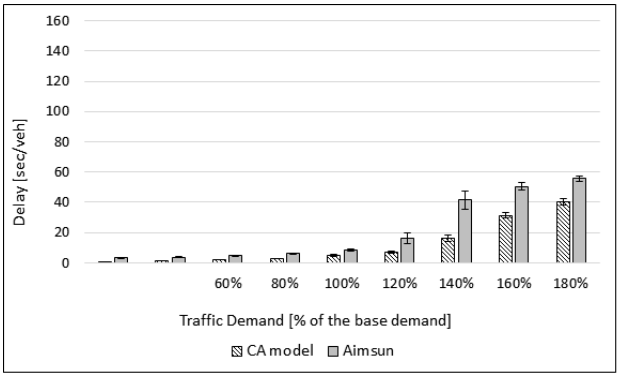

(a) Average travel time per vehicle (including cars and buses)

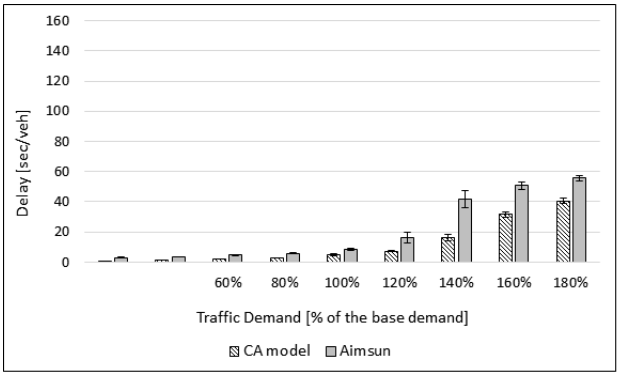

(b) Average travel time per car

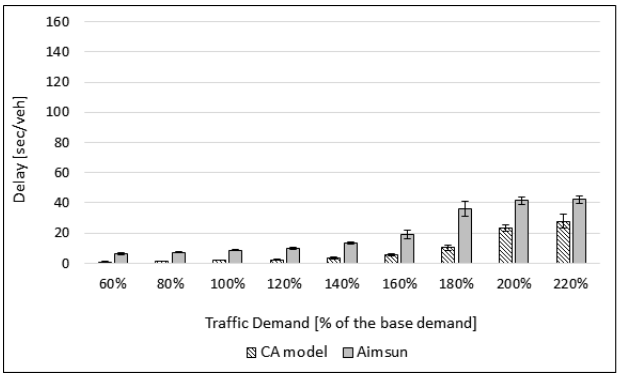

(c) Average travel time per bus

Figure 3.14: Comparison of CA and Aimsun models for the roundabout when buses are incorporated into the simulation using a simulation step of 1 sec in both models

Figure 3.15 shows the average travel times per vehicle at the signalized intersection and the presence of buses. Similar to the case of roundabouts, the average travel times

of cars (Figure 3.15b) have not been impacted by the presence of buses. At traffic demands of 60% to 180% of the base demand there are very small or statistically insignificant difference between the travel times estimated by the CA model and Aimsun. At traffic demands of 200% and 220% of the base demand, which represent saturated and oversaturated traffic conditions, the CA model results in higher travel times per car shown by Figure 3.15b. As explained earlier, the higher travel times estimated by the CA model could be due to the fixed gap acceptance over time while in the Aimsun, accepted critical gap decreases as the waiting time of a vehicle increases.

Figure 3.15c shows that the estimated travel times per bus by the CA model is lower than the travel times estimated by Aimsun for traffic demands of 60% to 140% of the base demand, which is due to the higher acceleration rates of buses in the CA model.

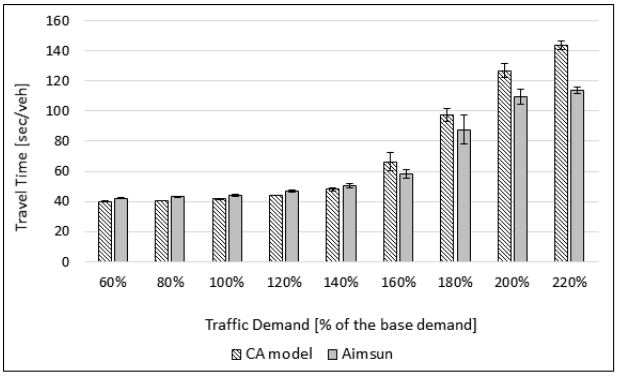

(a) Average travel time per vehicle

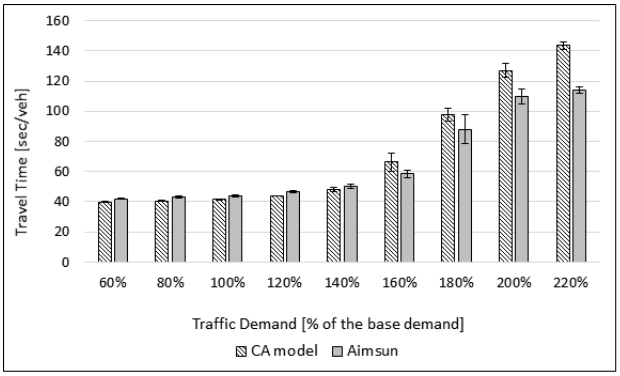

(b) Average travel time per car

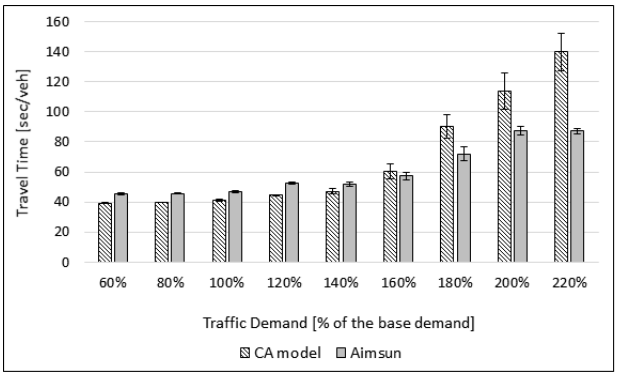

(c) Average travel time per bus

Figure 3.15: Comparison of CA and Aimsun models for the signalized intersection when buses are incorporated into the simulation using a simulation step of 1 sec in both models

Figure 3.16 shows average delays estimated by the CA model and Aimsun when buses are included in the simulations. As expected, the average delay of cars have not

changed compared to the scenarios without buses. Figure 3.16c shows the average delay per bus estimated by the CA model is lower than delays estimated by Aimsun for traffic demands up to 140% of the base demand, which is due to the lower acceleration rates of buses in the CA model. At high traffic demands (higher than 180% of the base demand) the CA model estimates higher delay than Aimsun, which is explained by the varying gap acceptance behavior in Aimsun.

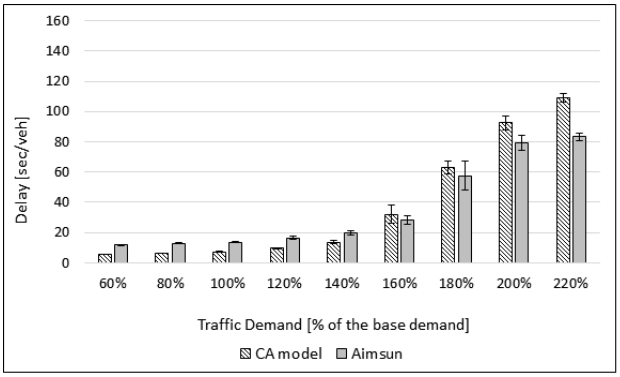

(a) Average travel time per vehicle

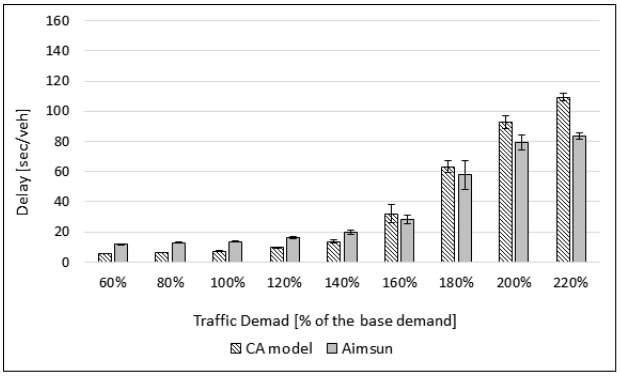

(b) Average travel time per car

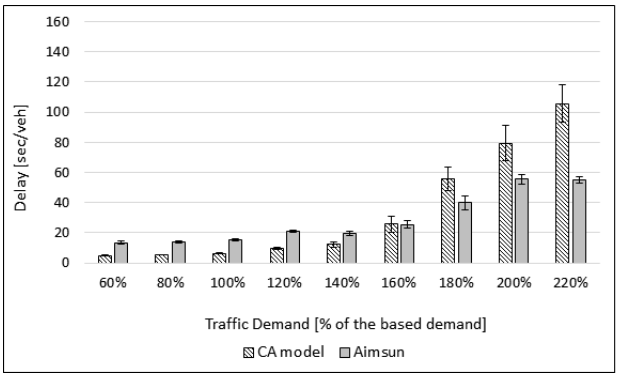

(c) Average travel time per bus

Figure 3.16: Comparison of CA and Aimsun models for the Signalized intersection when buses are incorporated into the simulation using a simulation step of 1 sec in both models

The results of the evaluation tests show that buses do not have significant effects on the operation of cars in neither the CA nor Aimsun. The current CA model is

not able to reflect the lower accelerate rates of buses. Thus, it was expected not to see any impact on average travel times and delays. However, even in Aimsun, which assumes lower acceleration rates for buses, no significant change on average travel time and delays per car is observed. The lower acceleration rates of buses in Aimsun led to higher travel times and delays per bus.

Although bus operational measures are underestimated by the CA model, the pattern shown by both CA and Aimsun models for roundabouts and signalized intersections is similar. Therefore, we can use to model to compare the performance of the roundabout and signalized intersection. To sum up, the CA model is used to perform sensitivity analysis for traffic demands of 60% to 160% of the base demand with and without the presence of buses at the roundabout and intersection.

3.5.2 Sensitivity Analysis with Respect to Varying Total Traffic Demand

The results of sensitivity analysis are presented in two subsections: when buses are included in the simulation and when they are not included.

3.5.2.1 Experiments without Buses

Figure 3.17 shows the estimated operational and environmental performance measures at the roundabout and signalized intersection for various levels of traffic demands (traffic demands of 60% to 160% of the base demand, for which the CA models have been validated) when buses are not included in the simulation. Average travel time, delay, number of stops, and NO_x and CO emission per vehicle for the entire time of traveling in the network are presented. It should be noted that the CA model overestimates the number of stops because any deceleration from speed of 1 cell/simulation step (16.8 mph) leads to a stop while in the real-world a vehicle may decelerates from the same speed without reaching a complete stop. However, we can use the CA model to compare the impact of increases in traffic demand on the number of stops at the roundabout and the signalized intersection.

Figure 3.17a shows that travel time at the roundabout is lower than the travel time at the signalized intersection for all traffic demands and the differences are statistically significant. As traffic demand increases, travel times at both the signalized intersection and the roundabout increase. However, the rate of increase of travel time at the signalized intersection is higher than the roundabout. Replacing a signalized intersection with a roundabout can reduce travel time from 4.5% (at 60% of the base traffic demand) to 32% (at 160% of the base demand). Figure 3.17b shows that average delay at the roundabout is considerably improved compared to the signalized intersection. At traffic demand of 60% of the base demand, average delay at the roundabout is less than 1 sec while average delay at the signalized intersection is 5 sec. The difference between delay at the roundabout and the signalized intersection increases to 23 sec at traffic demand of 160% of the base demand. The reason is that at signalized intersections vehicles may have unnecessary stops and imposed delay due to red signal.

Figure 3.17c shows that the number of stops at the roundabout is lower than the signalized intersections for lower traffic demands. As traffic demand increases, the difference between the number of stops at the roundabout and signalized intersection decreases such that there is no statistically significant difference at traffic demand of 160% of the base demand. The reason for this pattern is that at lower traffic demands and conflicting traffic traveling within the roundabout, vehicles can travel more smoothly. However, at signalized intersections and low traffic demands, there are always some unnecessary stops due to red signals even when there is no crossing traffic. At higher traffic demands, the number of stops to conflicting traffic at roundabouts increases with a high rate. In addition, SYNCHRO optimizes signal timing considering the number of stops as well as delay (i.e. the main objective is to minimize delay. The number of stops and queue length are also considered by applying penalties for these performance measures).

In addition to better operational performance, the roundabout leads to improved NO_x and CO emissions per vehicle at all traffic demands according to Figures 3.17d and 3.17e. The difference of emissions at roundabouts and signalized intersections is higher for lower traffic demands, which is the same pattern as for the number of stops shown in Figure 3.17c. Both roundabout and signalized intersections show small yet statistically significant increases in emissions as the traffic demand increases.

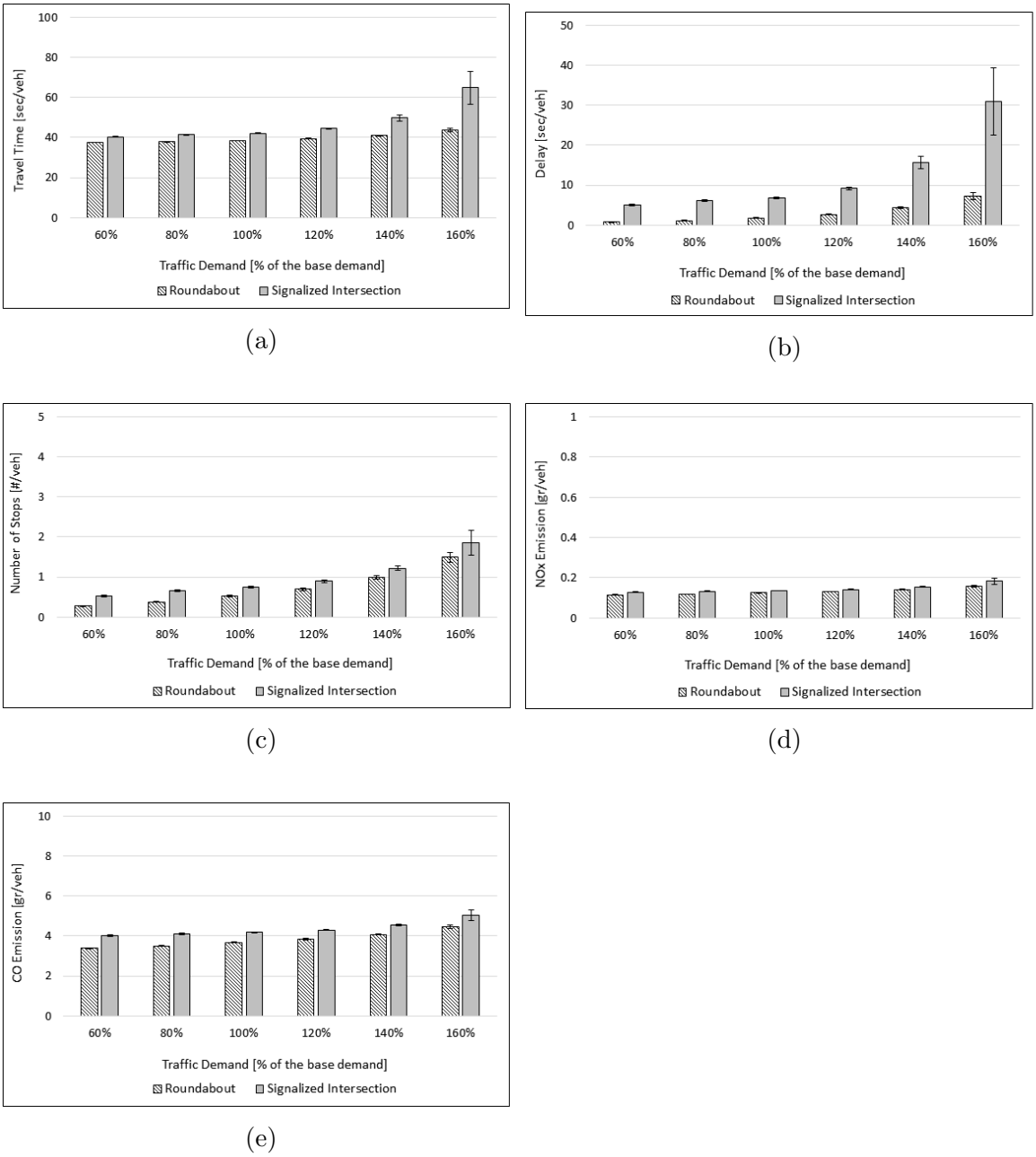

Figure 3.17: Sensitivity analysis with respect to total traffic demand without the presence of buses

3.5.2.2 Simulations with Buses

This subsection presents the results of sensitivity analysis with respect to total traffic demand when buses are included in the experiments. Average travel times, delays,

number of stops, and CO, CO_2, and NO_x emissions are presented for cars and buses separately.

Figure 3.18 shows the operational performance measures (i.e. average travel time, delay, and number of stops) for cars and buses at the roundabout and signalized intersection. As mentioned earlier, cars and buses have the same acceleration rates and speeds in the CA model. As a result, thy have the same operational performance as shown in Figure 3.18. For the entire range of traffic demands from 60% to 160% of the base demand, the roundabout results in lower travel time and delay compared to the signalized intersection. The higher travel times and delays can be due to the unnecessary imposed delays to vehicles at a red signal when there is no crossing traffic. In addition, a steady increase in average travel time and delay is observed at the roundabout as traffic demand increases. However, there is a sharp increase in travel time and delay at the signalized intersection from traffic demand of 140% to 160%. This shows the higher sensitivity of a signalized intersection's performance to traffic demand when the demand gets close to the saturated traffic conditions.

Figure 3.18e and 3.18f show that roundabouts lead to lower number of stops compared to signalized intersections for all traffic demands. However, as traffic demand increases from 60% to 140% of the base demand, the difference between the number of stops at the roundabout and signalized intersection decreases and a the demand of 140%, this difference is statistically insignificant. This shows the higher sensitivity of number of stops at the roundabout to traffic demand, which can be the result of vehicles stops to conflicting traffic traveling within the roundabout. However, at traffic demand of 160% of the base demand, the difference of number of stops at the roundabout and signalized intersection increases again (i.e. lower number of stops at the roundabout). As mentioned earlier, the sensitivity of signalized intersection's performance to traffic demand when the traffic condition is close to saturated conditions is higher compared to the roundabout.

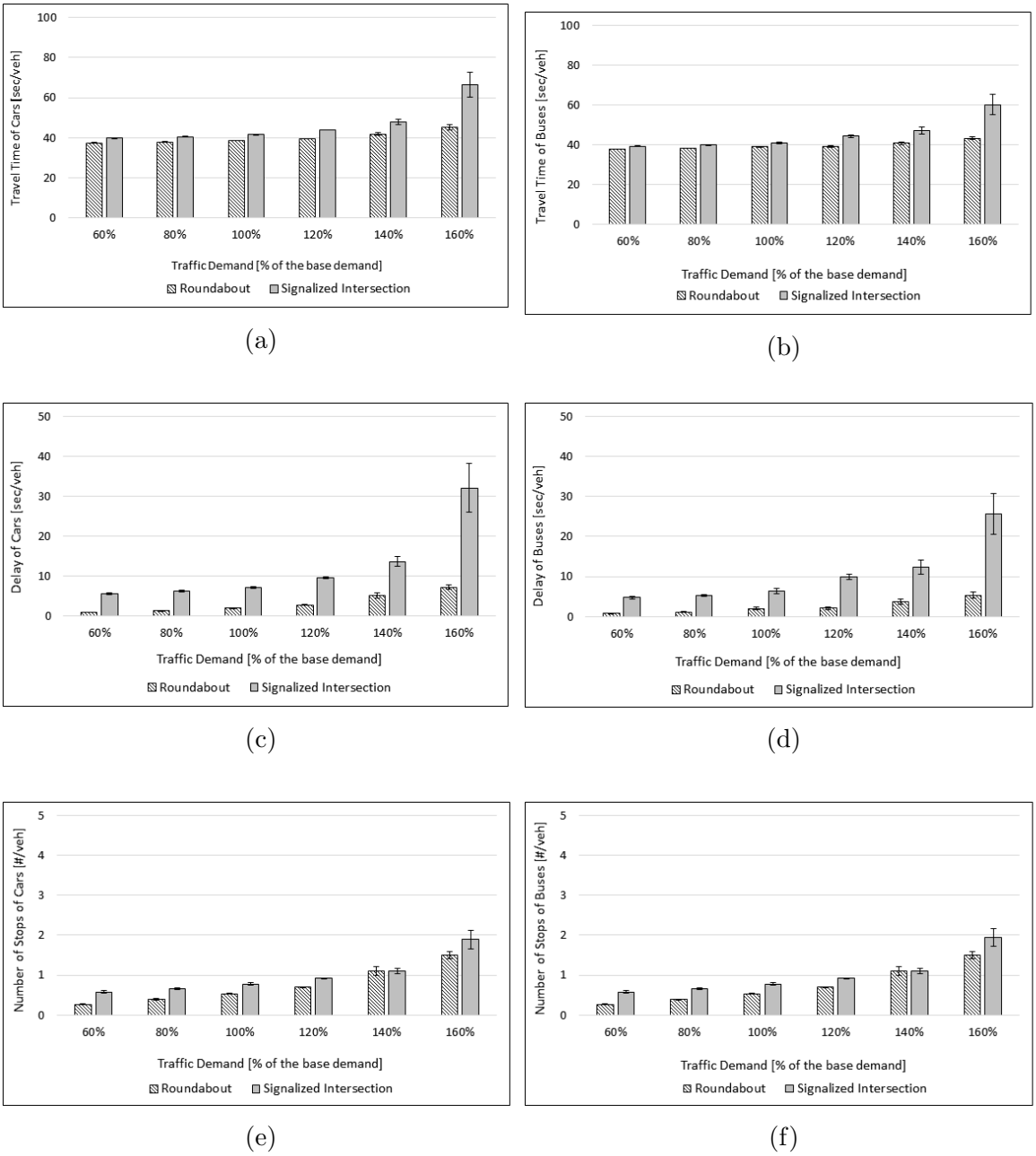

Figure 3.18: Sensitivity of operational performance measures at roundabouts and signalized intersections with respect to total traffic demand when buses are included in the experiments

Figure 3.19 shows the sensitivity of emissions of cars and buses at the roundabout and signalized intersection to total traffic demand. According to Tables 3.5 and 3.6,

gasoline cars have significantly lower NO_x emission rates than diesel buses. As a results, the average emissions produced by cars and presented in Figure 3.19a are considerably lower than the average emissions produced by buses and presented in Figure 3.19b. In addition, Figures 3.19a and 3.19b show that at traffic demands of 60% to 140% of the base demand, the roundabout and signalized intersection result in similar NO_x emission levels produced by cars and buses. However, at traffic demand of 160% of the base demand, the roundabout results in respectively 0.03 gr/veh (17%) and 0.68 gr/veh (13%) lower NO_x emission for cars and buses compared to the signalized intersection. This is expected because of the higher number of stops and delays at the signalized intersection at traffic demand of 160% of the base demand.

Tables 3.5 and 3.6 show that gasoline cars have a considerably higher CO emission rate than diesel buses during an acceleration event that happens at high speed (acceleration from speed of 1 cell/simulation step to 2 cell/simulation step) than diesel buses buses. This results in higher values of CO emissions for cars than buses at both the roundabout and signalized intersection. Figure 3.19c shows that roundabouts lead to lower CO emissions than signalized intersections. As traffic demand increases from 60% to 140% of the base demand, the difference between CO emissions at the roundabout and signalized intersection decreases from 0.62 gr/veh to 0.51 gr/veh. At traffic demand of 160% of the base demand, this difference increases again to 0.60 gr/veh. The pattern of CO emission changes at the roundabout and signalized intersection is similar to the pattern observed for number of stops in Figure 3.18e. Unlike to cars, buses do not have different emissions at the roundabout and signalized intersection at any traffic demand. This can be due to the lower difference of buses' emission rates at different speed and acceleration levels compared to cars.

Tables 3.5 and 3.6 show the higher CO_2 emission rates of diesel buses compared to gasoline cars. This results in lower emission produced by cars as presented in Figure 3.19e than the emissions of buses as presented in Figure 3.19f. Figure 3.19e shows that

there is a small yet statistically significant difference between the CO_2 emissions of cars at the roundabout and signalized intersection. The roundabout results in around 6 gr/veh higher CO_2 emission (despite its lower delays and number of stops) compared to the signalized intersection. This small difference can be due to the longer traveled distance within the roundabout than signalized intersection. Figure 3.19f shows the the emissions produced by buses at the roundabout and signalized intersection do not have a statistically significant difference at any traffic demand except the demand of 160% of the base demand, at which the roundabout leads to lower CO_2 emission than signalized intersection.

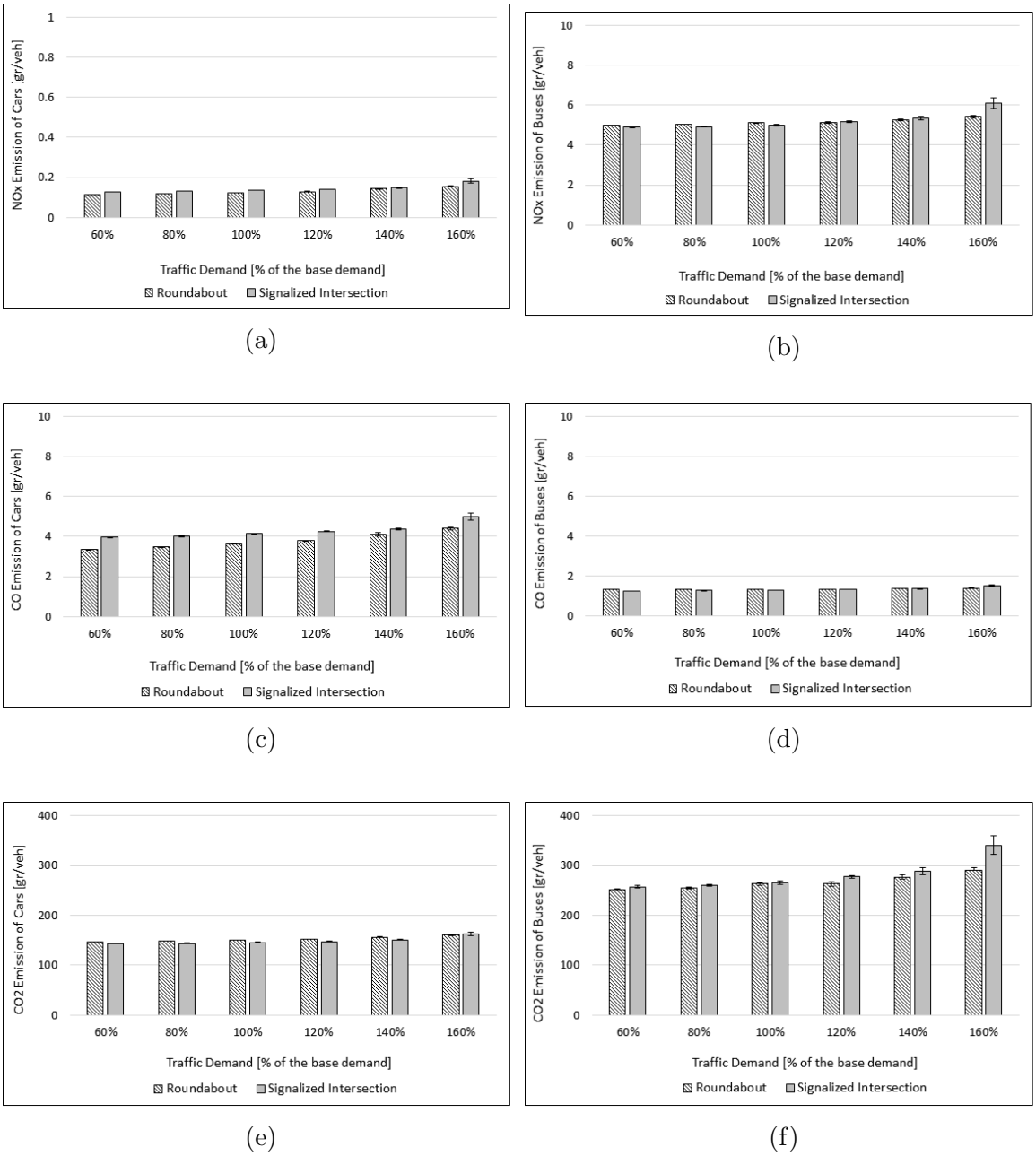

Figure 3.19: Sensitivity of environmental performance measures at roundabouts and signalized intersections with respect to total traffic demand when buses are included in the experiments

3.5.3 Sensitivity Analysis with Respect to Left Turn Ratio

This subsection presents the results of sensitivity analysis with respect to left turning ratio. Results are presented in two sections when the left turning ratio only on northbound and southbound approaches change or the left turning ratio on all approaches change. In the current scenarios only cars are included in the simulation and the left turning ratio of car demand varies across scenarios.

3.5.3.1 Varying Left Turning Ratio on Northbound and Southbound Approaches

This subsection presents the results of sensitivity analysis with respect to left turn ratio on northbound and southbound approaches. Figure 3.20 shows that the operational and environmental performance of roundabout does not change with varying traffic demand on only northbound and southbound approaches (at a constant total demand of 300 veh/hr on each approach). However, there are small yet statistically significant increases in emissions as well as operational and environmental performance measures at the signalized intersection. Figures 3.20a and 3.20b show increases of 2.6 sec and 2.3 sec in the average travel time and delay at the signalized intersection from scenario 1 to 4. Figure 3.20c also shows that the number of stops at the intersection increases by 0.36 (60%) from scenario 1 to 4. the changes in NO_x emissions are statistically insignificant from scenarios 1 to 4 according to Figure 3.20d, but Figure 3.20e shows an increase of 0.6 gr/veh (16%) in CO emission at the signalized intersection.

The above results show that roundabouts can better control left turning demand compared to signalized intersection and they can be considered as a promising alternative for signalized intersection at sites with high left turning traffic.

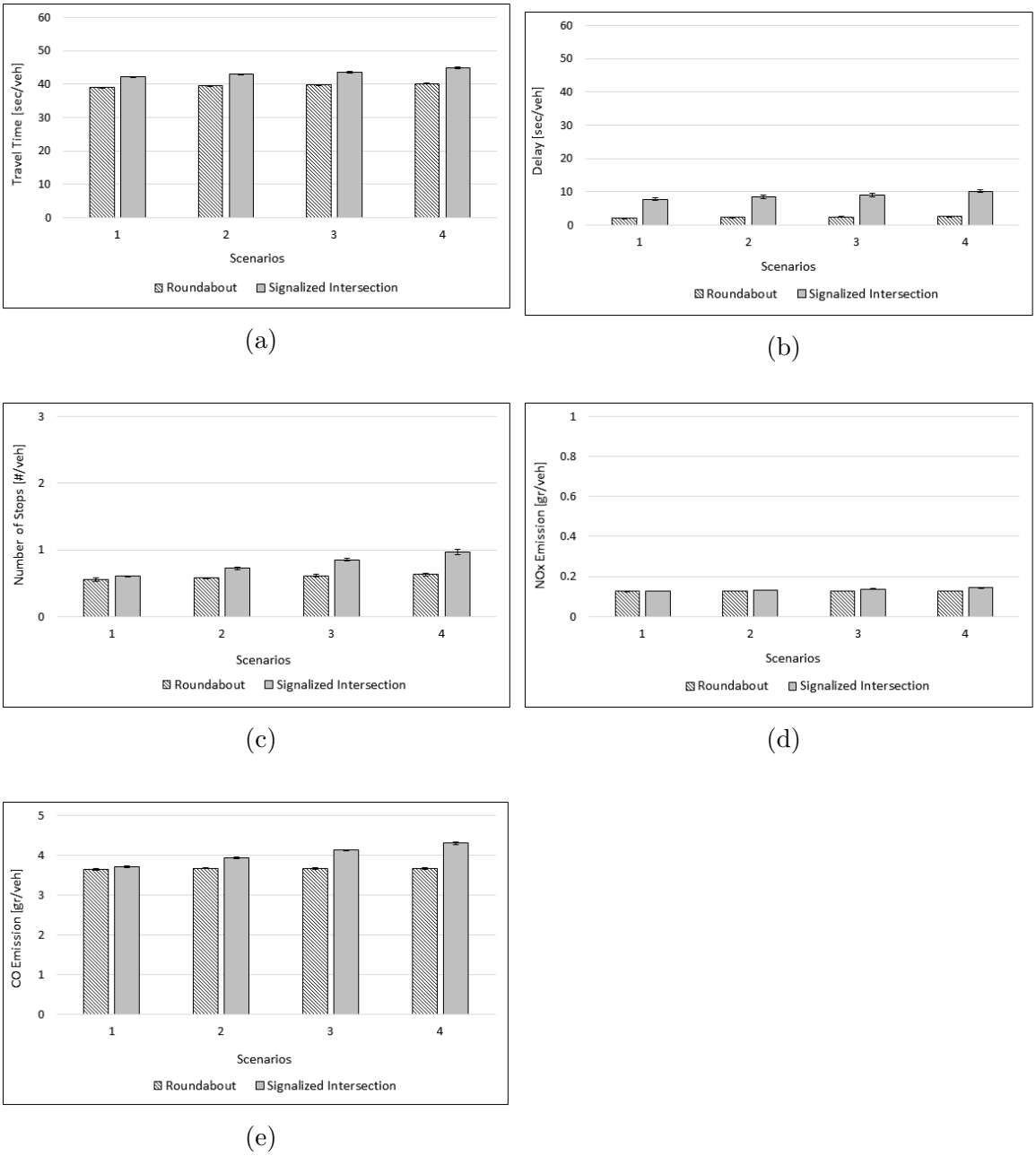

Figure 3.20: Sensitivity analysis with respect to the left turn ratio on northbound and southbound approaches when buses are not included in the experiments

3.5.3.2 Varying Left Turning Ratio on all Approaches

Figures 3.21a to 3.21c show that the operational performance of both the roundabout and the signalized intersection is affected by changing left turning ratio on all

approaches. Travel time at the roundabout and signalized intersection respectively increases by 2.6 sec and 4.2 sec from scenario 1 to scenario 4. Average delay increases 1.5 sec and 3.6 sec at the roundabout and signalized intersection from scenario 1 to scenario 4. Figure 3.21c shows the number of stops increases by 0.2 (34%) at the roundabout and 0.7 (116%) at the signalized intersection. Although travel time, delay, and number of stops increase at both types of intersections, the roundabout can better control left turning traffic and results in lower increases in these performance measures.

Furthermore, Figures 3.21d and 3.21e show that NO_x and CO emissions at roundabout are not sensitive to left turning ratio when overall traffic remains the same. However, NO_x and CO emissions at the signalized intersection increases respectively by 0.04 gr/veh (26%) and 1.2 gr/veh (33%) from scenario 1 to scenario 4. The reason could be the higher rate of increase in the number of stops at the signalized intersection compared to the roundabout when the left turning ratio increases on all approaches.

To sum up, roundabouts more adequately control left turning traffic compared to signalized intersections. Therefore, replacing signalized intersections with roundabouts, results in improved operational and environmental performance measures.

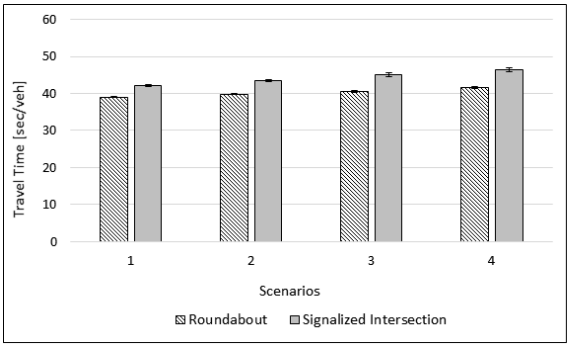

(a)

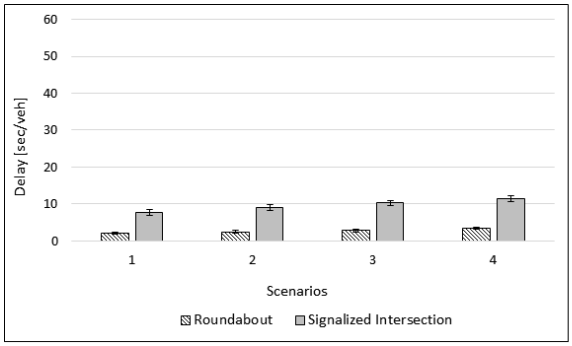

(b)

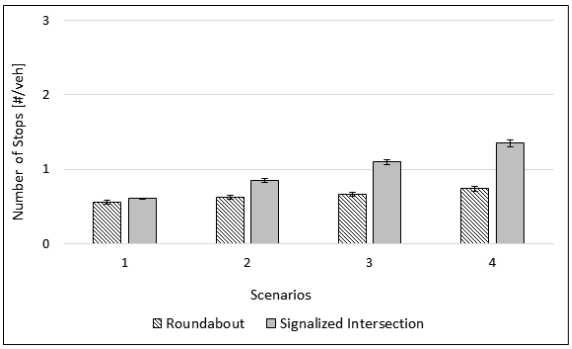

(c)

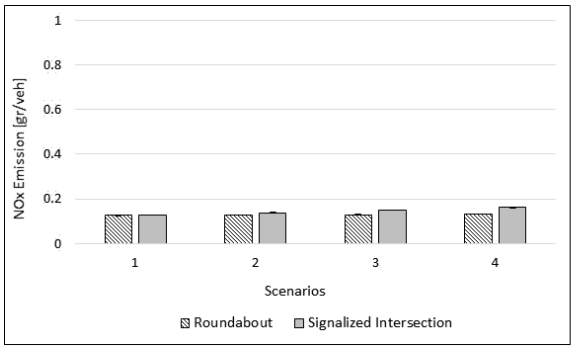

(d)

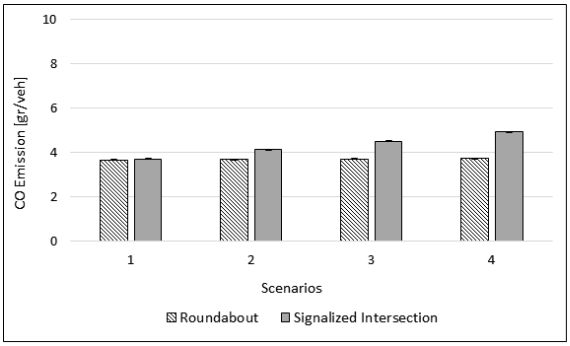

(e)

Figure 3.21: Sensitivity analysis with respect to the left turn ratio on all approaches when buses are not included in the experiments

3.5.4 Sensitivity Analysis with Respect to the Pedestrian Volume

This section present the results of sensitivity analysis with respect to the pedestrian volume. Various levels of pedestrian volume, 0%, 40%, 60%, 80%, 100%, 120%, and

140% of the base volume are paired with the base traffic demand in these sensitivity analysis scenarios. Results are presented in two subsections with and without buses in the experiments.

3.5.4.1 Simulations without Buses

Figure 3.22 shows the sensitivity of performance measures to the pedestrian volume at the roundabout and signalized intersection when buses are not considered in the simulations. It is shown that the performance of the signalized intersection is not affected by increased pedestrian volume across the designed scenarios. This is because at signalized intersections pedestrians cross the street in the same direction as through traffic on each link. As a result, only right and left turning traffic can be affected by pedestrians, but those impacts are not significant in current scenarios with the base traffic demand. Unlike signalized intersections, both operational and environmental performance of roundabout is impacted by pedestrian crossings. Increase in pedestrian volume from 0 to 140% of the base volume results in increases of average travel time, delay, number of stops, NO_x and CO emissions by respectively, 2.9 sec (8%), 2.9 sec (161%), and 0.4 gr/veh (11%). Therefore, at sites with high pedestrian volume, the impact of pedestrians on the performance measures should be considered. Despite the sensitivity of the roundabout performance to pedestrian volume, roundabouts have better operational and environmental performance than signalized intersections at the base traffic demand and any pedestrian volume.

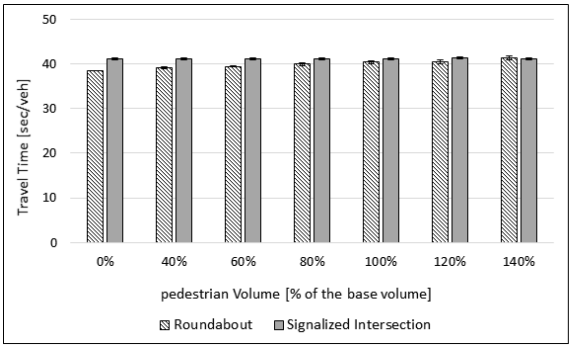

(a)

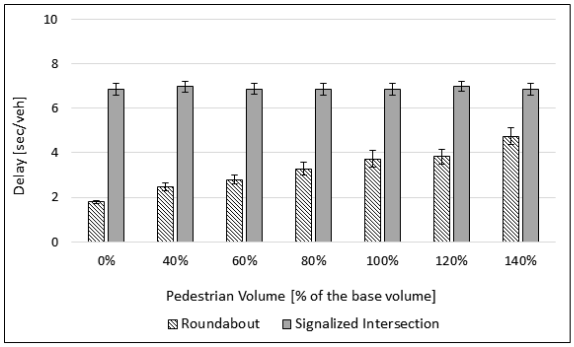

(b)

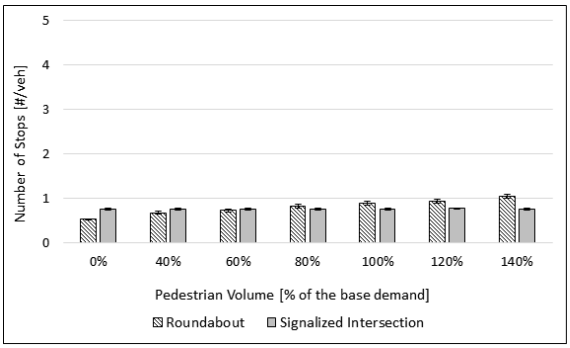

(c)

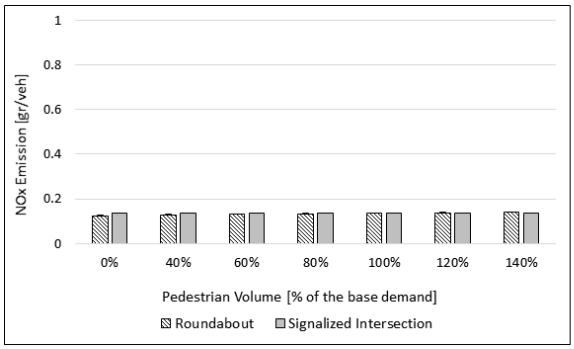

(d)

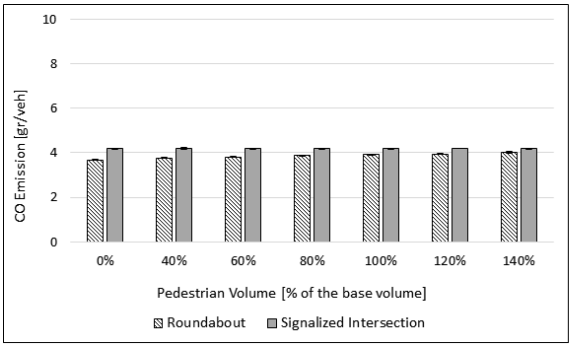

(e)

Figure 3.22: Sensitivity analysis with respect to the pedestrian volume when buses are not included in the experiments

3.5.4.2 Simulations with Buses

Figure 3.23 shows the sensitivity of operational performance measures (i.e. average travel times, delay, and number of stops) at roundabouts and signalized intersections

with respect to pedestrian volume when buses are incorporated into the simulations. In the real-world, when presence of buses and pedestrians are paired at the intersection, the operation of buses as well as other traffic could be affected more than the condition at which there is no bus at the intersection. In the real-world buses have lower acceleration rate than cars. As a result, when a bus yields to a pedestrian, it takes longer time that it accelerates again and moves at the previous speed compared to the time that a car needs to reach its previous speed after a stop. Consequently, if there is a queue behind the stopped vehicle, higher delay is imposed to the vehicles in the queue. However, the current CA model does not account for the lower acceleration rate of buses. As a result, no difference is observed in car operations in these experiments when buses are considered or not.

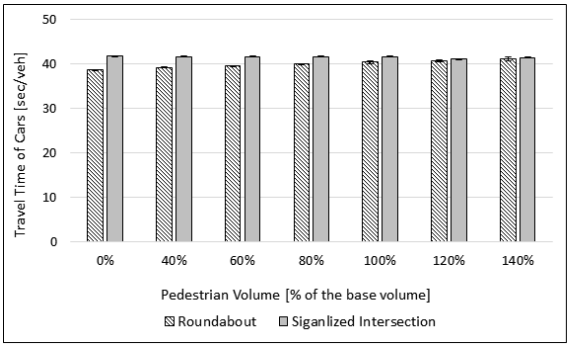

(a)

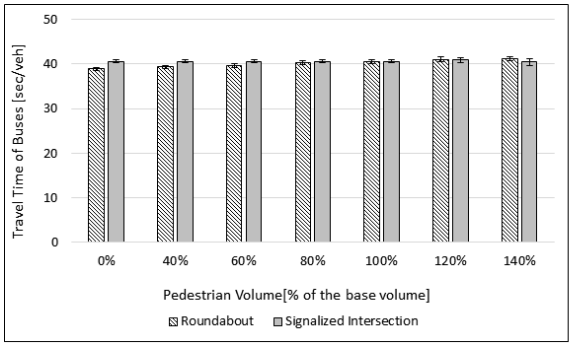

(b)

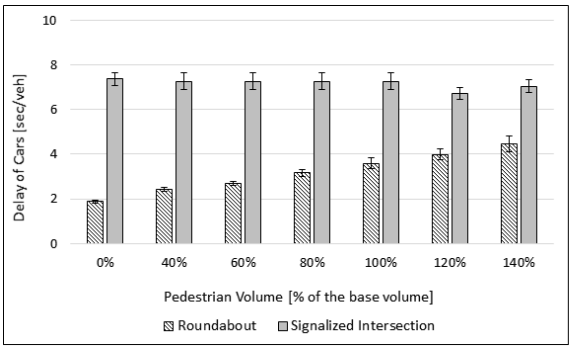

(c)

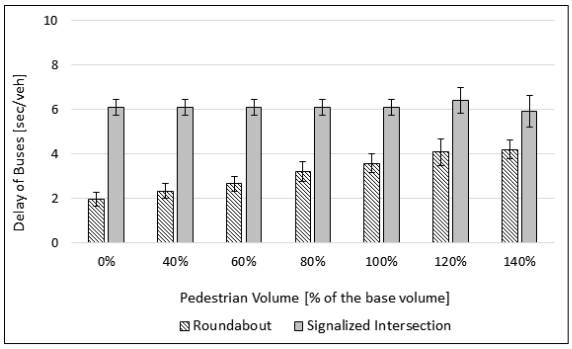

(d)

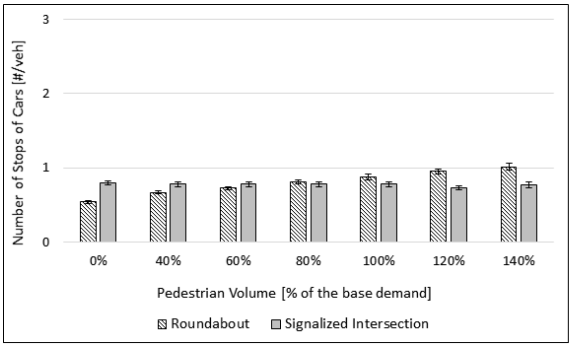

(e)

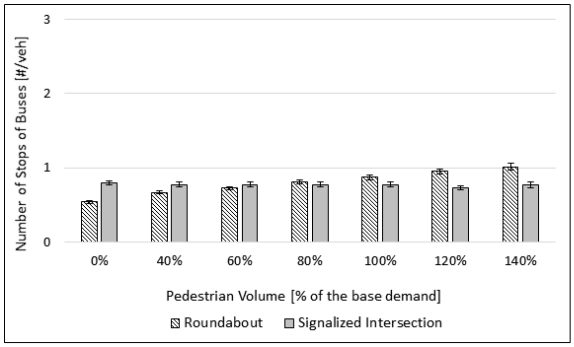

(f)

Figure 3.23: Sensitivity of operational performance measures of roundabouts and signalized intersections with respect to pedestrian volume with the presence of buses

Figure 3.24 shows the average emissions at the roundabout and signalized intersection when buses are included in the simulations. As expected, the average emission of cars is not affected by the presence of buses. Figure 3.24b shows that the average NO_x

emission of buses is 0.4 gr/veh higher at the roundabout compared to the signalized intersection. CO and CO_2 emissions at the roundabout and signalized intersection do not have a statistically significant difference.

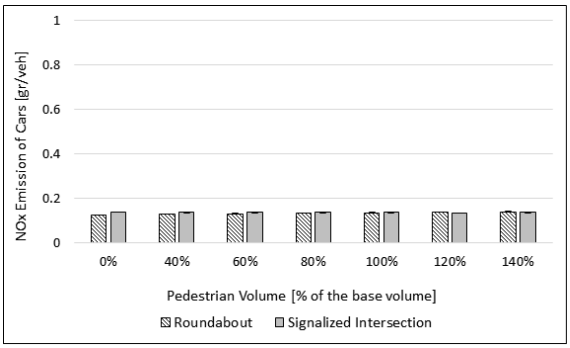

(a)

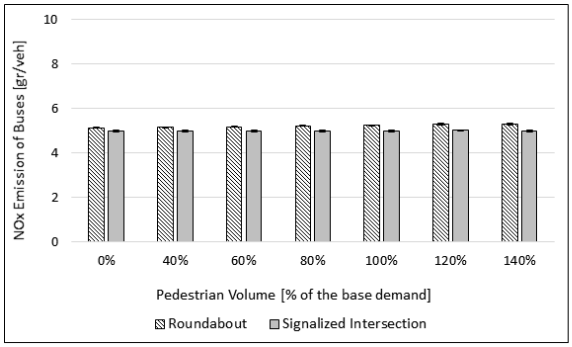

(b)

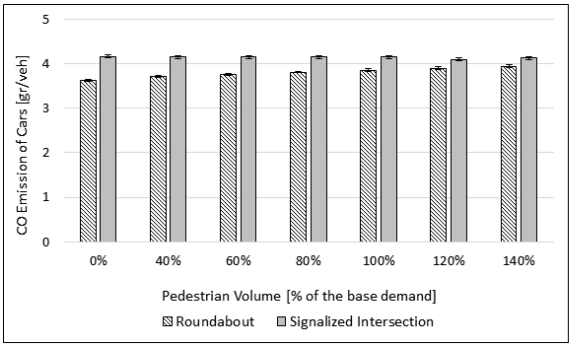

(c)

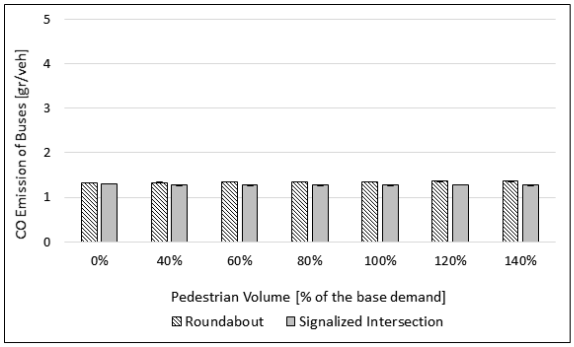

(d)

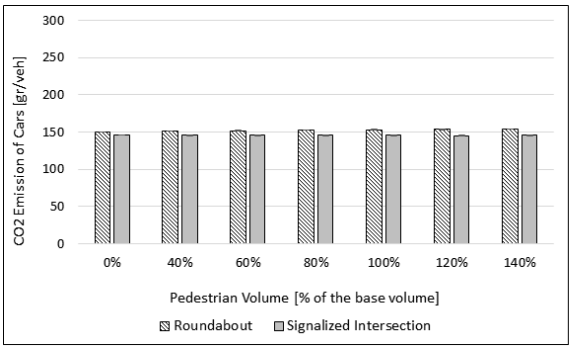

(e)

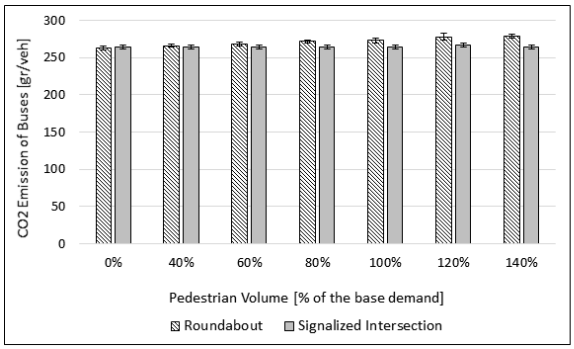

(f)

Figure 3.24: Sensitivity of emissions at roundabouts and signalized intersections with respect to pedestrian volume when buses are included in the experiments

3.6 Summary of Findings

CA-based simulation models for a roundabout and signalized intersections with single-lane approaches are developed and compared with results from the Aimsun microsimulation tool. The models are able to incorporate the effect of different traffic demands, turning ratios, and pedestrian volume and they can approximate vehicles' speed profiles to be used for emission estimation. The CA-based simulation model needs less calibration effort than the other existing simulation models. The calibration steps required for a CA-based roundabout model are as follows:

- Cell length: in a CA-based model, cells should be of the same length or shorter than the shortest moving object considered in the simulation.
- Simulation step: A simulation step should be selected such that it results in reasonable reaction times, critical gap, and follow up headway at the roundabout.
- Speed limits: in the CA model, vehicles cannot have higher speeds than the sections' speed limits. Therefore, it is recommended to select speed limits based on real-world trajectories not the posted speed limits at the site.
- Critical gap: A spatial interpretation of critical gap as the number of empty cells in the circular area can be used in the CA-based simulation model for roundabouts.
- Follow up headway: follow up headway in the CA-based model is twice the simulation step.

The CA-based models are used to analyze the sensitivity of operational and environmental performance of each type of intersection with respect to total traffic demand, left turning ratio, and pedestrian volume. Results show that roundabouts have better operational and environmental performance than signalized intersections

at undersaturated traffic conditions. Also, both the roundabout and signalized intersection result in steady increases in the performance measures as total traffic demand increases from 60% to 160% of the base demand. However, higher rate of changes in performance measures are observed at higher traffic demands as the intersection becomes more congested. Furthermore, roundabouts' operation is less sensitive to left turning traffic compared to signalized intersections' operation. Finally, signalized intersections are not sensitive to the changes in pedestrian volume while both operational and environmental performance measures at the roundabout increase significantly as pedestrian volume increases. Despite this fact, roundabouts still have a better performance than signalized intersection at the base traffic demand and any pedestrian volume in terms of delay, number of stops, and emissions.

One of the shortcomings of the CA-based simulation model is rough speed estimations and acceleration/deceleration rates as a result of a small simulation step. However, the speed fluctuations and interactions with other vehicles and pedestrians require using a small simulation step. This study showed that transit operations cannot be simulated using a cell length of 7.5 m and simulation step of 1 sec since it results in high acceleration/deceleration rates for transit vehicles. This issue can be addressed by using shorter cells in the model and considering a higher number of cells for each vehicle. In addition, future studies can be performed to analyze and compare more complicated intersection layouts (i.e. number of lane groups) and signal settings.

CHAPTER 4

CONCLUSION

Signalized intersections have a major role in traffic congestion and air quality. There is an imperative need to address these issues using the limited funds and infrastructure. Adequate signal control strategies are cost-effective tools to improve the sustainability of traffic networks.

In addition, the increased popularity of roundabouts necessitates comprehensive studies of their operational and environmental performance. Thus, simple simulation tools are required to facilitate the evaluation of roundabouts against other types of intersections.

4.1 Summary of Findings

A real-time bi-objective signal control strategy is developed for isolated intersections, which operate at undersaturated traffic conditions. The proposed signal control system optimizes a weighted combination of total vehicle delay (or person delay) and emissions and it accounts for delay experienced by auto and transit users as well as different emission levels produced by each type of vehicle. This system is able to address the issue of serving transit vehicles that arrive at the same time at the intersection by taking into account the impact each transit vehicles have on total delay and emissions. This study presents optimal solutions and the trade-offs between delay and emissions and their impact on transit operation for different combinations of the two conflicting objectives. The presented Pareto Frontiers help authorities to make informed decisions regarding the appropriate choice of objective function for a

specific site and meeting emission standards considering the impact on transit operation at an intersection. The main findings from the evaluation tests on the proposed bi-objective signal control system are as follows:

- Two objectives vehicle delay (or person delay) and emissions could be highly conflicting depending on the pollutant and emission rates used. Therefore, appropriate weights for each objective should be used to achieve the achieve desirable levels of delay and emissions.

- When a combination of total vehicle delay and CO emissions is optimized, transit vehicles do not receive priority since they do not have higher emission rates than auto vehicles. However, when a combination of total vehicle delay and NO_x emissions is optimized and if the general traffic conditions allow, transit vehicles receive priority due to their higher NO_x emission rates.

- When a combination of total person delay and CO emissions is optimized, transit vehicles may receive priority due to their higher passenger occupancy if a high delay delay weight is used in the objective function. Otherwise, if a high emission weight is used, they do not get priority. If a combination of total person delay and NO_x is optimized, transit vehicles may receive priority with any delay or emission weight used, since they have higher passenger occupancy and emission rates, but these two objectives are not highly conflicting.

- The proposed system deals with the issue of serving conflicting transit vehicles that arrive during the same cycle. If a high delay weight is used in the objective function that considers total person delay as well as emissions, the transit vehicle with higher passenger occupancy may receive priority. If a high emission weight is used in the objective function, transit vehicles receive priority based on the potential contribution they have on emissions improvement.

CA-based models for roundabouts and signalized intersections with single-lane approaches are also developed and validated for undersaturated traffic conditions. The CA-based models need less calibration efforts compared to the existing microsimulation models and can be used easily to estimate emissions based on vehicle trajectories. The models were used to study and compare the operational and environmental performance of roundabouts and signalized intersections under different traffic demands, left turning ratios, and pedestrian volumes. In addition, some simple steps to calibrate such models for roundabouts are provided. The main findings of the evaluation tests using the CA-based models are as follows:

- Roundabouts lead to lower delay and emissions than signalized intersection at undersaturated traffic conditions.
- Both roundabouts and signalized intersections show steady increase in delay and emissions as traffic demand increase (in the range of undersaturated traffic conditions).
- Roundabout control left turning vehicles more adequately compared to signalized intersections.
- Roundabouts' operational and environmental performance is sensitive to pedestrian volume, but the performance of signalized intersections is not affected by pedestrian crossings.
- To simulate transit operations using the CA model, it is necessary to account for their lower acceleration/deceleration rates.

4.2 Future Work

The developed signal control system and the CA-based models can be improved or extended in several ways. Some areas for future research are as follows:

- Extending the signal control system to be used for oversaturated conditions,
- Improving the performance of the signal control system by relaxing the assumptions of constant cycle length and phase sequence,
- Improving the accuracy of the CA-based models for roundabouts and signalized intersections by assuming shorter cells and consequently smaller speed bins and acceleration/deceleration rates,
- Simulating transit operations using the CA-based models through considering lower acceleration/deceleration rates for them compared to autos
- Extending the CA-based models to more complicated roundabout and intersection layouts and signal settings.

BIBLIOGRAPHY

[1] Aimsun users manual v8 — page layout — shape. https://www.scribd.com/document/266245543/Aimsun-Users-Manual-v8. (Accessed on 02/25/2018).

[2] California air basins. https://www.arb.ca.gov/desig/airbasins/airbasins.htm. (Accessed on 02/09/2018).

[3] Center for environmental research & technology: Comprehensive modal emission model (cmem). http://www.cert.ucr.edu/cmem/. (Accessed on 02/05/2018).

[4] Description and history of the mobile highway vehicle emission factor model — moves and other mobile source emissions models — us epa. https://www.epa.gov/moves/description-and-history-mobile-highway-vehicle-emission-factor-model. (Accessed on 12/26/2017).

[5] Google maps. https://www.google.com/maps/@42.395151,-72.5263408,410m/data=!3m1!1e3. (Accessed on 02/25/2018).

[6] Map: California map for local air district websites. https://www.arb.ca.gov/capcoa/dismap.htm. (Accessed on 02/09/2018).

[7] Ms sedco intersector microwave motion and presence sensor software changes — ms sedco. http://mssedco.com/intersector-changes/. (Accessed on 02/10/2018).

[8] Official release of emfac2011 motor vehicle emission factor model for use in the state of california. https://www.gpo.gov/fdsys/pkg/FR-2013-03-06/pdf/2013-05245.pdf. (Accessed on 02/04/2018).

[9] Pareto efficiency. https://en.wikipedia.org/wiki/Pareto$_e ff iciency$.($Accessedon$02/05/2018).

[10] The smartest project: Analysis of micro-simulation tools. http://www.its.leeds.ac.uk/projects/smartest/append3d.htmla32. (Accessed on 02/09/2018).

[11] TRansportatoin ANalysis SIMulation Systems. http://ndssl.vbi.vt.edu/transims-docs.html. Accessed: 2017-11/20.

[12] Abrams, Daniel S, Fitzpatrick, Cole D, Tang, Yue, and Knodler, Michael A. A spatial and temporal analysis of driver gap acceptance behavior at modern roundabouts. In *92nd Annual Meeting of the Transportation Research Board, Washington, DC January* (2013).

[13] Anderson, Jessica, Sayers, Tessa, and Bell, Michael. The objectives of traffic signal control. *Traffic engineering & control 39*, 3 (1998), 167–170.

[14] Barth, Matthew, An, Feng, Younglove, Theodore, Levine, C, Scora, G, Ross, Marc, and Wenzel, Thomas. *Development of a comprehensive modal emissions model*. National Cooperative Highway Research Program, Transportation Research Board of the National Academies, 2000.

[15] Barth, Matthew, An, Feng, Younglove, Theodore, Scora, George, Levine, Carrie, Ross, Marc, and Wenzel, Thomas. Comprehensive modal emission model (cmem), version 2.0 users guide. *University of California, Riverside* (2000).

[16] Bellman, Richard E, and Zadeh, Lotfi Asker. Decision-making in a fuzzy environment. *Management science 17*, 4 (1970), B–141.

[17] Belz, Nathan P, Aultman-Hall, Lisa, and Montague, James. Influence of priority taking and abstaining at single-lane roundabouts using cellular automata. *Transportation research part C: emerging technologies 69* (2016), 134–149.

[18] Brian Park, Byungkyu, Yun, Ilsoo, and Ahn, Kyoungho. Stochastic optimization for sustainable traffic signal control. *International journal of sustainable transportation 3*, 4 (2009), 263–284.

[19] Chamberlin, Robert, Swanson, Ben, Talbot, Eric, Dumont, Jeff, and Pesci, Stephen. Analysis of moves and cmem for evaluating the emissions impact of an intersection control change. In *Transportation Research Board 90th Annual Meeting* (2011), no. 11-0673.

[20] Chimdessa, Yadeta, Kassa, Semu M, and Lemecha, Legesse. Efficiency of roundabouts as compared to traffic light controlled intersections in urban road networks. *Momona Ethiopian Journal of Science 5*, 2 (2013), 81–100.

[21] Choi, David, Beardsley, Megan, Brzezinski, David, Koupal, John, and Warila, James. Moves sensitivity analysis: the impacts of temperature and humidity on emissions. In *MOVES Workshop* (2011).

[22] Christofa, Eleni, Papamichail, Ioannis, and Skabardonis, Alexander. Person-based traffic responsive signal control optimization. *IEEE Transactions on Intelligent Transportation Systems 14*, 3 (2013), 1278–1289.

[23] Clean Air Technologies International, Inc. OEM 2100. http://globalmrv.com/, Accessed February 2015.

[24] Coelho, Margarida C, Farias, Tiago L, and Rouphail, Nagui M. Effect of roundabout operations on pollutant emissions. *Transportation Research Part D: Transport and Environment 11*, 5 (2006), 333–343.

[25] Echab, H, Ez-Zahraouy, H, and Lakouari, N. Simulation study of interference of crossings pedestrian and vehicle traffic at a single lane roundabout. *Physica A: Statistical Mechanics and its Applications 461* (2016), 854–864.

[26] Echab, H, Lakouari, N, Ez-Zahraouy, H, and Benyoussef, A. Simulation study of traffic car accidents at a single lane roundabout. *International Journal of Modern Physics C 27*, 01 (2016), 1650009.

[27] Floudas, Christodoulos A. *Nonlinear and mixed-integer optimization: fundamentals and applications*. Oxford University Press, 1995.

[28] Frey, H Christopher, Rouphail, Nagui M, and Zhai, Haibo. Speed- and facility-specific emission estimates for on-road light-duty vehicles on the basis of real-world speed profiles. *Transportation Research Record: Journal of the Transportation Research Board 1987*, 1 (2006), 128–137.

[29] Frey, H Christopher, Unal, Alper, Chen, Jianjun, and Li, Song. Modeling mobile source emissions based upon in-use and second-by-second data: Development of conceptual approaches for epas new moves model. In *Proceedings, Annual Meeting of the Air and Waste Management Association, Pittsburgh* (2003).

[30] Frey, Henry Christopher, Rouphail, Nagui M, Unal, A, and Colyar, James D. Measurement of on-road tailpipe co, no, and hydrocarbon emissions using a portable instrument. In *Proceedings, Annual Meeting of the Air & Waste Management Association* (2001), Citeseer.

[31] Gates, Tim J, Noyce, David A, Bill, Andrea R, Van Ee, Nathanael, and Gates, TJ. Recommended walking speeds for pedestrian clearance timing based on pedestrian characteristics. In *Proceeding of TRB 2006 Annual Meeting* (2006).

[32] Guo, Rui, and Zhang, Yu. The relationship between mobility and environmental externalities at signalized intersections. In *Transportation Research Board 93rd Annual Meeting* (2014), no. 14-3347.

[33] Hallmark, Shauna L, and Mudgal, Abhisek. Comparison of vsp profiles for three types of intersection control and implications for emissions. In *Intelligent Transportation Systems (ITSC), 2012 15th International IEEE Conference on* (2012), IEEE, pp. 415–420.

[34] Hellinga, Bruce, Khan, Mohammad Ali, and Fu, Liping. Analytical emission models for signalised arterials.

[35] Hitchcock, Owen, and Gayah, Vikash. Methods to identify candidate solutions in multi-objective signal timing optimization. *Transportation Research Record: Journal of the Transportation Research Board* (2018).

[36] Huang, Ding-wei. Phase diagram of a traffic roundabout. *Physica A: Statistical Mechanics and its Applications 383*, 2 (2007), 603–612.

[37] Jackson, Meredith, and Rakha, Hesham A. Are roundabouts environmentally friendly? an evaluation for uniform approach demands. In *90th Transportation Research Board Annual Meeting, Washington, DC, USA* (2011).

[38] Jeihani, Mansoureh, Ahn, Kyoungho, Hobeika, Antoine G, Sherali, Hanif D, and Rakha, Hesham A. Comparison of transims'light duty vehicle emissions with on-road emission measurements. In *Journal of the Transportation Research Forum* (2010), vol. 45.

[39] Khalighi, Farnoush. A real-time signal control system to minimize emissions at isolated intersections.

[40] Khalighi, Farnoush. Scholarworks@ umassamherst.

[41] Kosonen, Iisakki. Multi-agent fuzzy signal control based on real-time simulation. *Transportation Research Part C: Emerging Technologies 11*, 5 (2003), 389–403.

[42] Koupal, John, Michaels, Harvey, Cumberworth, Mitch, Bailey, Chad, and Brzezinski, Dave. Epa's plan for moves: a comprehensive mobile source emissions model. In *Proceedings of the 12th CRC On-Road Vehicle Emissions Workshop, San Diego, CA* (2002), pp. 15–17.

[43] Kun, Chen, and Lei, Yu. Microscopic traffic-emission simulation and case study for evaluation of traffic control strategies. *Journal of Transportation Systems Engineering and Information Technology 7*, 1 (2007), 93–99.

[44] Kvatch, IA, Dravitzki, VK, and Brown, DN. On-board vehicle emission measurement technique for the determination of the effect of route attributes on emission rates. In *ARRB TRANSPORT RESEARCH LTD CONFERENCE, 19TH, 1998, SYDNEY, NEW SOUTH WALES, AUSTRALIA* (1998).

[45] Lee, Jee-Hyong, Lee, Keon-Myung, and Lee-Kwang, Hyung. Fuzzy controller for intersection group. In *Industrial Automation and Control: Emerging Technologies, 1995., International IEEE/IAS Conference on* (1995), IEEE, pp. 376–382.

[46] Leonard, II, John D, and Rodegerdts, Lee A. Comparison of alternate signal timing policies. *Journal of transportation engineering 124*, 6 (1998), 510–520.

[47] Li, Meng, Boriboonsomsin, Kanok, Wu, Guoyuan, Zhang, Wei-Bin, and Barth, Matthew. Traffic energy and emission reductions at signalized intersections: a study of the benefits of advanced driver information. *International Journal of Intelligent Transportation Systems Research 7*, 1 (2009), 49–58.

[48] Li, Pengfei, Mirchandani, Pitu, and Zhou, Xuesong. Simulation-based traffic signal optimization to minimize fuel consumption and emission: A lagrangian relaxation approach. *Transportation Research Board* (2015).

[49] Li, Xiugang, Li, Guoqiang, Pang, Su-Seng, Yang, Xiaoguang, and Tian, Jialin. Signal timing of intersections using integrated optimization of traffic quality, emissions and fuel consumption: a note. *Transportation Research Part D: Transport and Environment 9*, 5 (2004), 401–407.

[50] Li, Zhi-Chun, and Ge, Xiao-Yan. Traffic signal timing problems with environmental and equity considerations. *Journal of advanced transportation 48*, 8 (2014), 1066–1086.

[51] Louis, Marie. Multi-criteria decision making when planning sustainable multimodal transportation routes in a linear corridor.

[52] Macioszek, Elżbieta. The comparison of models for follow-up headway at roundabouts. In *Scientific And Technical Conference Transport Systems Theory And Practice* (2017), Springer, pp. 16–26.

[53] Małecki, Krzysztof, and Watróbski, Jarosław. Cellular automaton to study the impact of changes in traffic rules in a roundabout: A preliminary approach. *Applied Sciences 7*, 7 (2017), 742.

[54] Midenet, Sophie, Boillot, Florence, and Pierrelée, Jean-Claude. Signalized intersection with real-time adaptive control: on-field assessment of co 2 and pollutant emission reduction. *Transportation Research Part D: Transport and Environment 9*, 1 (2004), 29–47.

[55] Nagel, Kai, and Schreckenberg, Michael. A cellular automaton model for freeway traffic. *Journal de physique I 2*, 12 (1992), 2221–2229.

[56] Oda, Toshihiko, Kuwahara, Masao, and Niikura, Satoshi. Traffic signal control for reducing vehicle carbon dioxide emissions on an urban road network. *Proc. 11th World Congr. ITS* (2004), 1–8.

[57] Pappis, Costas P, and Mamdani, Ebrahim H. A fuzzy logic controller for a trafc junction. *IEEE Transactions on Systems, Man, and Cybernetics 7*, 10 (1977), 707–717.

[58] Pareto, V. Course deconomie politique, lausanne, rouge, 1896. *ParetoCourse deconomie politique1896* (1896).

[59] Rakha, Hesham, Ahn, Kyoungho, and Trani, Antonio. Development of vt-micro model for estimating hot stabilized light duty vehicle and truck emissions. *Transportation Research Part D: Transport and Environment 9*, 1 (2004), 49–74.

[60] Rakha, Hesham, Ahn, Kyoungho, and Trani, Antonio. Development of vt-micro model for estimating hot stabilized light duty vehicle and truck emissions. *Transportation Research Part D: Transport and Environment 9*, 1 (2004), 49–74.

[61] Rakha, Hesham, Medina, A, Sin, H, Dion, F, Van Aerde, M, and Jenq, J. Traffic signal coordination across jurisdictional boundaries: Field evaluation of efficiency, energy, environmental, and safety impacts. *Transportation Research Record: Journal of the Transportation Research Board*, 1727 (2000), 42–51.

[62] Rodegerdts, Lee. *Roundabouts in the United States*, vol. 572. Transportation Research Board, 2007.

[63] Rouphail, Nagui M, Frey, H Christopher, Colyar, James D, and Unal, Alper. Vehicle emissions and traffic measures: exploratory analysis of field observations at signalized arterials. In *80th Annual Meeting of the Transportation Research Board, Washington, DC* (2001).

[64] Salamati, Katy, Rouphail, Nagui M, Frey, H Christopher, Liu, Bin, and Schroeder, Bastian J. Simplified method for comparing emissions in roundabouts and at signalized intersections. *Transportation Research Record: Journal of the Transportation Research Board*, 2517 (2015), 48–60.

[65] Schmöcker, Jan-Dirk, Ahuja, Sonal, and Bell, Michael GH. Multi-objective signal control of urban junctions–framework and a london case study. *Transportation Research Part C: Emerging Technologies 16*, 4 (2008), 454–470.

[66] Shabihkhani, Rooholamin, and Gonzales, Eric J. Analytical model for vehicle emissions at a signalized intersection: Integrating traffic and microscopic emissions models. In *Transportation Research Board 92nd Annual Meeting* (2013), no. 13-5208.

[67] Shindell, Drew T. The social cost of atmospheric release. *Climatic Change 130*, 2 (2015), 313–326.

[68] Skabardonis, Alexander, Geroliminis, Nikolas, and Christofa, Eleni. Prediction of vehicle activity for emissions estimation under oversaturated conditions along signalized arterials. *Journal of Intelligent Transportation Systems 17*, 3 (2013), 191–199.

[69] Stathopoulos, Fotis G, and Noland, Robert B. Induced travel and emissions from traffic flow improvement projects. *Transportation Research Record: Journal of the Transportation Research Board 1842*, 1 (2003), 57–63.

[70] Stevanovic, Aleksandar, Stevanovic, Jelka, and Kergaye, Cameron. Optimization of traffic signal timings based on surrogate measures of safety. *Transportation research part C: emerging technologies 32* (2013), 159–178.

[71] Stevanovic, Aleksandar, Stevanovic, Jelka, So, Jaehyun, and Ostojic, Marija. Multi-criteria optimization of traffic signals: Mobility, safety, and environment. *Transportation Research Part C: Emerging Technologies 55* (2015), 46–68.

[72] Stevanovic, Aleksandar, Stevanovic, Jelka, Zhang, Kai, and Batterman, Stuart. Optimizing traffic control to reduce fuel consumption and vehicular emissions. *Transportation Research Record: Journal of the transportation research board 2128*, 1 (2009), 105–113.

[73] Sun, Dazhi, Benekohal, Rahim F, and Waller, S Travis. Multiobjective traffic signal timing optimization using non-dominated sorting genetic algorithm. In *Intelligent Vehicles Symposium, 2003. Proceedings. IEEE* (2003), IEEE, pp. 198–203.

[74] Tao, Fei, Shi, Qinyi, and Yu, Lei. Evaluation of effectiveness of coordinated signal control in reducing vehicle emissions during peak hours versus nonpeak hours. *Transportation Research Record: Journal of the Transportation Research Board*, 2233 (2011), 45–52.

[75] Teply, Stan, Allingham, DI, Richardson, DB, and Stephenson, BW. Canadian capacity guide for signalized intersections.

[76] Unal, Alper, Rouphail, Nagui M, and Frey, H Christopher. Effect of arterial signalization and level of service on measured vehicle emissions. *Transportation Research Record: Journal of the Transportation Research Board 1842*, 1 (2003), 47–56.

[77] Várhelyi, András. The effects of small roundabouts on emissions and fuel consumption: a case study. *Transportation Research Part D: Transport and Environment 7*, 1 (2002), 65–71.

[78] Von Neumann, John. The general and logical theory of automata. *Cerebral mechanisms in behavior 1*, 41 (1951), 1–2.

[79] Wang, Ruili, and Ruskin, Heather J. Modeling traffic flow at a single-lane urban roundabout. *Computer Physics Communications 147*, 1-2 (2002), 570–576.

[80] Xia, Haitao, Boriboonsomsin, Kanok, and Barth, Matthew. Dynamic eco-driving for signalized arterial corridors and its indirect network-wide energy/emissions benefits. *Journal of Intelligent Transportation Systems 17*, 1 (2013), 31–41.

[81] Xia, Haitao, Boriboonsomsin, Kanok, Schweizer, Friedrich, Winckler, Andreas, Zhou, Kun, Zhang, Wei-Bin, and Barth, Matthew. Field operational testing of eco-approach technology at a fixed-time signalized intersection. In *Intelligent Transportation Systems (ITSC), 2012 15th International IEEE Conference on* (2012), IEEE, pp. 188–193.

[82] Xiaohong, CHEN, Dalin, QIAN, and Donghua, SHI. Multi-objective optimization method of signal timing for the non-motorized transport at intersection. *Journal of Transportation Systems Engineering and Information Technology 11*, 2 (2011), 106–111.

[83] Xu, Feng, and Tian, Zong. Driver behavior and gap-acceptance characteristics at roundabouts in california. *Transportation Research Record: Journal of the Transportation Research Board*, 2071 (2008), 117–124.

[84] Zamanipour, Mehdi, Head, Larry, and Ding, Jun. Priority system for multimodal traffic signal control. In *Transportation Research Board 93rd Annual Meeting* (2014), no. 14-3579.

[85] Zeng, Weiliang, He, Zhaocheng, and Chen, Ningning. A multi-objective optimization model and a decision-making method for traffic signal control. In *Proceedings of the 10th International Conference of Chinese Transportation Professionals, Beijing, China* (2010), pp. 1507–1517.

[86] Zhai, Haibo, Frey, H Christopher, and Rouphail, Nagui M. A vehicle-specific power approach to speed-and facility-specific emissions estimates for diesel transit buses. *Environmental science & technology 42*, 21 (2008), 7985–7991.

[87] Zhang, Lihui, Yin, Yafeng, and Chen, Shigang. Robust signal timing optimization with environmental concerns. *Transportation Research Part C: Emerging Technologies 29* (2013), 55–71.

[88] Zhang, Yingying, Xumei, Chen, Zhang, Xiao, Guohua, Song, Yanzhao, Hao, and Lei, Yu. Assessing effect of traffic signal control strategies on vehicle emissions. *Journal of Transportation Systems Engineering and Information Technology 9*, 1 (2009), 150–155.

[89] Zhou, Shenpei, Yan, Xinping, and Wu, Chaozhong. Optimization model for traffic signal control with environmental objectives. In *Natural Computation, 2008. ICNC'08. Fourth International Conference on* (2008), vol. 6, IEEE, pp. 530–534.

[90] Zhou, Zhanhong, and Cai, Ming. Intersection signal control multi-objective optimization based on genetic algorithm. *Journal of Traffic and Transportation Engineering (English Edition) 1*, 2 (2014), 153–158.

[91] Züger, P, Porchet, A, and Burch, D. Roundabouts: fuel consumption, emissions of pollutants, crossing times. In *Proceeding of the 1st Swiss Transport Research Conference, Monte Verità/Ascona* (2001).